G-matrix Fourier Transform (GFT) Projection NMR Spectroscopy

Theory and Application

The 'NMR sampling problem':
minimal measurement times scale with Πn_j

1 scan *per* second
16 complex points *per* dimension =>

- 1D -> 1 second
- 2D -> ~0.5 minutes
- 3D -> ~0.3 hours
- 4D -> ~9 hours
- 5D -> ~12 days
- 6D -> ~1.1 years

Importance for NMR at highest magnetic fields

- '**Sampling demand**' in each indirect dimension scales with the magnetic field strength
  => 4D at 900 versus 600 MHz ^{1}H resonance frequency is **3.4-times larger**

- **Sensitivity increases with magnetic field strength**

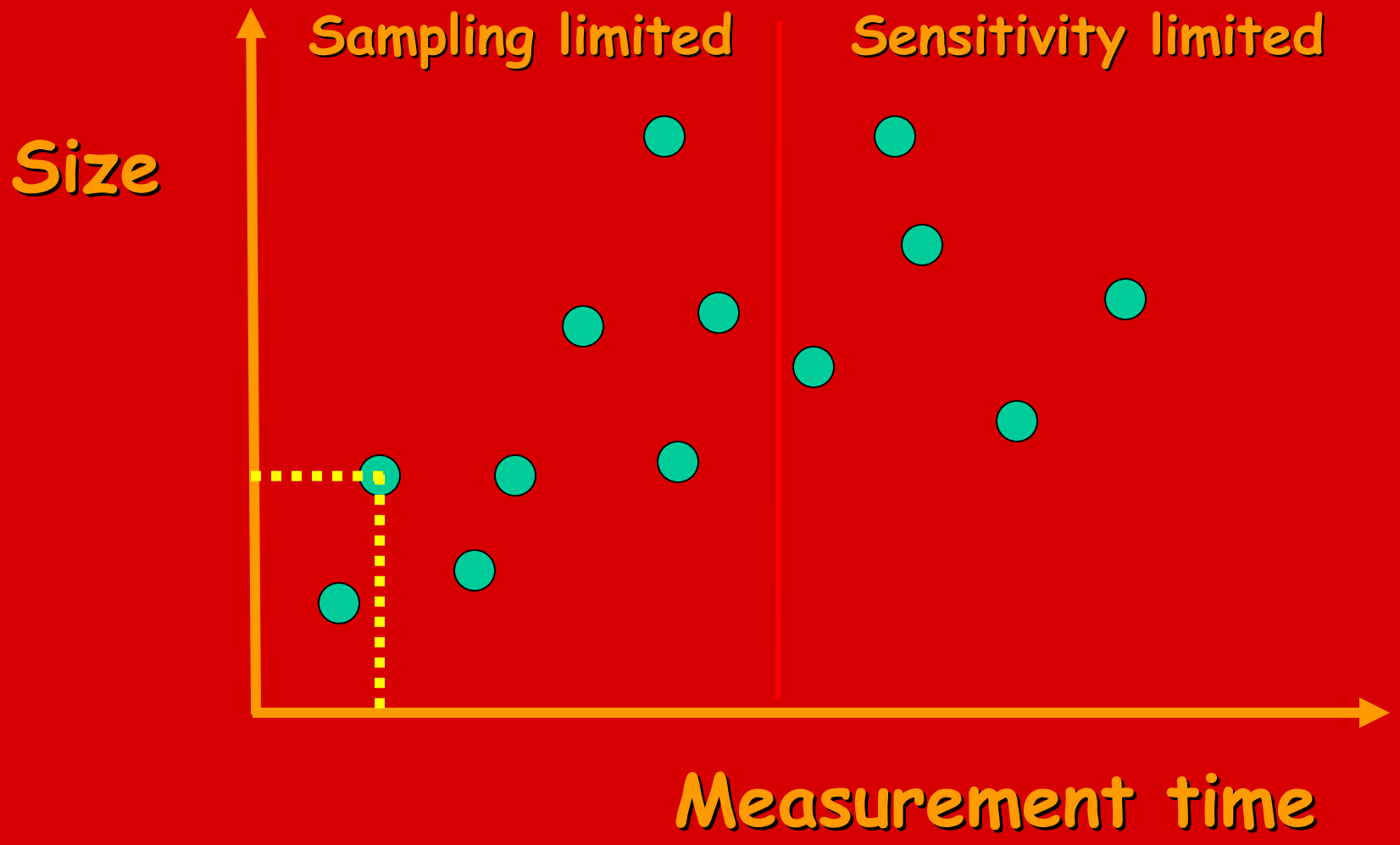
Sampling limited
Sensitivity limited
Size
Measurement time

Projection NMR:
a solution of the
NMR sampling problem…

…avoid many dimensions…

Major developments in the 1970-1980s (Richard Ernst and coworkers)

- 'Skewed projections' of homo-nuclear 2D *J*-spectra were calculated using the '**projection cross-section**' theorem to obtain decoupled 1D ^{1}H NMR spectra;
  no joint incrementation of shift evolution periods or phase-sensitive signal detection

- 'Accordion NMR': *joint sampling of chemical shift evolution period and 'mixing time' in EXSY -> **Reduction in dimensionality***

Early 1990s:

Demand for an approach in which chemical shifts are jointly sampled in a phase-sensitive manner….

Reduced-dimensionality (RD) NMR and its variants:

'Modules' for GFT projection NMR

RD NMR Spectroscopy

(Szyperski, Wider, Bushweller, Wuthrich. JACS 115, 1993)

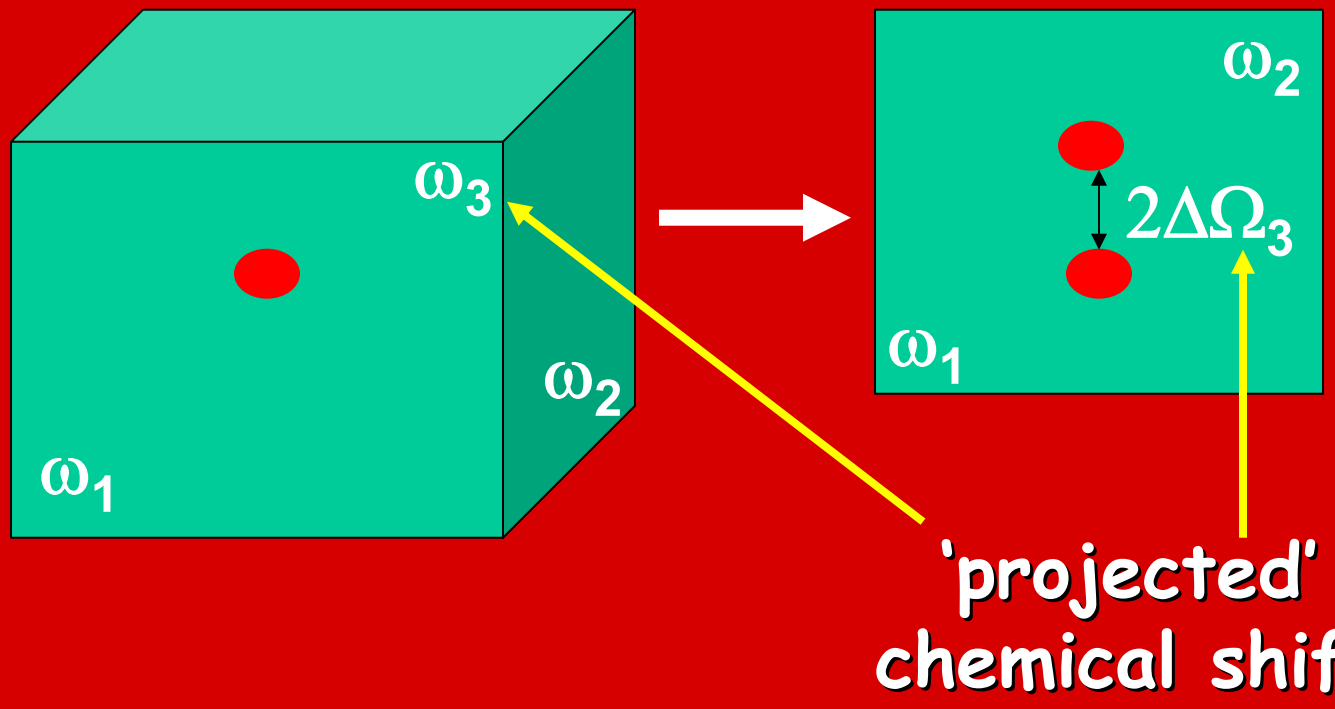

Challenge: keep information upon projection

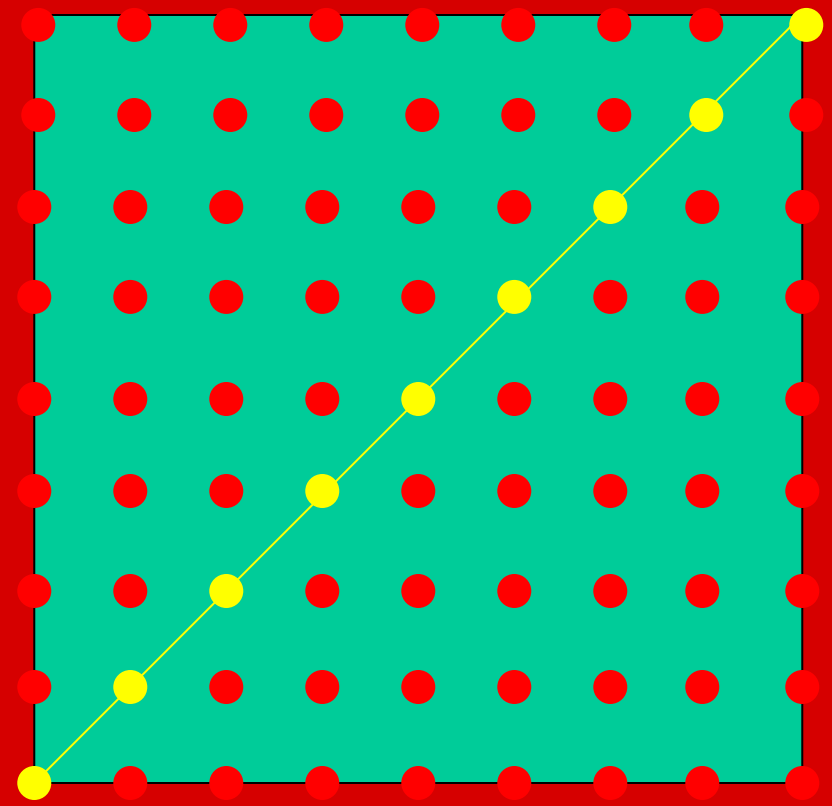

Transfer amplitude ~ $e^{i\Omega_K t}\cos(\Omega_S t)$

J. Am. Chem. Soc. v 115
p. 9307 Szyperski

J-9308-M2

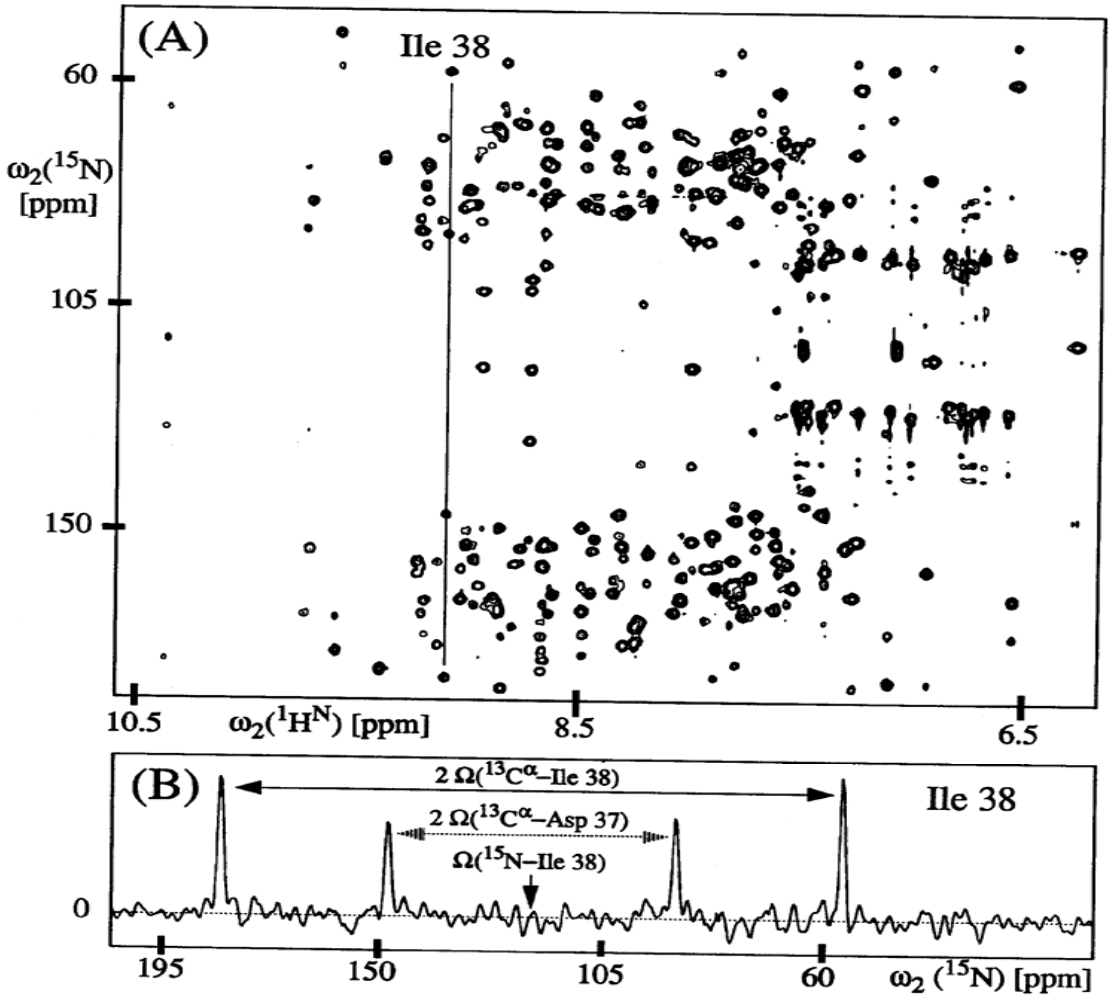

Fig. S1

2D RD HNNCA
Szyperski et al.,
JACS 115, 1993
Suppl. Material

RD NMR variants…

1. Scaling of shift evolution periods

(Szyperski et al., JACS 115,1993)

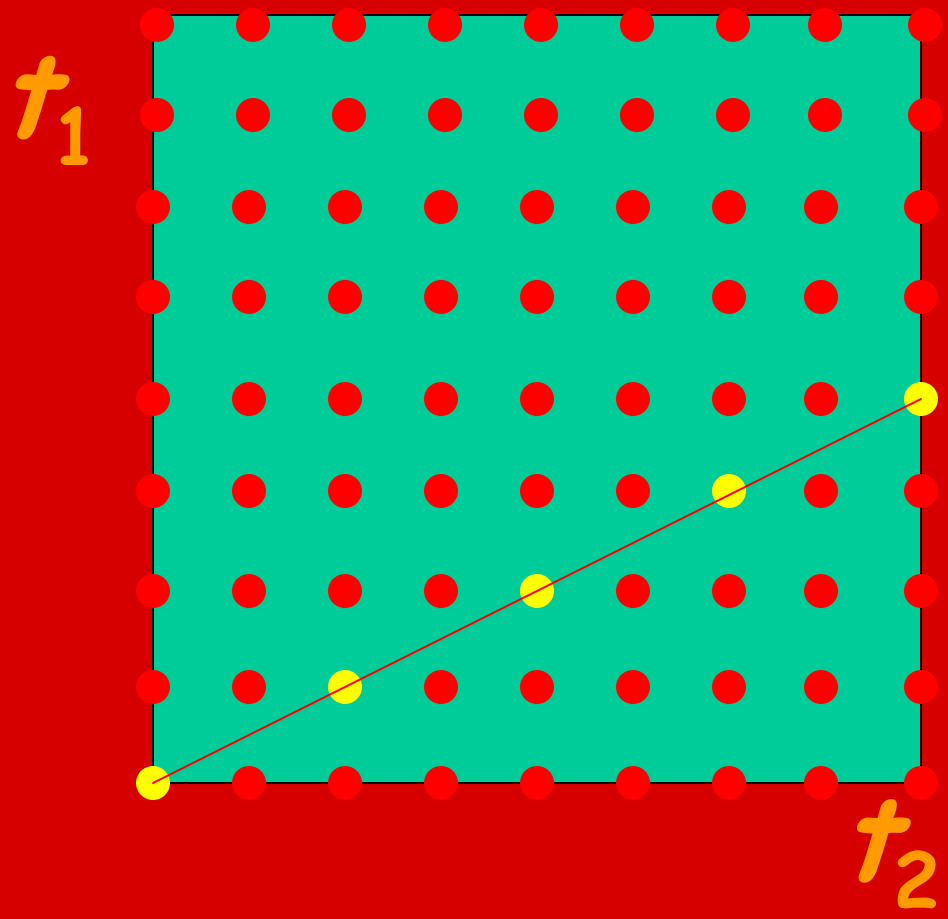
t_1
t_2

3D $\underline{H}^{\alpha/\beta}\underline{C}^{\alpha/\beta}$(CO)NHN, a Projected 4D NMR Experiment for Sequential Correlation of Polypeptide $^{1}H^{\alpha/\beta}$, $^{13}C^{\alpha/\beta}$ and Backbone ^{15}N and $^{1}H^{N}$ Chemical Shifts

THOMAS SZYPERSKI, MAURIZIO PELLECCHIA, AND KURT WÜTHRICH

Institut für Molekularbiologie und Biophysik, Eidgenössische Technische Hochschule-Hönggerberg, CH-8093 Zurich, Switzerland

Received June 29, 1994

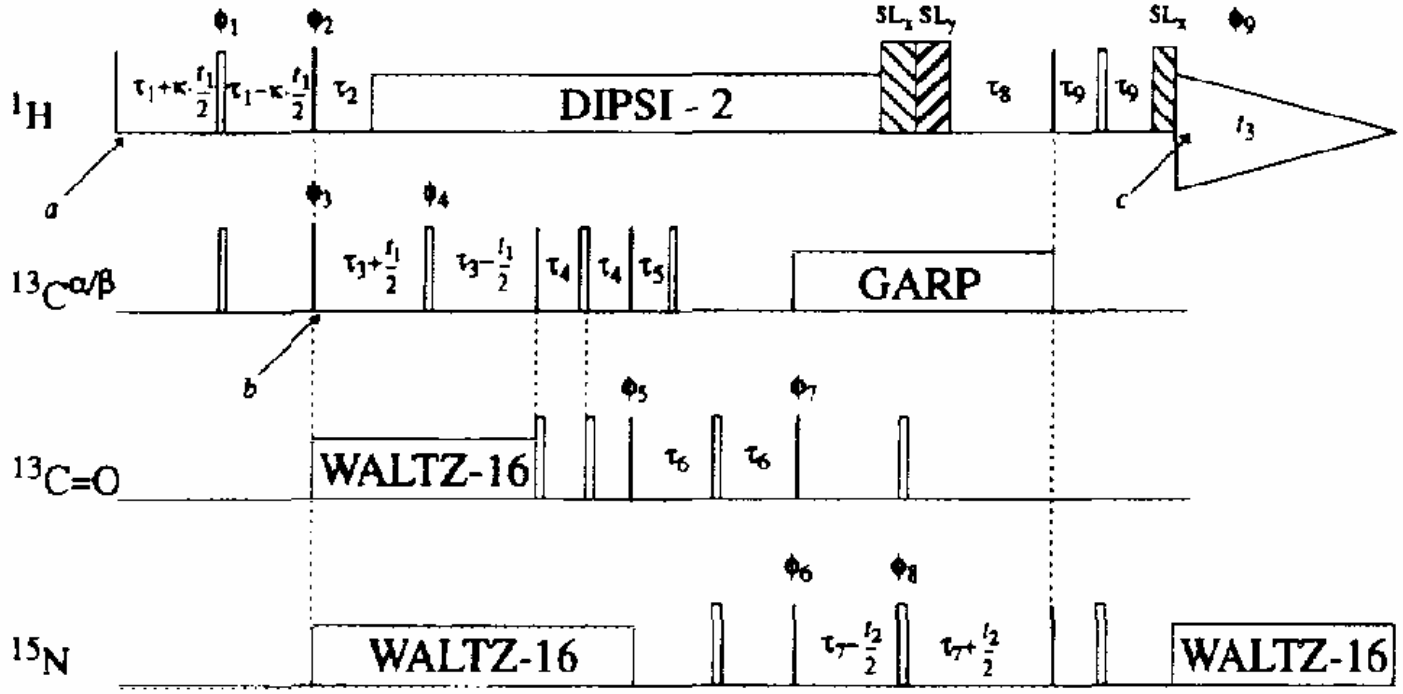

'tilted projected spectrum'

NMRFam Workshop 06/06/06

$t_1(^{13}C\alpha\beta)$

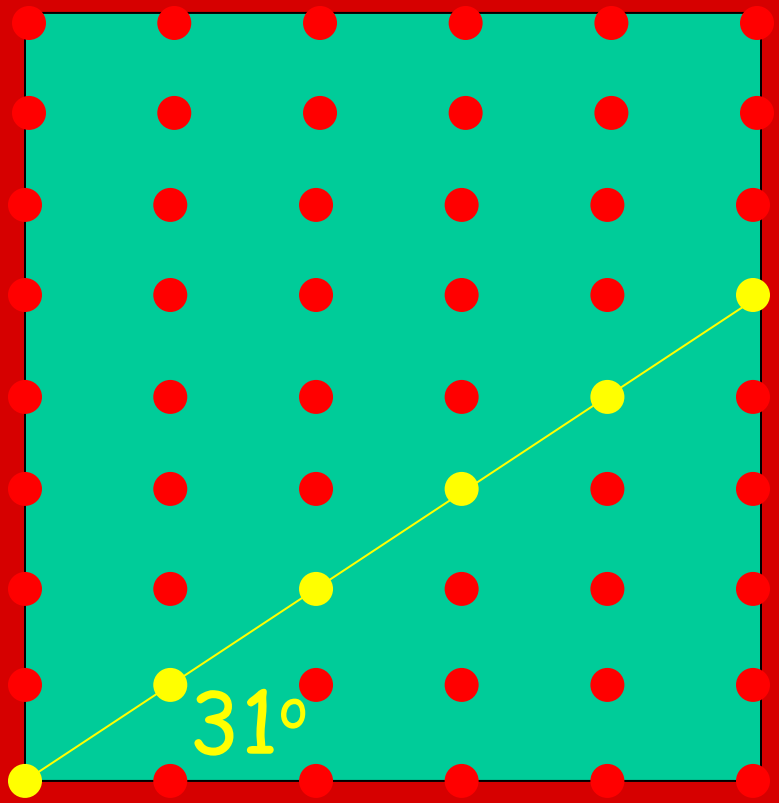

$\kappa = 1.65$

$t_2(^{1}H\alpha\beta)$

2. Central peak detection

(Szyperski et al., JMR B108, 1995; JACS 118,1996)

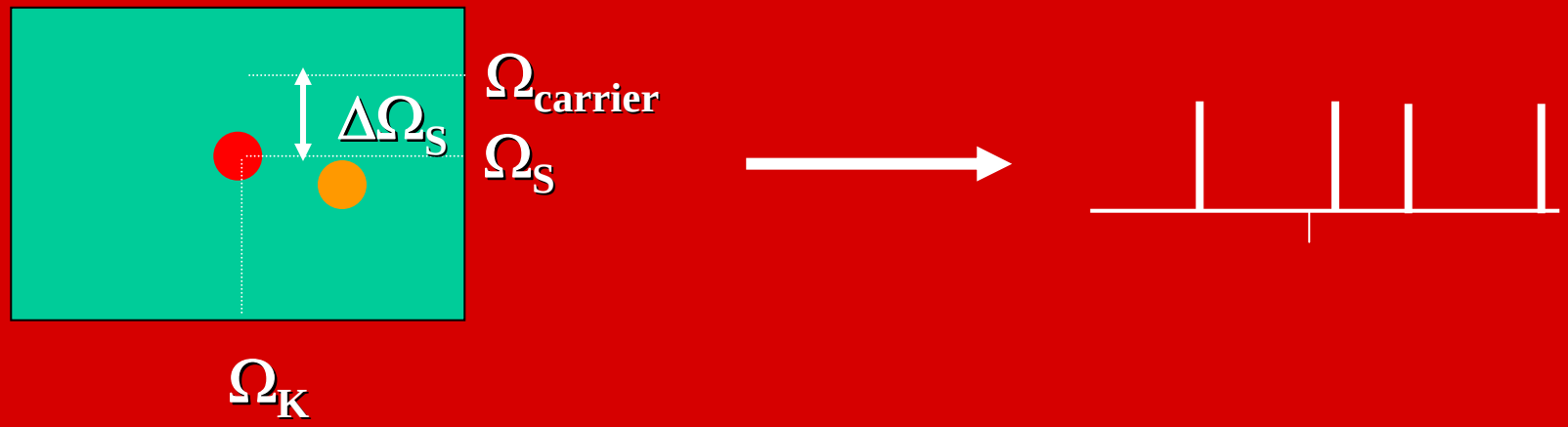
$\Omega_{carrier}$
$\Delta\Omega_S$
Ω_S
Ω_K

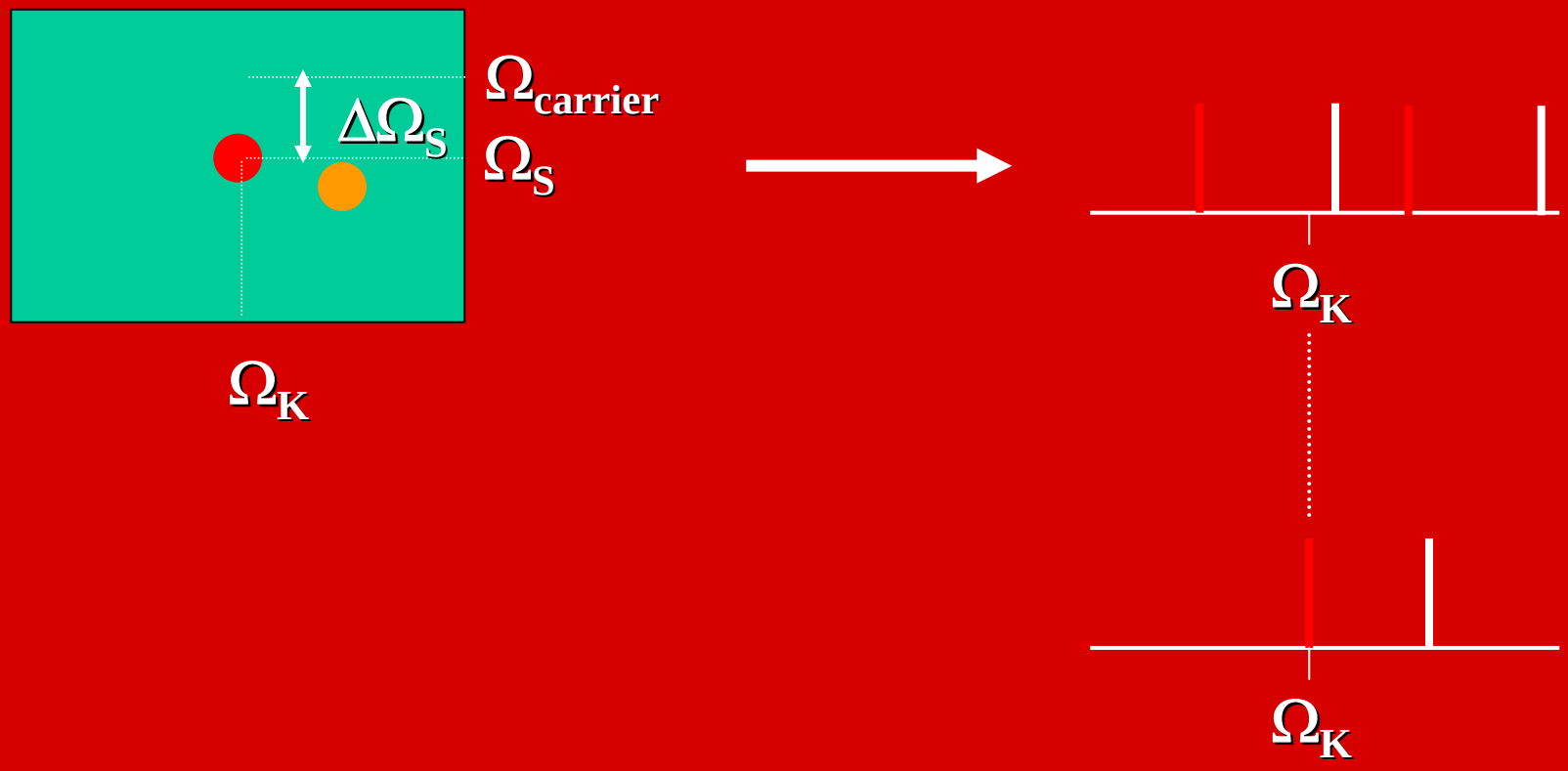

central peak detection

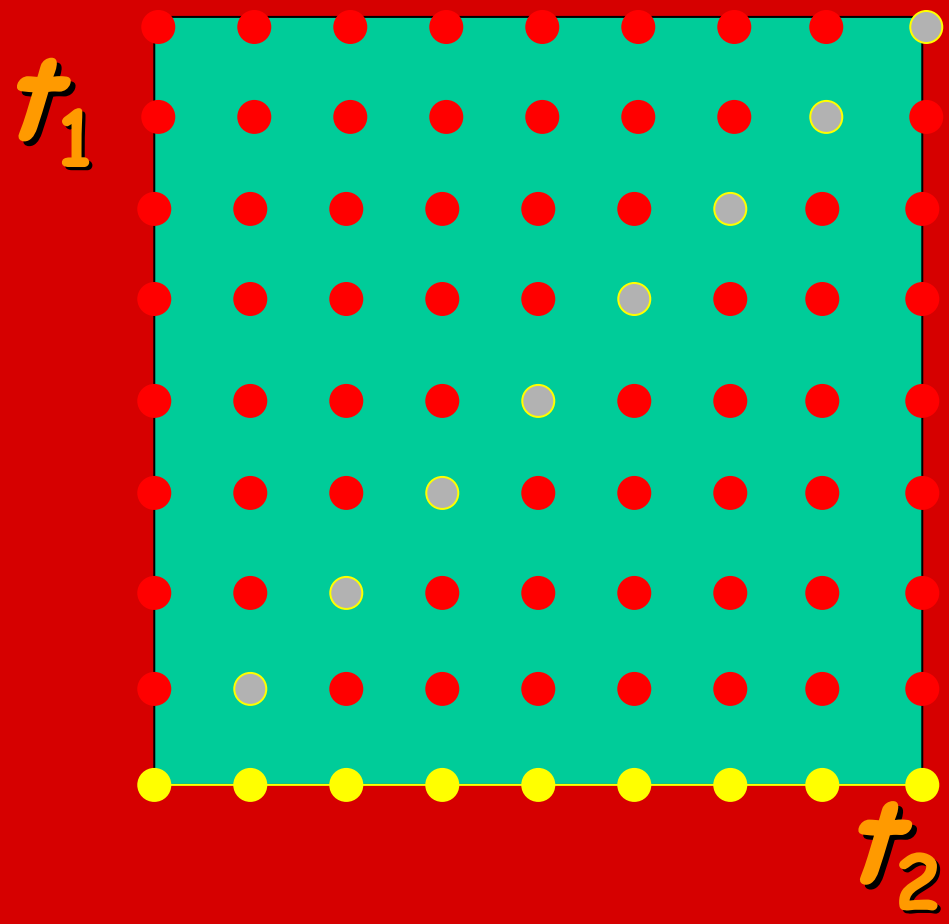

central peak detection ⇔
'orthogonal projections'

Identification of shift multiplets

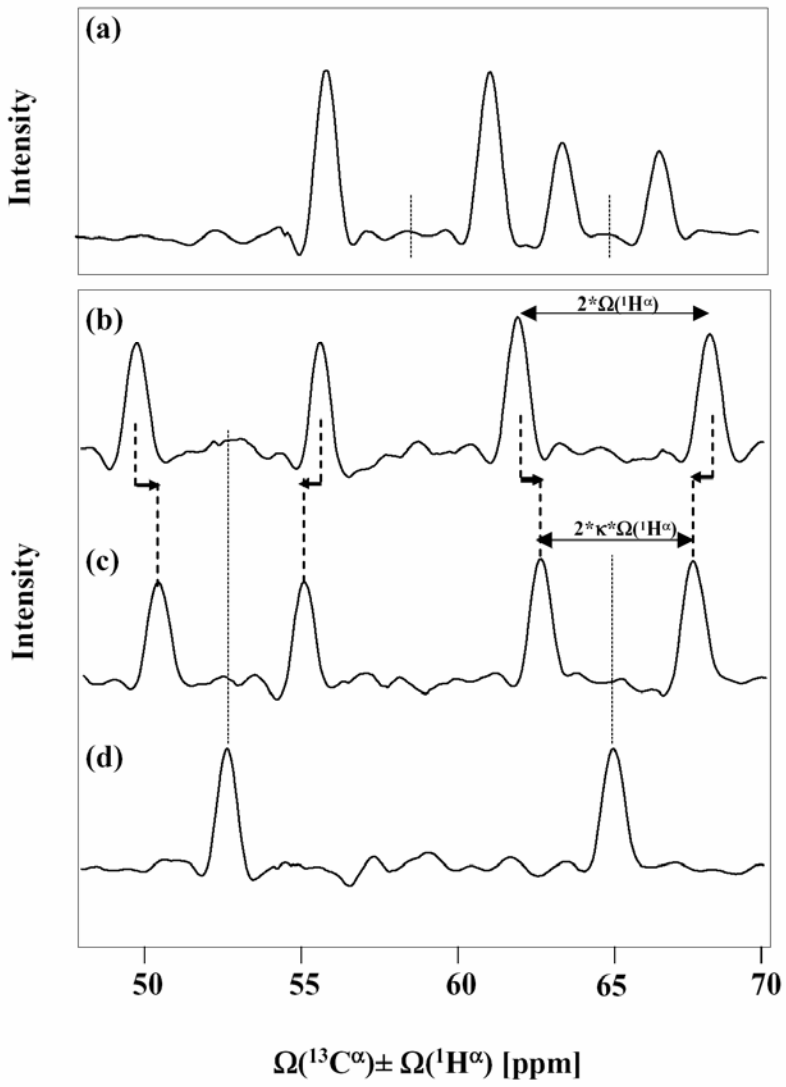

'spin relaxation time labeling'

variation of scaling of evolution periods

central peak detection

3. 'Phase-sensitive' RD NMR

(Marion and coworkers, JMR B109, 1995)

Transfer amplitude ~ $e^{i\Omega_K t}\cos(\Omega_S t)$

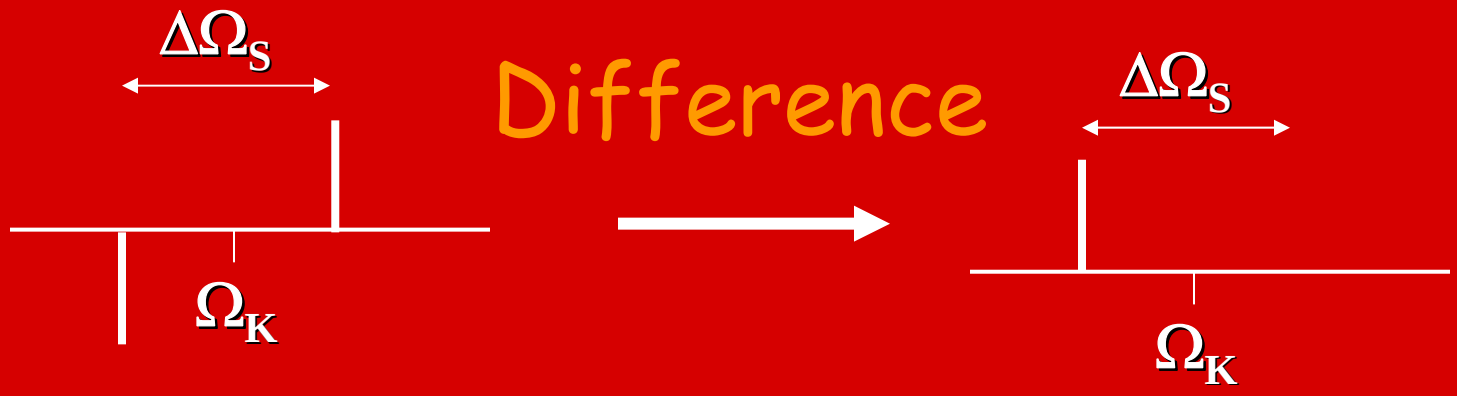

Transfer amplitude ~ $e^{i\Omega_K t}\sin(\Omega_S t)$

The alternative:
TPPI combined with scaling of shift evolution periods

A Novel Reduced-Dimensionality Triple-Resonance Experiment for Efficient Polypeptide Backbone Assignment, 3D CO HN N CA

THOMAS SZYPERSKI, DANIEL BRAUN, CÉSAR FERNÁNDEZ, CHRISTIAN BARTELS, AND KURT WÜTHRICH

Institut für Molekularbiologie und Biophysik, Eidgenössische Technische Hochschule-Hönggerberg, CH-8093 Zürich, Switzerland

Received May 26, 1995

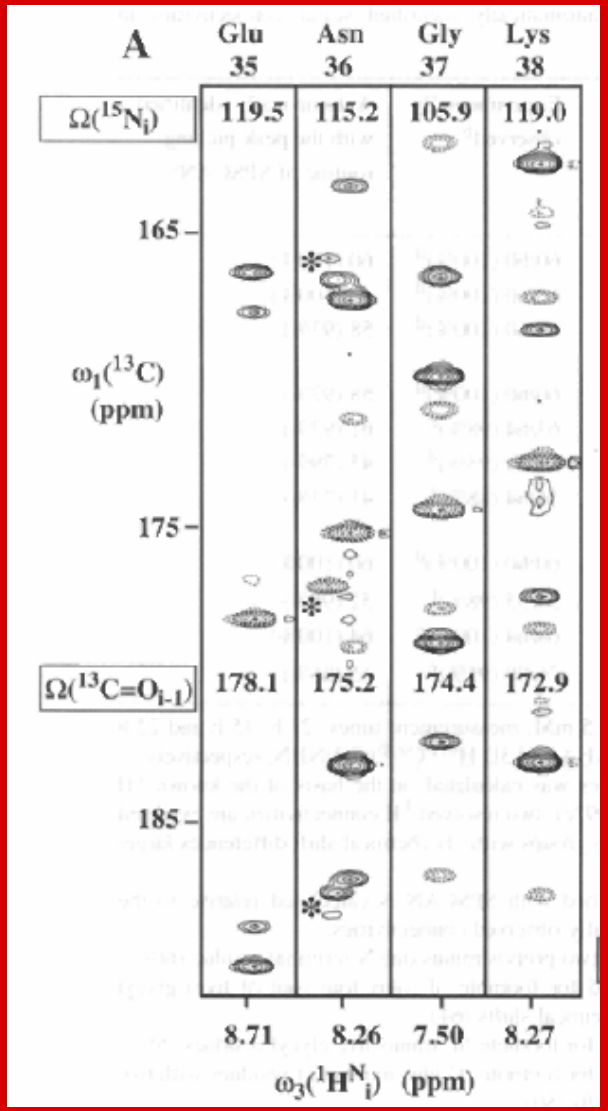

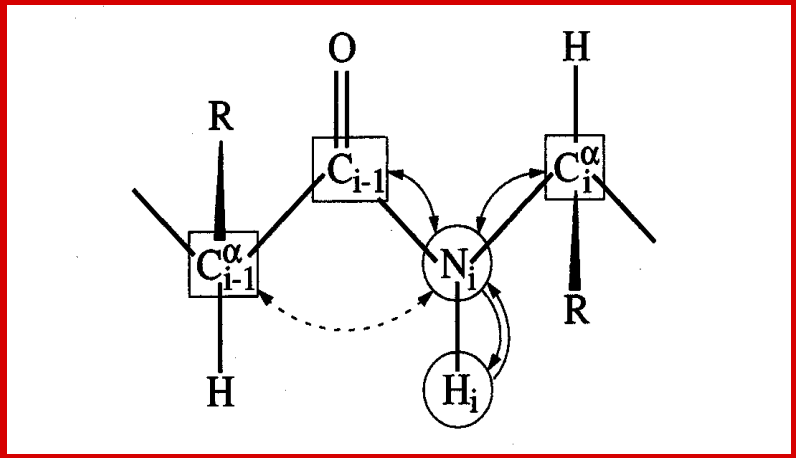

Journal of Biomolecular NMR, 11: 387–405, 1998.
KLUWER/ESCOM

Sequential resonance assignment of medium-sized $^{15}N/^{13}C$-labeled proteins with projected 4D triple resonance NMR experiments

Thomas Szyperski*, Bogdan Banecki**, Daniel Braun & Ralf W. Glaser***
Institut für Molekularbiologie und Biophysik, Eidgenössische Technische Hochschule-Hönggerberg, CH-8093 Zürich, Switzerland

Received 12 September 1997; Accepted 27 November 1997

4. 'Double RD NMR'

(Lohr and coworkers, JBNMR 1995)

A new triple-resonance experiment for the sequential assignment of backbone resonances in proteins

Frank Löhr and Heinz Rüterjans*

Institut für Biophysikalische Chemie, Johann Wolfgang Goethe Universität Frankfurt am Main, Biozentrum, Marie Curie Strasse 9, D-60439 Frankfurt am Main, Germany

Received 31 January 1995
Accepted 30 March 1995

Keywords: Triple-resonance NMR spectroscopy; Sequential assignment; Reduced dimensionality; *Desulfovibrio vulgaris* flavodoxin

3D {HACA},{CON} HN

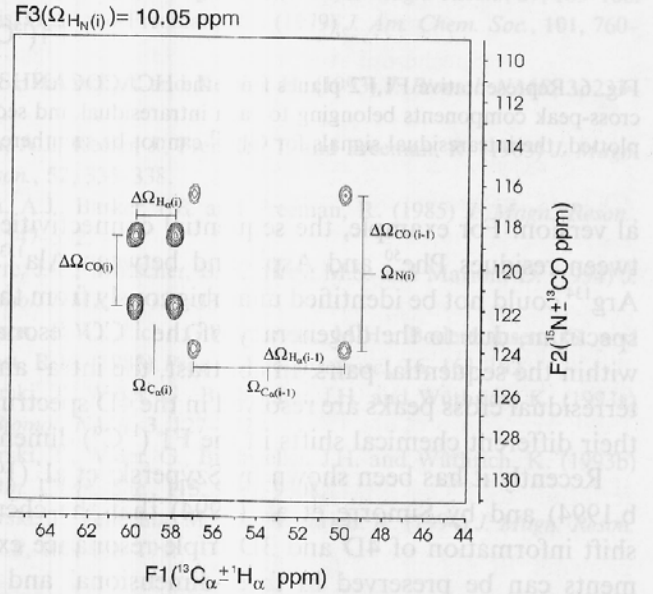

Fig. 5. Expansion of an F1,F2-slice of the HCACOCANH spectrum obtained with the pulse sequence from Fig. 1C. The intraresidual correlation for Cys^{90} (residue i) of *D. vulgaris* flavodoxin and the sequential Ala^{89}/Cys^{90} correlation are shown. The midpoints of the rectangles appear at the ^{15}N chemical shift of Cys^{90} and the $^{13}C^{\alpha}$ chemical shifts of Cys^{90} and Ala^{89}, which can be read directly from the scales at the F1 and F2 axes. $^{1}H^{\alpha}$ and ^{13}CO chemical shifts are obtained from the splittings along the two indirectly detected dimensions. The splittings (in Hz) are scaled down using the factors x = 0.625 and y = 0.2, such that 1 ppm splitting in F1 corresponds to $\Delta\Omega(H^{\alpha}) = 0.2$ ppm and 1 ppm splitting in F2 corresponds to $\Delta\Omega(CO) = 1$ ppm.

Journal of Magnetic Resonance **156,** 262–268 (2002)
doi:10.1006/jmre.2002.2537

2D HNN(CO)CAHA

Novel 2D Triple-Resonance NMR Experiments for Sequential Resonance Assignments of Proteins

Keyang Ding and Angela M. Gronenborn[1]

Laboratory of Chemical Physics, National Institute of Diabetes and Digestive and Kidney Diseases, National Institutes of Health, Bethesda, Maryland 20892

Received January 17, 2002; revised March 19, 2002; published online June 20, 2002

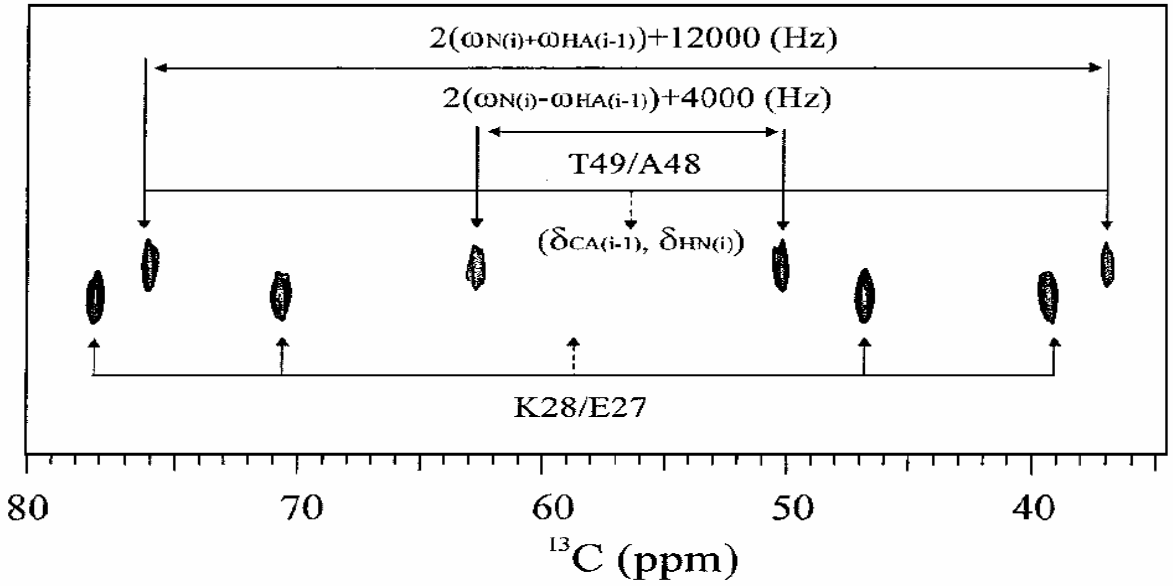

FIG. 6. Expansion of the boxed region in Fig. 5A comprising the cross peaks of K28/E27 and T49/A48 in 2D HN(CO)CAHA. The centers for the cross-peak

Generalization of RD NMR:

G-matrix Fourier Transform NMR Spectroscopy

(*JACS* 2003, *125*, 1385)

Defining features of GFT NMR

- **Repeated joint sampling** of an arbitrary number of indirect chemical shift evolution periods so that transfer amplitudes are generated which are proportional to **all possible permutations of cosine and sine modulations** of the individual shifts

- **Linear combination** of the sub-spectra resulting from such sampling which yields **edited sub-spectra** containing signals encoding **phase-sensitively detected linear combinations** of the jointly sampled shifts

4D FT NMR spectrum

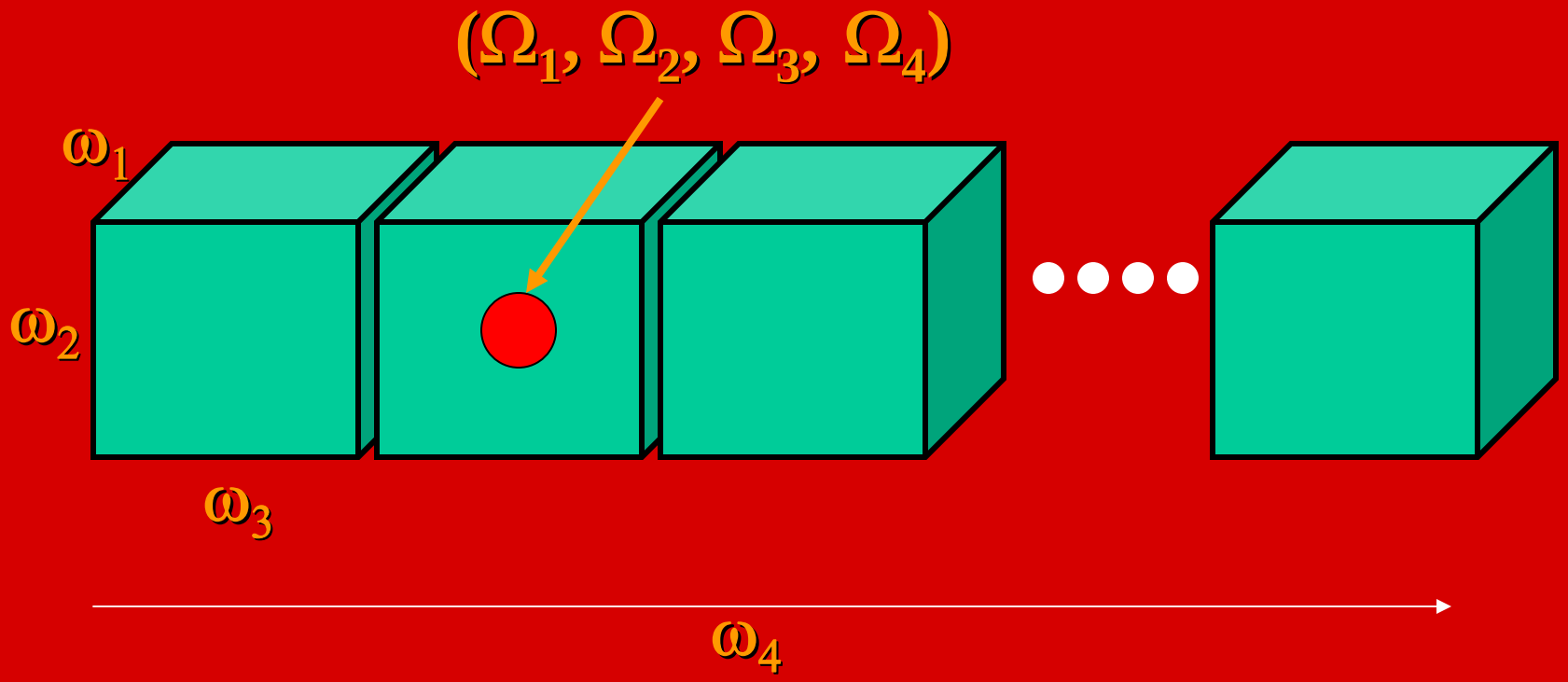

(4,2)D GFT NMR experiment

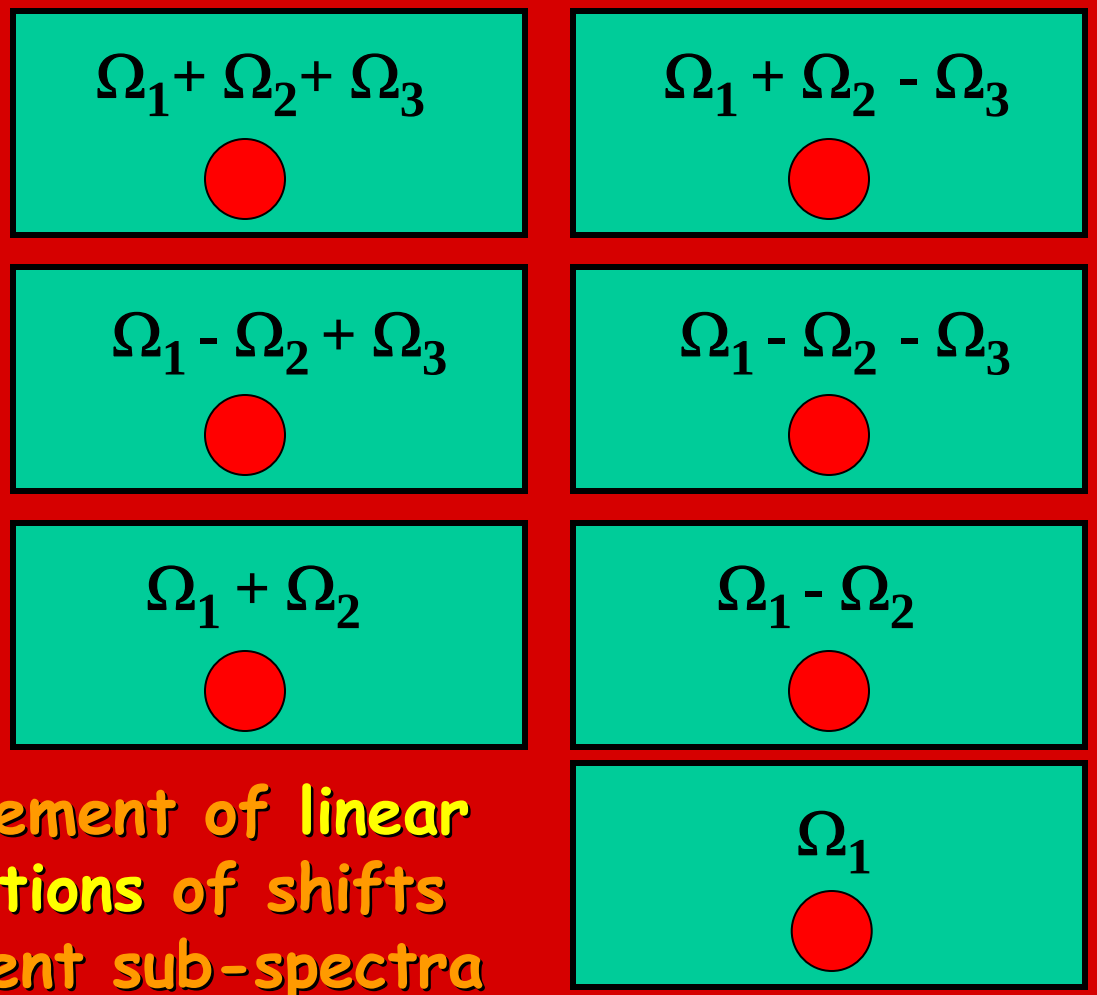

…measurement of **linear combinations** of shifts in different sub-spectra

…**precision** arises from over-determination

(4,2)D GFT NMR

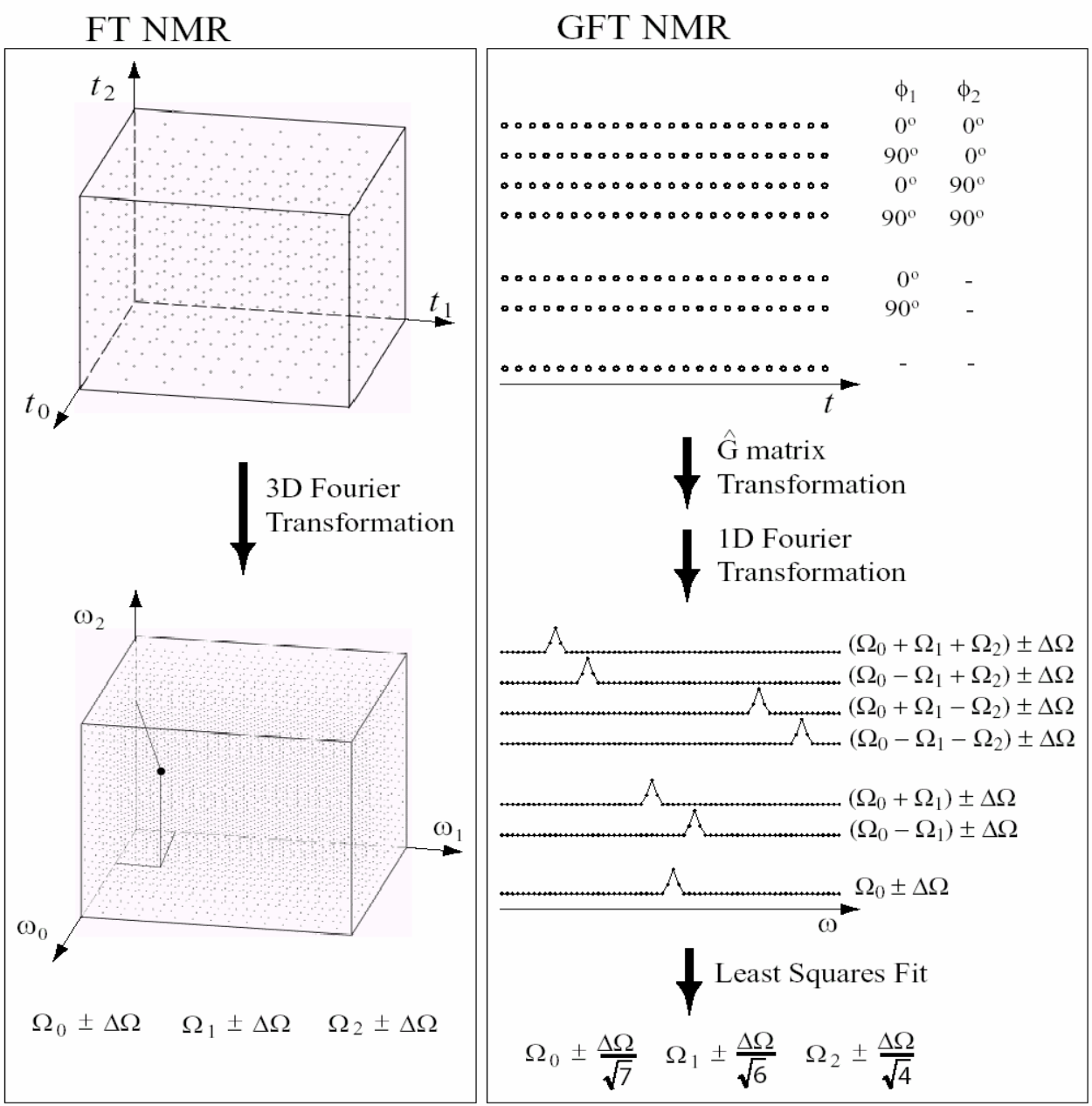
FT NMR
GFT NMR
t_2
t_1
t_0
3D Fourier Transformation
ω_2
ω_1
ω_0
$\Omega_0 \pm \Delta\Omega$ $\Omega_1 \pm \Delta\Omega$ $\Omega_2 \pm \Delta\Omega$
ϕ_1 ϕ_2
0° 0°
90° 0°
0° 90°
90° 90°
0° -
90° -
- -
t
$\hat{G}$ matrix Transformation
1D Fourier Transformation
$(\Omega_0 + \Omega_1 + \Omega_2) \pm \Delta\Omega$
$(\Omega_0 - \Omega_1 + \Omega_2) \pm \Delta\Omega$
$(\Omega_0 + \Omega_1 - \Omega_2) \pm \Delta\Omega$
$(\Omega_0 - \Omega_1 - \Omega_2) \pm \Delta\Omega$
$(\Omega_0 + \Omega_1) \pm \Delta\Omega$
$(\Omega_0 - \Omega_1) \pm \Delta\Omega$
$\Omega_0 \pm \Delta\Omega$
ω
Least Squares Fit
$\Omega_0 \pm \frac{\Delta\Omega}{\sqrt{7}}$ $\Omega_1 \pm \frac{\Delta\Omega}{\sqrt{6}}$ $\Omega_2 \pm \frac{\Delta\Omega}{\sqrt{4}}$

Joint Sampling of 3D Subspace of an ND FT NMR Experiment

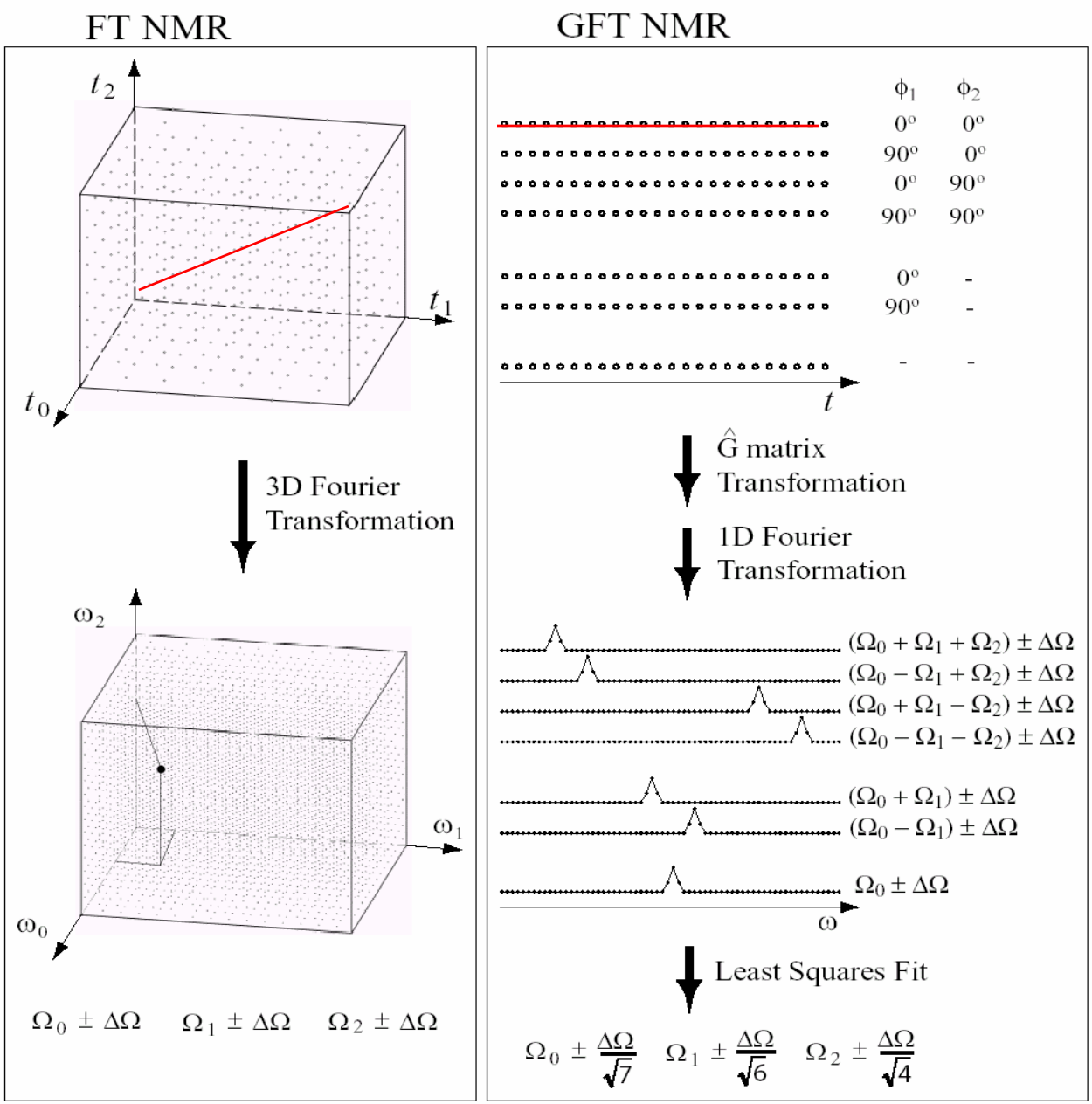

$\cos(\Omega_0 t)$	$\cos(\Omega_1 t)\ \cos(\Omega_2 t)$
$\cos(\Omega_0 t)$	$\sin(\Omega_1 t)\ \cos(\Omega_2 t)$
$\cos(\Omega_0 t)$	$\cos(\Omega_1 t)\ \sin(\Omega_2 t)$
$\cos(\Omega_0 t)$	$\sin(\Omega_1 t)\ \sin(\Omega_2 t)$

FT NMR

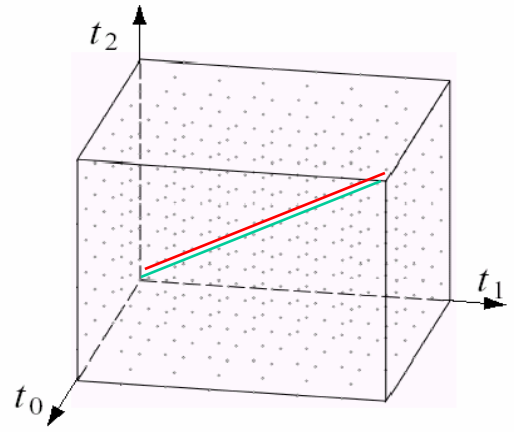

3D Fourier Transformation

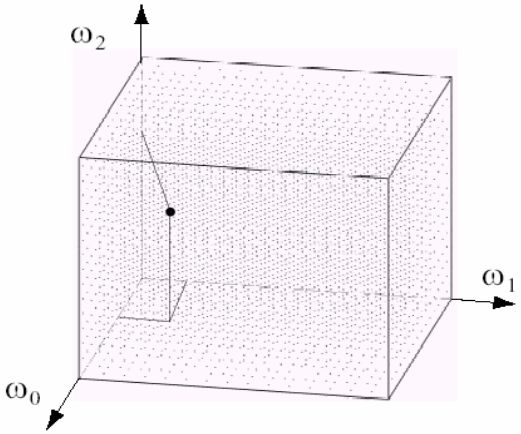

$\Omega_0 \pm \Delta\Omega$ $\Omega_1 \pm \Delta\Omega$ $\Omega_2 \pm \Delta\Omega$

GFT NMR

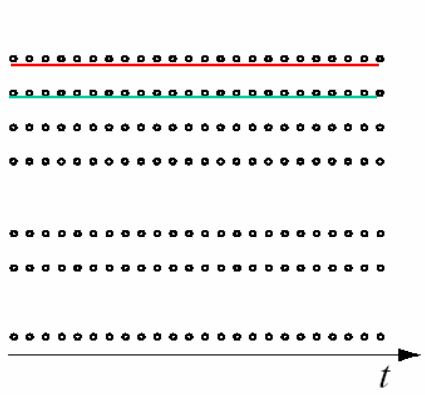

$\hat{G}$ matrix Transformation

1D Fourier Transformation

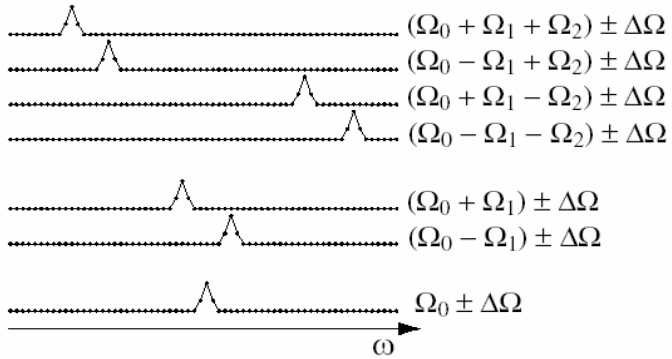

Least Squares Fit

$\Omega_0 \pm \frac{\Delta\Omega}{\sqrt{7}}$ $\Omega_1 \pm \frac{\Delta\Omega}{\sqrt{6}}$ $\Omega_2 \pm \frac{\Delta\Omega}{\sqrt{4}}$

$\cos(\Omega_0 t)$	$\cos(\Omega_1 t)$	$\cos(\Omega_2 t)$
$\cos(\Omega_0 t)$	$\sin(\Omega_1 t)$	$\cos(\Omega_2 t)$
$\cos(\Omega_0 t)$	$\cos(\Omega_1 t)$	$\sin(\Omega_2 t)$
$\cos(\Omega_0 t)$	$\sin(\Omega_1 t)$	$\sin(\Omega_2 t)$

FT NMR

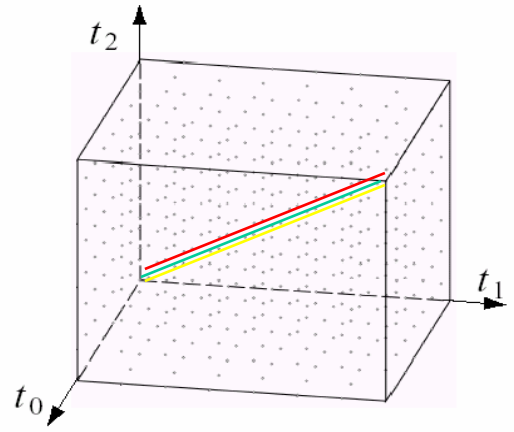

3D Fourier Transformation

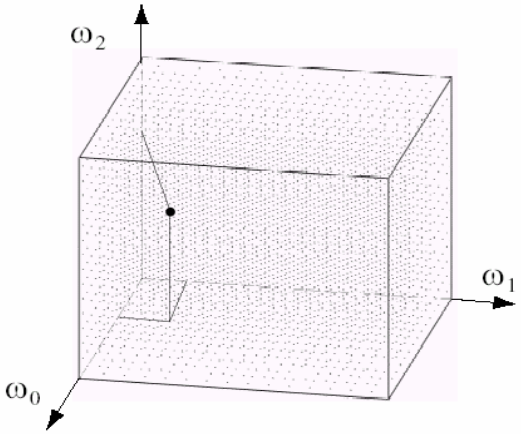

$\Omega_0 \pm \Delta\Omega$ $\Omega_1 \pm \Delta\Omega$ $\Omega_2 \pm \Delta\Omega$

GFT NMR

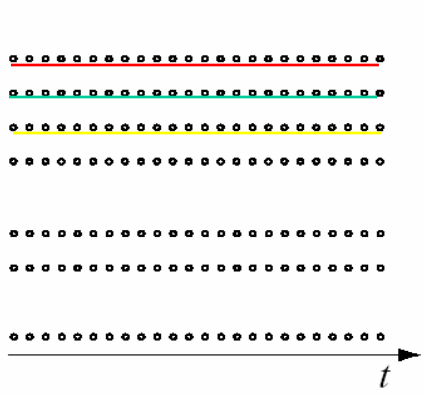

$\hat{G}$ matrix Transformation

1D Fourier Transformation

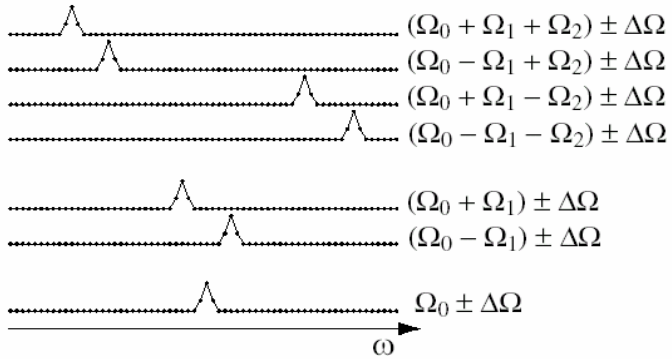

Least Squares Fit

$\Omega_0 \pm \frac{\Delta\Omega}{\sqrt{7}}$ $\Omega_1 \pm \frac{\Delta\Omega}{\sqrt{6}}$ $\Omega_2 \pm \frac{\Delta\Omega}{\sqrt{4}}$

$\cos(\Omega_0 t)$	$\cos(\Omega_1 t)$	$\cos(\Omega_2 t)$
$\cos(\Omega_0 t)$	$\sin(\Omega_1 t)$	$\cos(\Omega_2 t)$
$\cos(\Omega_0 t)$	$\cos(\Omega_1 t)$	$\sin(\Omega_2 t)$
$\cos(\Omega_0 t)$	$\sin(\Omega_1 t)$	$\sin(\Omega_2 t)$

FT NMR

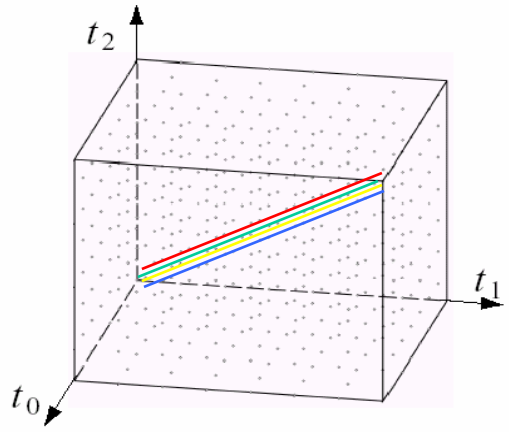

3D Fourier Transformation

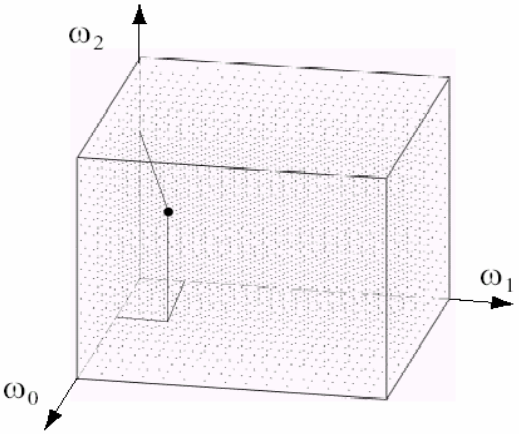

$\Omega_0 \pm \Delta\Omega$ $\Omega_1 \pm \Delta\Omega$ $\Omega_2 \pm \Delta\Omega$

GFT NMR

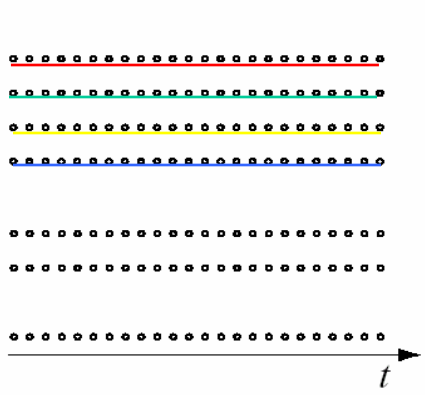

$\hat{G}$ matrix Transformation

1D Fourier Transformation

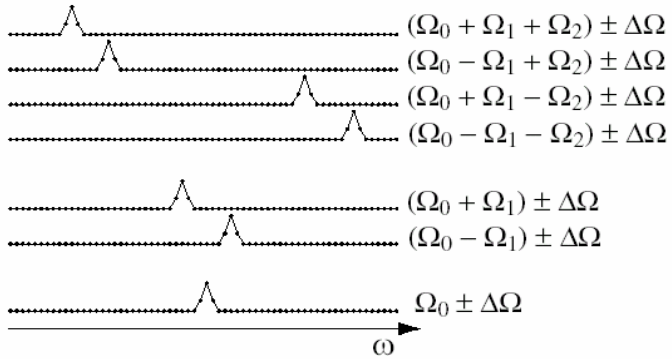

Least Squares Fit

$\Omega_0 \pm \frac{\Delta\Omega}{\sqrt{7}}$ $\Omega_1 \pm \frac{\Delta\Omega}{\sqrt{6}}$ $\Omega_2 \pm \frac{\Delta\Omega}{\sqrt{4}}$

$\cos(\Omega_0 t)$	$\cos(\Omega_1 t)$	$\cos(\Omega_2 t)$
$\cos(\Omega_0 t)$	$\sin(\Omega_1 t)$	$\cos(\Omega_2 t)$
$\cos(\Omega_0 t)$	$\cos(\Omega_1 t)$	$\sin(\Omega_2 t)$
$\cos(\Omega_0 t)$	$\sin(\Omega_1 t)$	$\sin(\Omega_2 t)$

FT NMR

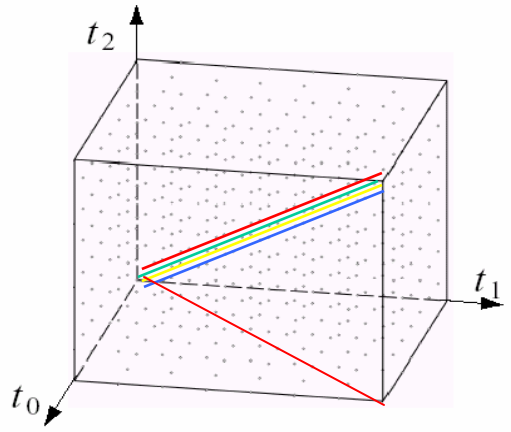

3D Fourier Transformation

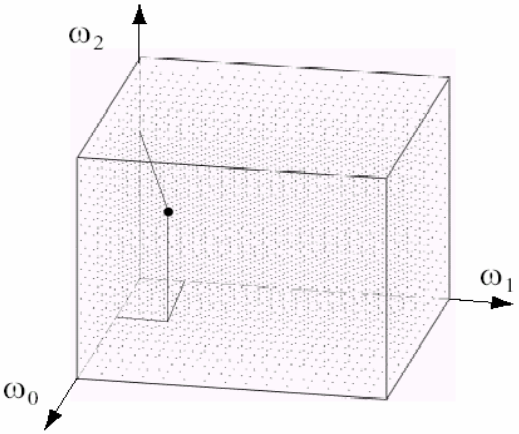

$\Omega_0 \pm \Delta\Omega$ $\Omega_1 \pm \Delta\Omega$ $\Omega_2 \pm \Delta\Omega$

GFT NMR

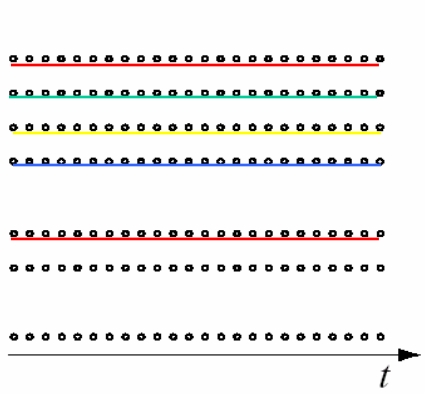

$\hat{G}$ matrix Transformation

1D Fourier Transformation

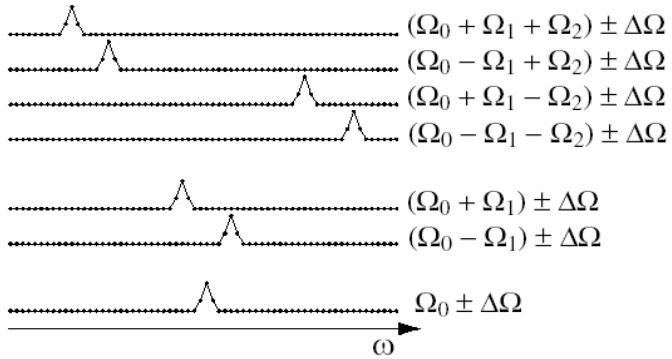

Least Squares Fit

$\Omega_0 \pm \frac{\Delta\Omega}{\sqrt{7}}$ $\Omega_1 \pm \frac{\Delta\Omega}{\sqrt{6}}$ $\Omega_2 \pm \frac{\Delta\Omega}{\sqrt{4}}$

$\cos(\Omega_0 t)\cos(\Omega_1 t)$

$\cos(\Omega_0 t)\sin(\Omega_1 t)$

FT NMR

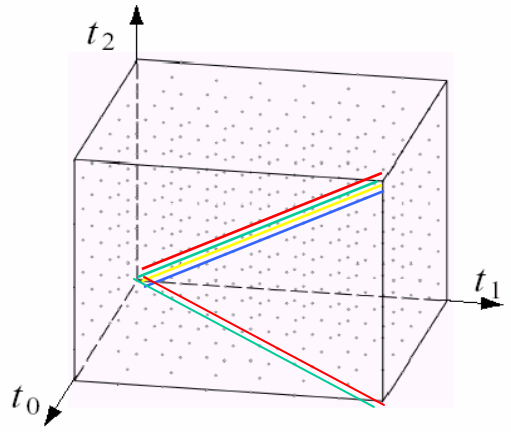

3D Fourier Transformation

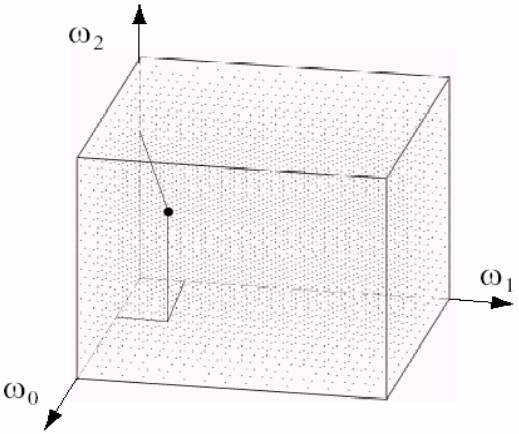

$\Omega_0 \pm \Delta\Omega$ $\Omega_1 \pm \Delta\Omega$ $\Omega_2 \pm \Delta\Omega$

GFT NMR

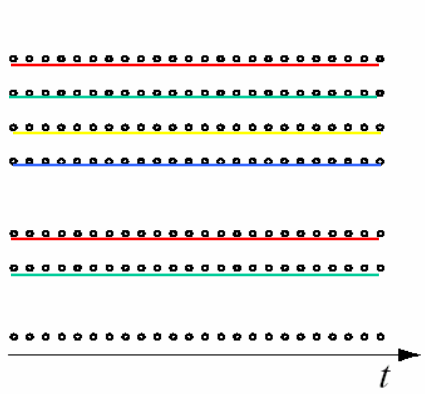

$\hat{G}$ matrix Transformation

1D Fourier Transformation

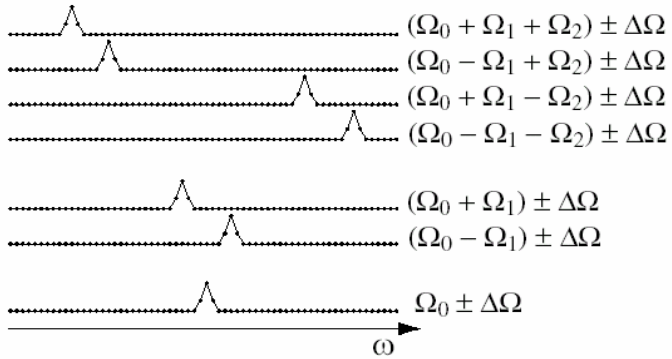

Least Squares Fit

$\Omega_0 \pm \frac{\Delta\Omega}{\sqrt{7}}$ $\Omega_1 \pm \frac{\Delta\Omega}{\sqrt{6}}$ $\Omega_2 \pm \frac{\Delta\Omega}{\sqrt{4}}$

$\cos(\Omega_0 t)\cos(\Omega_1 t)$

$\cos(\Omega_0 t)\sin(\Omega_1 t)$

FT NMR

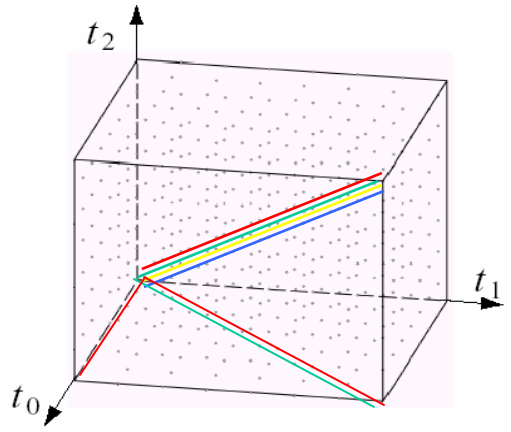

3D Fourier Transformation

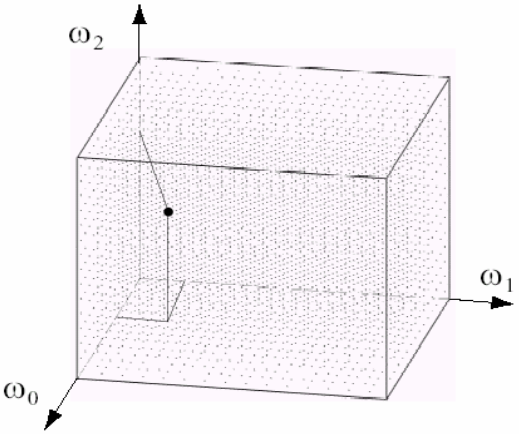

$\Omega_0 \pm \Delta\Omega$ $\Omega_1 \pm \Delta\Omega$ $\Omega_2 \pm \Delta\Omega$

GFT NMR

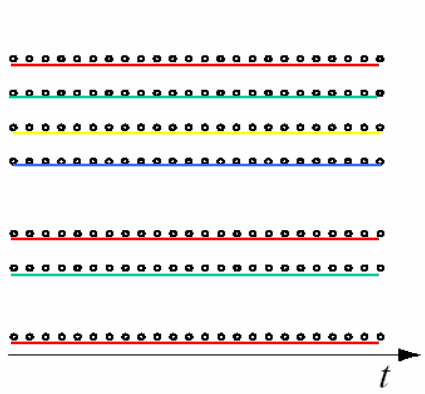

$\hat{G}$ matrix Transformation

1D Fourier Transformation

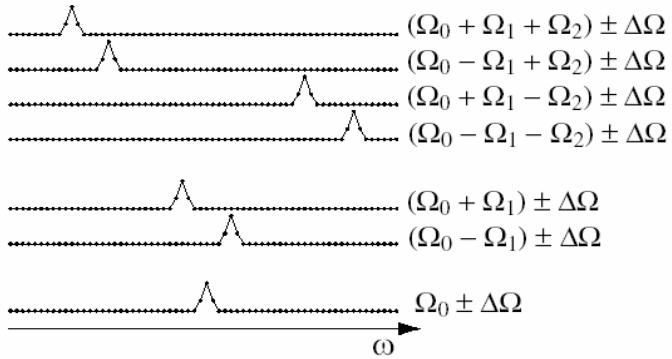

Least Squares Fit

$\Omega_0 \pm \frac{\Delta\Omega}{\sqrt{7}}$ $\Omega_1 \pm \frac{\Delta\Omega}{\sqrt{6}}$ $\Omega_2 \pm \frac{\Delta\Omega}{\sqrt{4}}$

$\cos(\Omega_0 t)$

FT NMR

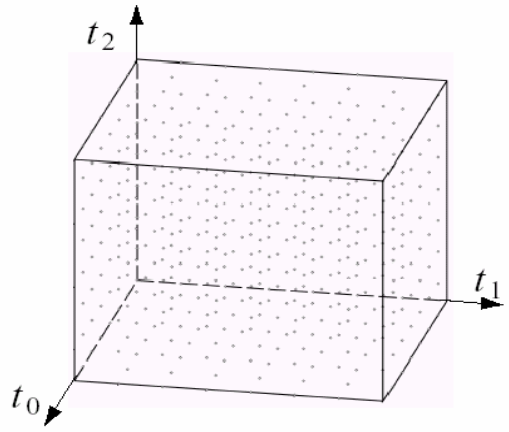

3D Fourier Transformation

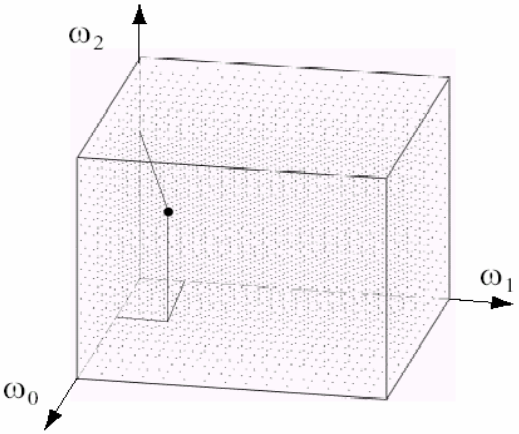

$\Omega_0 \pm \Delta\Omega$ $\Omega_1 \pm \Delta\Omega$ $\Omega_2 \pm \Delta\Omega$

GFT NMR

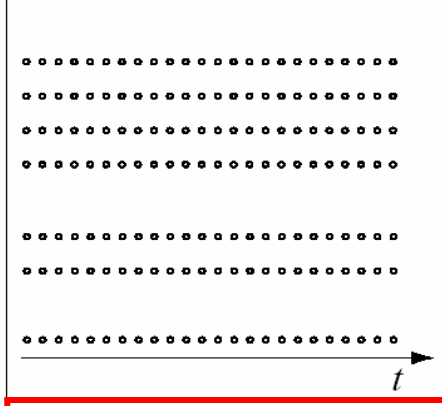

$\hat{G}$ matrix Transformation

1D Fourier Transformation

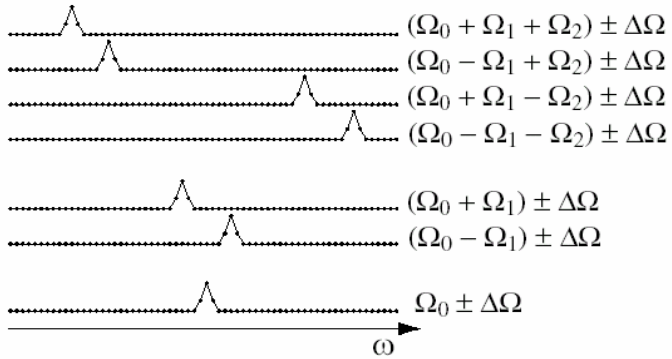

Least Squares Fit

$\Omega_0 \pm \frac{\Delta\Omega}{\sqrt{7}}$ $\Omega_1 \pm \frac{\Delta\Omega}{\sqrt{6}}$ $\Omega_2 \pm \frac{\Delta\Omega}{\sqrt{4}}$

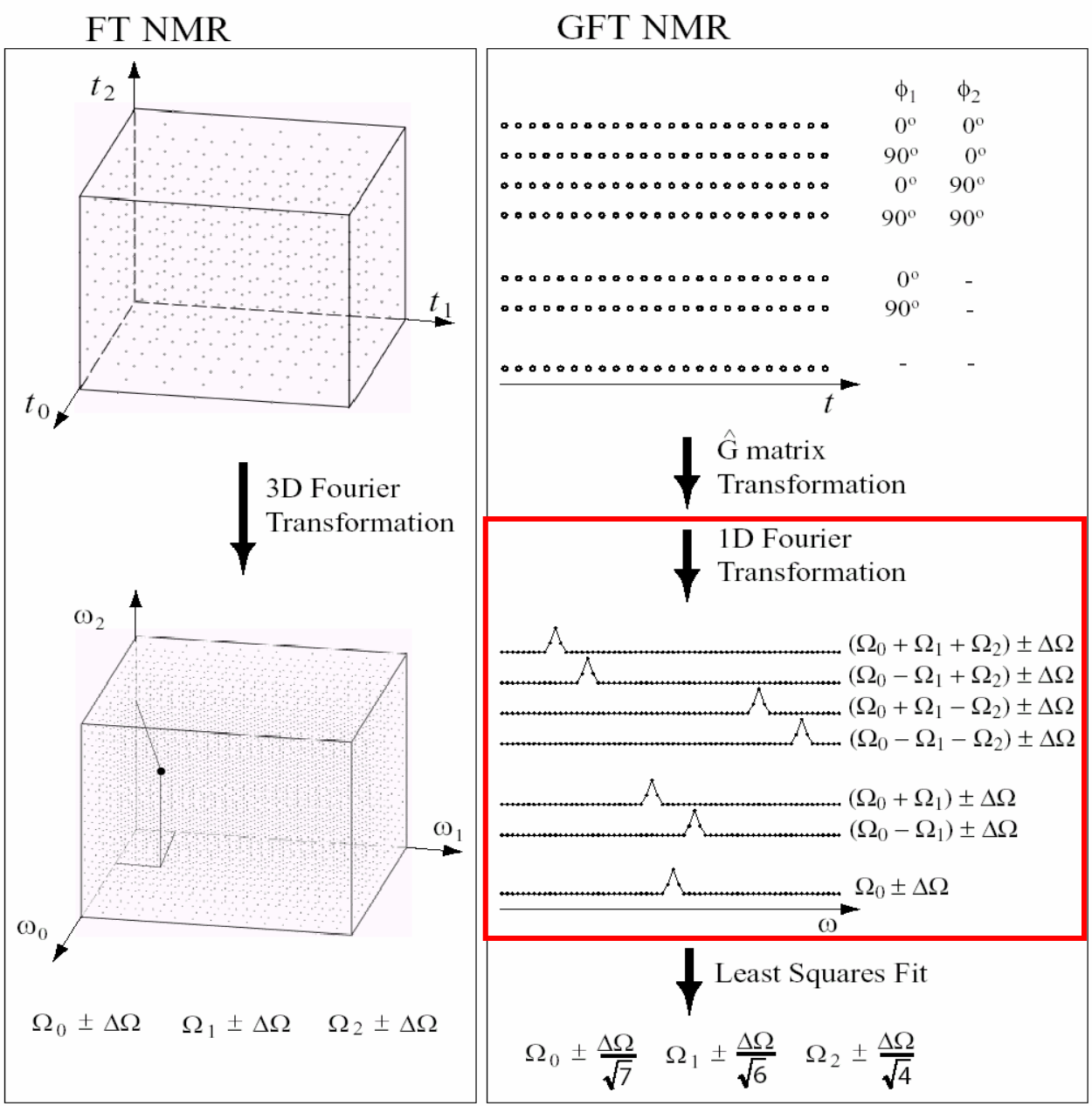

Complete sampling of linear combinations of chemical shifts

FT NMR

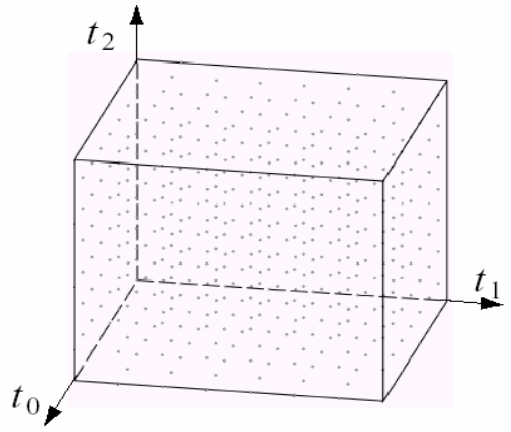

3D Fourier Transformation

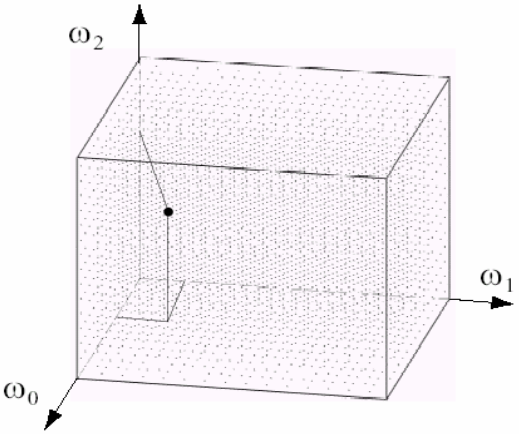

$\Omega_0 \pm \Delta\Omega$ $\Omega_1 \pm \Delta\Omega$ $\Omega_2 \pm \Delta\Omega$

GFT NMR

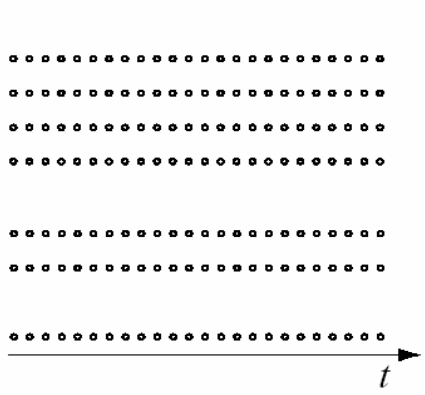

$\hat{G}$ matrix Transformation

1D Fourier Transformation

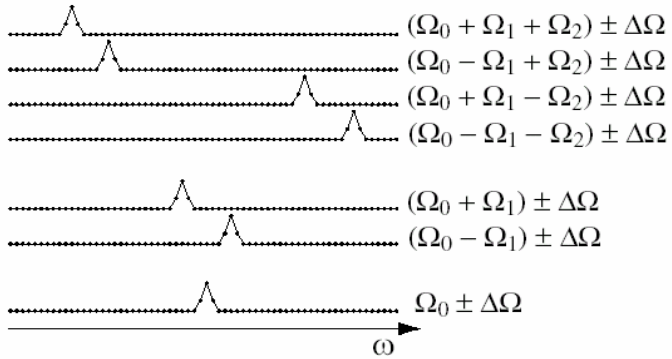

Least Squares Fit

$\Omega_0 \pm \frac{\Delta\Omega}{\sqrt{7}}$ $\Omega_1 \pm \frac{\Delta\Omega}{\sqrt{6}}$ $\Omega_2 \pm \frac{\Delta\Omega}{\sqrt{4}}$

The G-matrix:

Phase-sensitive detection of linear of combinations of chemical shifts combined with (time domain) editing into different sub-spectra

(4,2)D GFT NMR

$S_{1r} \propto \cos(\kappa_0 \Omega_0 t)*\cos(\kappa_1 \Omega_1 t)*\cos(\kappa_2 \Omega_2 t)$

$S_{1i} \propto \sin(\kappa_0 \Omega_0 t)*\cos(\kappa_1 \Omega_1 t)*\cos(\kappa_2 \Omega_2 t)$

$S_{2r} \propto \cos(\kappa_0 \Omega_0 t)*\sin(\kappa_1 \Omega_1 t)*\cos(\kappa_2 \Omega_2 t)$

$S_{2i} \propto \sin(\kappa_0 \Omega_0 t)*\sin(\kappa_1 \Omega_1 t)*\cos(\kappa_2 \Omega_2 t)$

$S_{3r} \propto \cos(\kappa_0 \Omega_0 t)*\cos(\kappa_1 \Omega_1 t)*\sin(\kappa_2 \Omega_2 t)$

$S_{3i} \propto \sin(\kappa_0 \Omega_0 t)*\cos(\kappa_1 \Omega_1 t)*\sin(\kappa_2 \Omega_2 t)$

$S_{4r} \propto \cos(\kappa_0 \Omega_0 t)*\sin(\kappa_1 \Omega_1 t)*\sin(\kappa_2 \Omega_2 t)$

$S_{4i} \propto \sin(\kappa_0 \Omega_0 t)*\sin(\kappa_1 \Omega_1 t)*\sin(\kappa_2 \Omega_2 t)$,

so that the vector $\mathbf{T}(2)=\mathbf{G}(2)\bullet\mathbf{S}(2)$ is given in complex notation by:

$$\mathbf{T}(2) = \begin{bmatrix} e^{i(\kappa_0*\Omega_0+\kappa_1*\Omega_1+\kappa_2*\Omega_2)t} \\ e^{i(\kappa_0*\Omega_0-\kappa_1*\Omega_1+\kappa_2*\Omega_2)t} \\ e^{i(\kappa_0*\Omega_0+\kappa_1*\Omega_1-\kappa_2*\Omega_2)t} \\ e^{i(\kappa_0*\Omega_0-\kappa_1*\Omega_1-\kappa_2*\Omega_2)t} \end{bmatrix} = \begin{bmatrix} 1 & i & i & -1 & i & -1 & -1 & -i \\ 1 & i & -i & 1 & i & -1 & 1 & i \\ 1 & i & i & -1 & -i & 1 & 1 & i \\ 1 & i & -i & 1 & -i & 1 & -1 & -i \end{bmatrix} \bullet \begin{bmatrix} s_{1r} \\ s_{1i} \\ s_{2r} \\ s_{2i} \\ s_{3r} \\ s_{3i} \\ s_{4r} \\ s_{4i} \end{bmatrix} \qquad (4).$$

Hence, the four linear combinations of chemical shifts, $\kappa_0*\Omega_0\pm\kappa_1*\Omega_1\pm\kappa_2*\Omega_2$, are measured in one of the four sub-spectra each.

Reduction of minimal measurement time

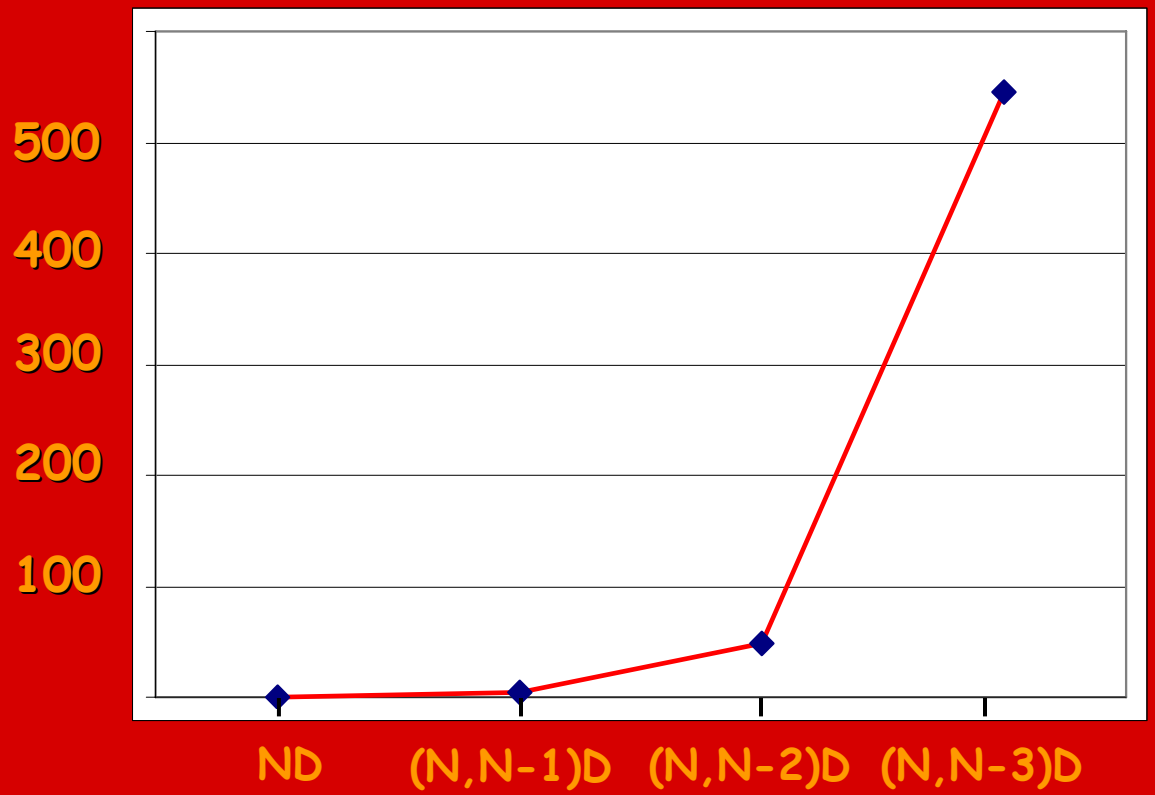

$$\frac{\prod_{1}^{K} n_i}{\sum_{1}^{K} n_i} * \frac{2^K}{2^{K+1}-1}$$

(5,2)D HACACONHN

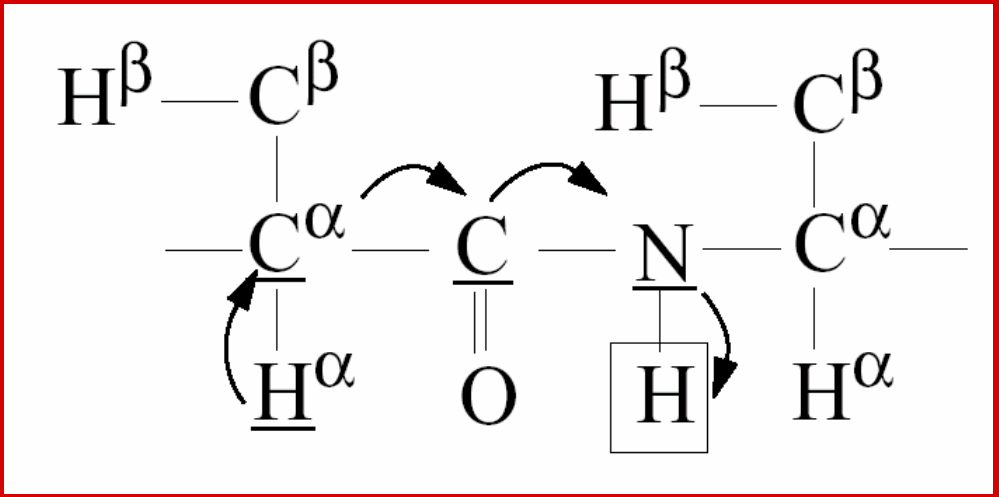

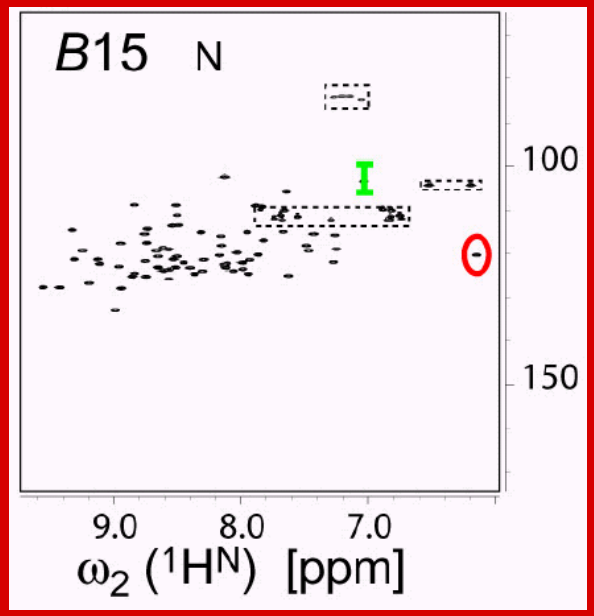

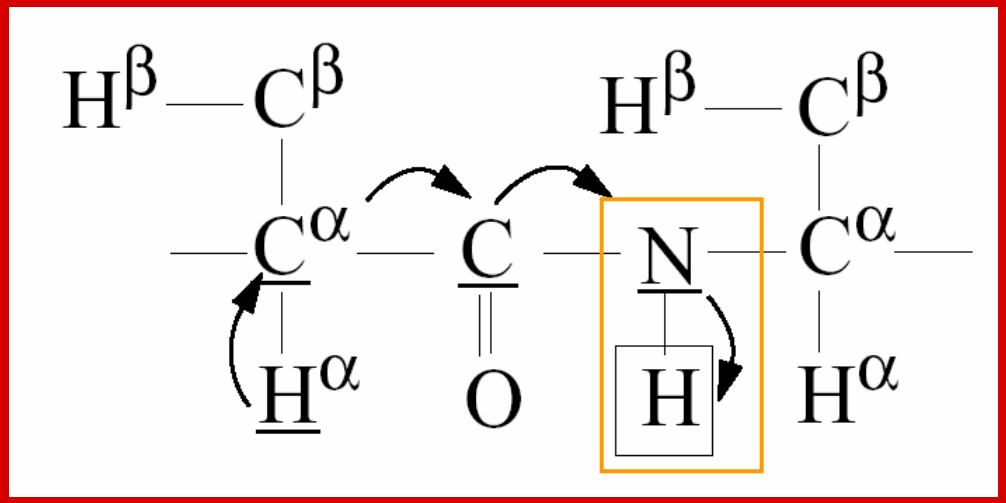

2D Information
13.8 min

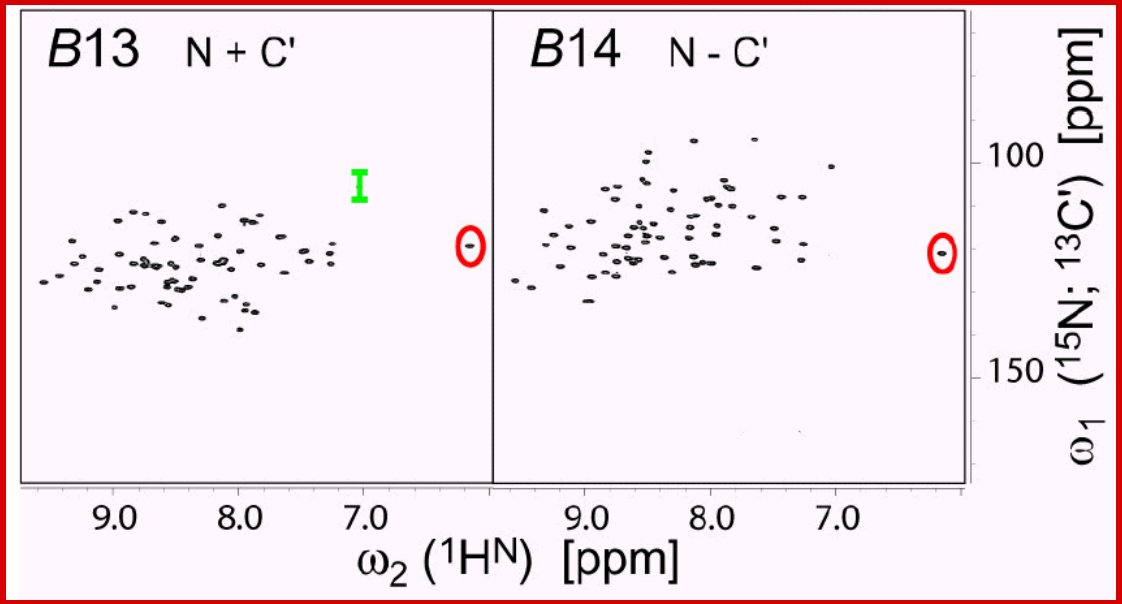

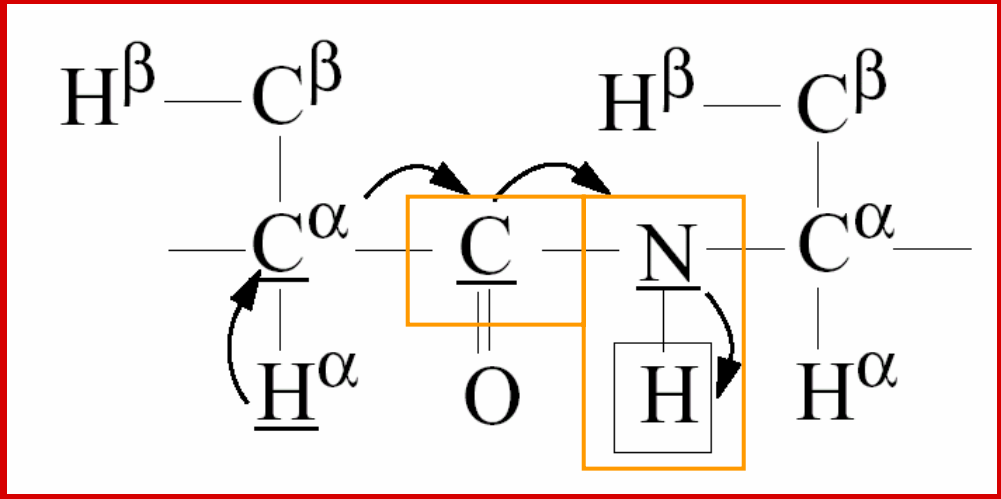

3D Information
+25.2 min

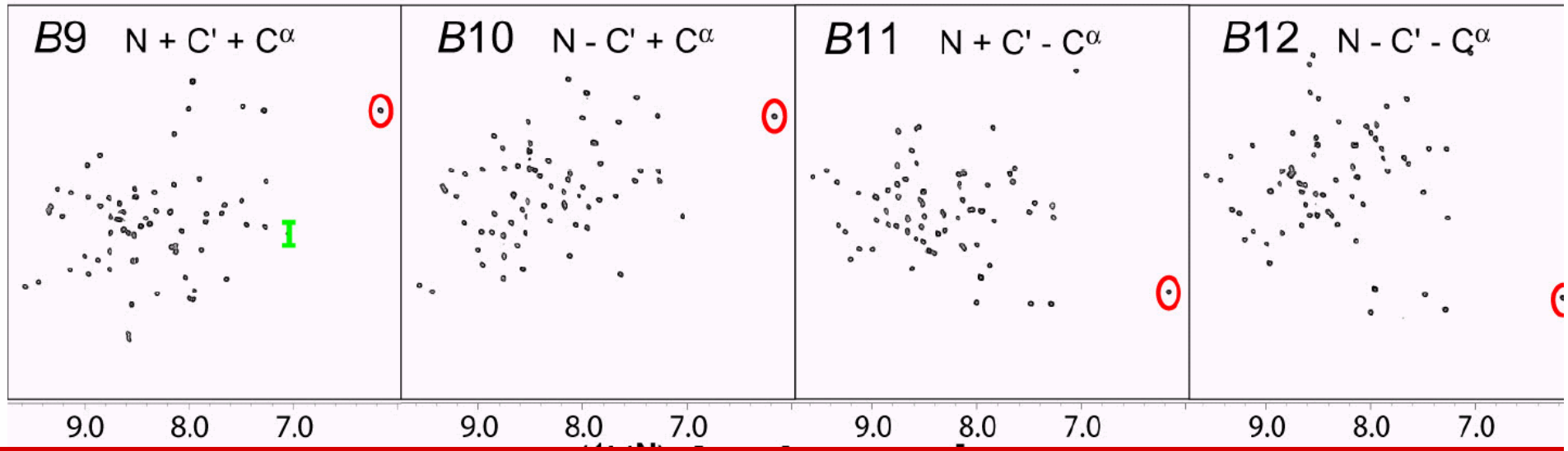

4D Information +52.8 min

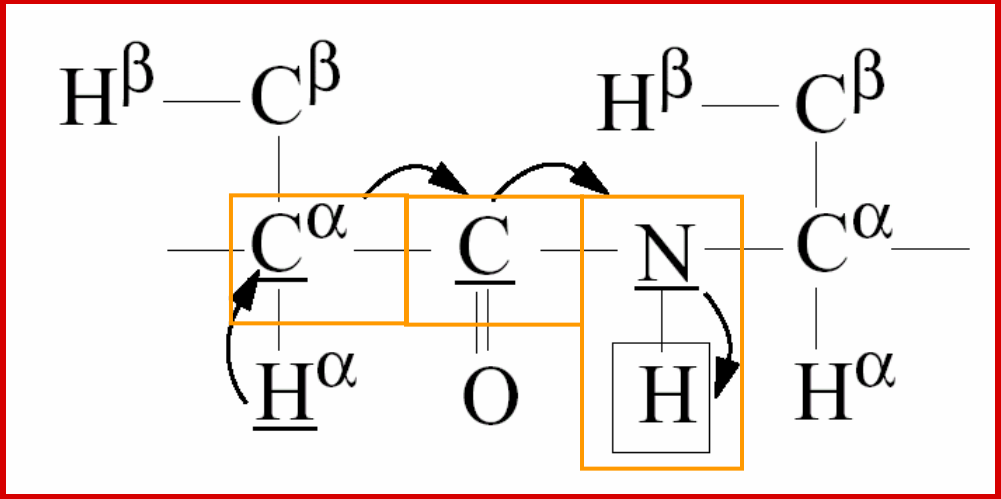

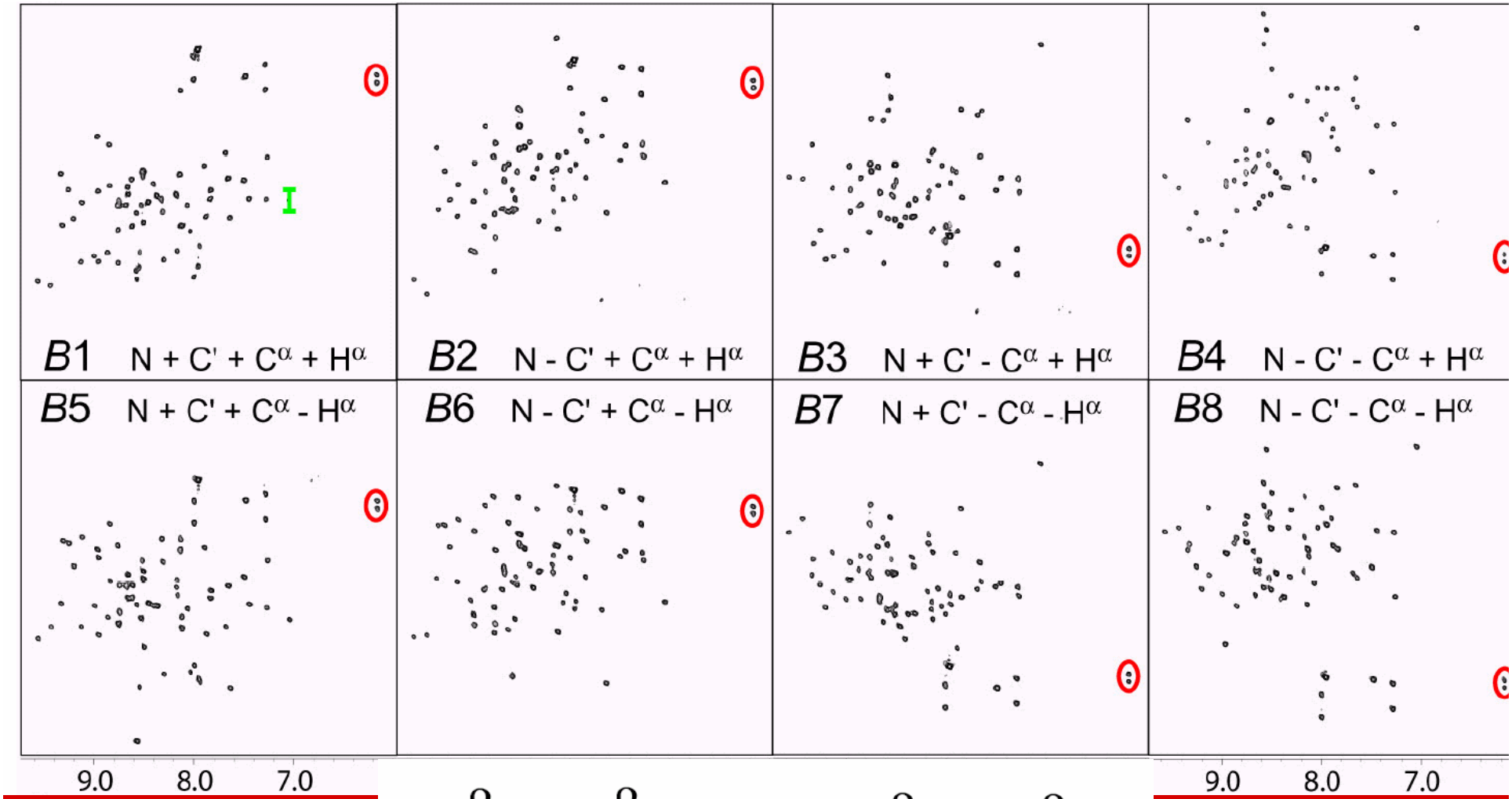

5D Information
+108 min

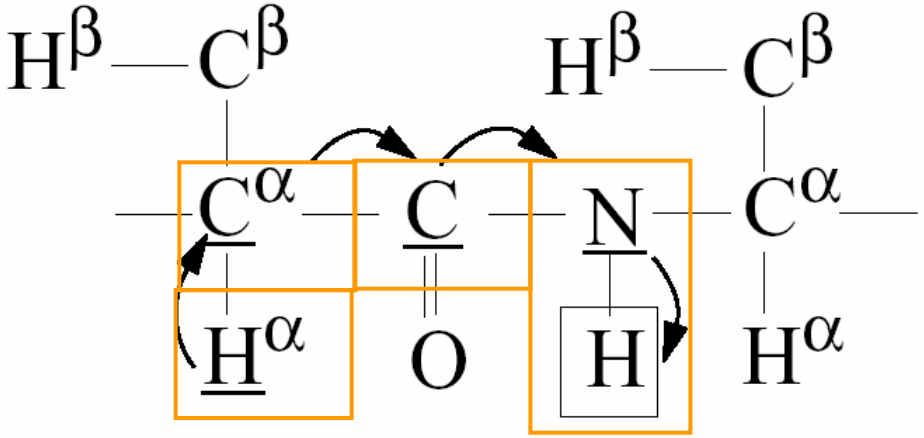

Features of GFT NMR

- Generally applicable acquisition scheme
- Accurate adaptation of measurement times to sensitivity requirement *without* sacrificing digital resolution or high dimensional correlation
- 5D or 6D feasible
- No additional hardware required
- Data size reduction
- Accelerated processing speed
- Robustness of data analysis

Time *versus* frequency domain editing

- Linear prediction ->
  time domain editing preferred

- Maximum entropy reconstruction,
  Filter-diagonalization etc.

GFT NMR –

methodological extensions…..

J|A|C|S
COMMUNICATIONS

Published on Web 03/12/2005

Resonance Assignment of Proteins with High Shift Degeneracy Based on 5D Spectral Information Encoded in G²FT NMR Experiments

Hanudatta S. Atreya, Alexander Eletsky, and Thomas Szyperski*

Department of Chemistry, State University of New York at Buffalo, Buffalo, New York 14260

Received December 10, 2004; E-mail: szypersk@chem.buffalo.edu

G²FT NMR

A contribution to establish NMR-based structural genomics of membrane proteins

NMRFam Workshop 06/06/06

G^2FT (5,3)D HN{N,CO}{$C^{\alpha\beta}C^{\alpha}$}

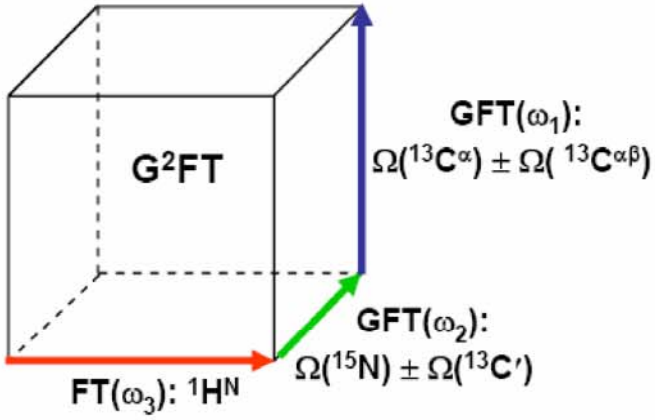

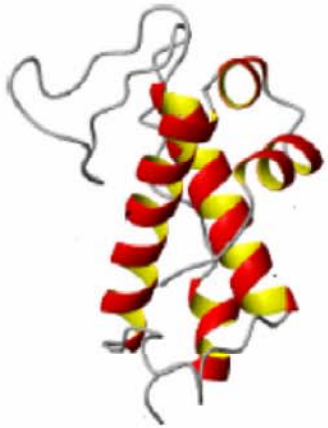

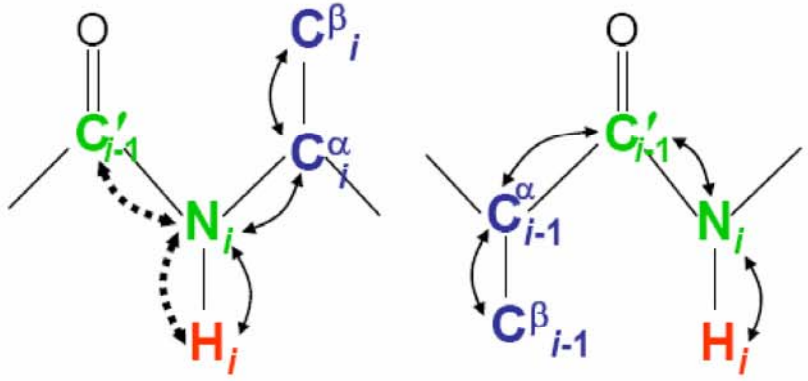

Longitudinal and transverse relaxation optimized GFT NMR: L-GFT-TROSY

Pervushin, K.; Vogeli, B.; Eletsky, A. *J. Am. Chem. Soc.* **2002**, *124*, 12898−12902.

9642–9647 | PNAS | June 29, 2004 | vol. 101 | no. 26

G-matrix Fourier transform NMR spectroscopy for complete protein resonance assignment

Hanudatta S. Atreya and Thomas Szyperski*

Departments of Chemistry and Structural Biology, State University of New York, Northeast Structural Genomics Consortium, Buffalo, NY 14260

Communicated by Herbert Hauptman, Hauptman–Woodward Medical Research Institute, Buffalo, NY, May 18, 2004 (received for review December 14, 2003)

A G-matrix Fourier transform (GFT) NMR spectroscopy-based strategy for resonance assignment of proteins is described. Each of the GFT NMR experiments presented here rapidly affords four-, five-, or six-dimensional spectral information in combination with precise measurements of chemical shifts. The resulting high information content enables one to obtain nearly complete assignments by using only four NMR experiments. For the backbone amide proton detected "out-and-back" experiments, data collection was further accelerated up to ≈2.5-fold by use of longitudinal ^{1}H relaxation optimization. The GFT NMR experiments were acquired for three proteins with molecular masses ranging from 8.6 to 17 kDa, demonstrating that the proposed strategy is of key interest for automated resonance assignment in structural genomics.

Nearly complete resonance assignments are generally considered a necessity for NMR-based protein structure determination (e.g., refs. 11 and 12). Here we describe a strategy for complete protein resonance assignment based on GFT NMR experiments affording accurate 4D, 5D, and 6D spectral information. Applications are presented for proteins with molecular masses ranging from 8.6 to 17 kDa.

Materials and Methods

NMR Spectrometer and Protein Samples. All measurements were performed at 25°C on Varian INOVA 600 and 750 MHz spectrometers, equipped with conventional $^{1}H/^{13}C/^{15}N$ triple-resonance probes, by using ≈1 mM solutions in 95% H_2O/5%

L-(4,3)D HNN(CO)$\underline{C}^{\alpha\beta}\underline{C}^{\alpha}$

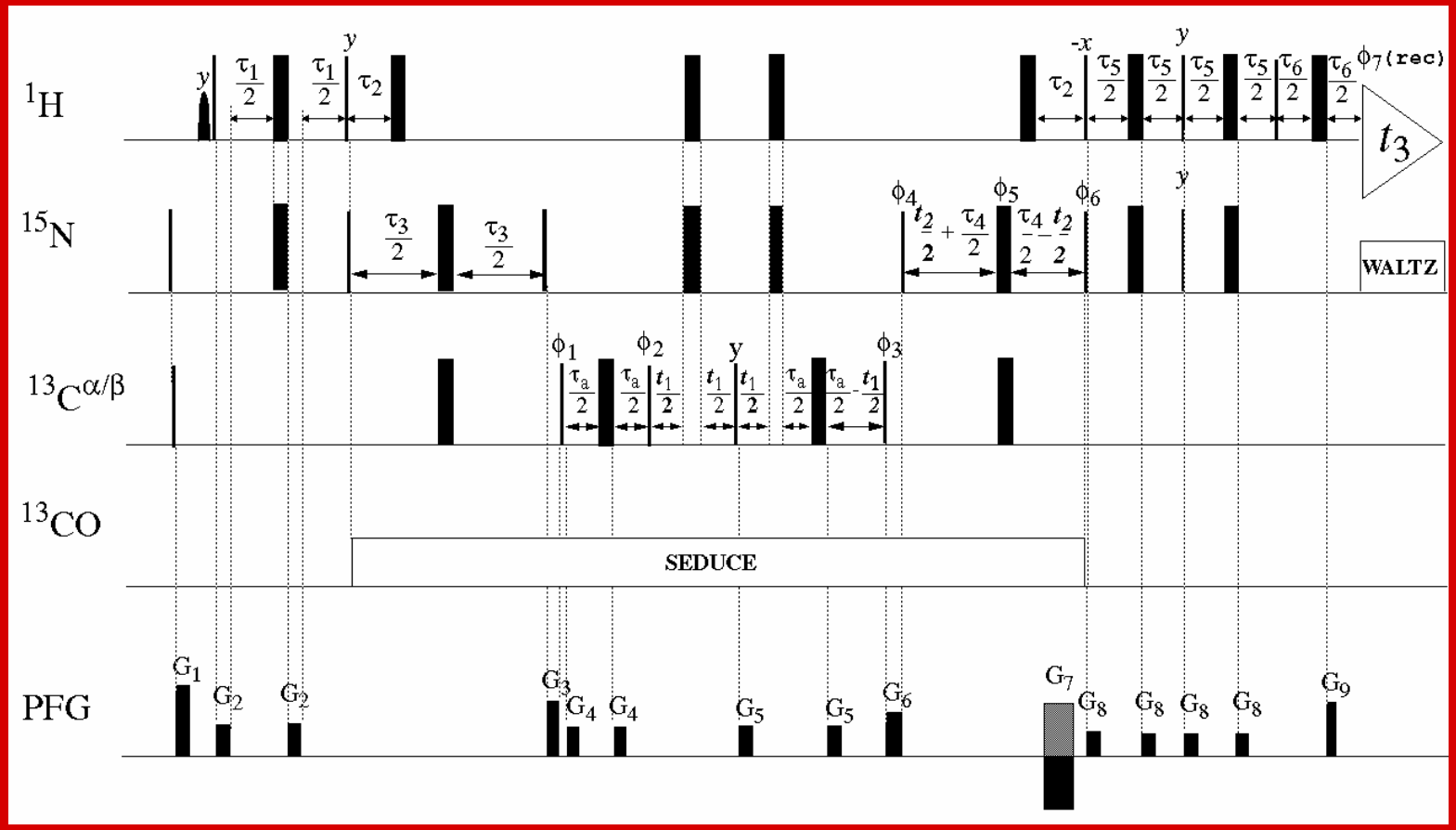

Water and aliphatic ^{1}H magnetization along +z at the start of signal detection

NMRFam Workshop 06/06/06

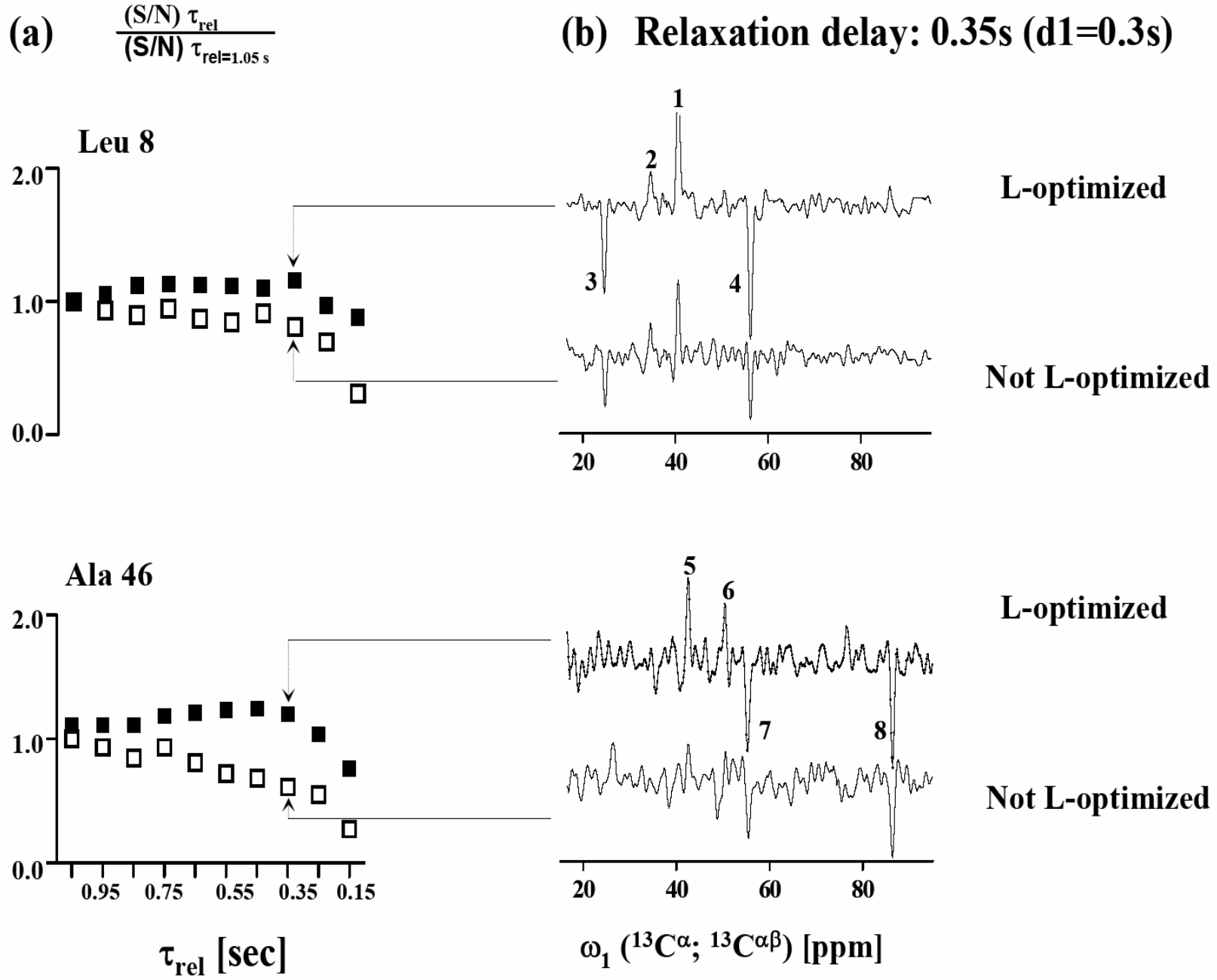
(a)
(S/N) τrel / (S/N) τrel=1.05 s
Leu 8
2.0
1.0
0.0
Ala 46
2.0
1.0
0.0
0.95
0.75
0.55
0.35
0.15
τrel [sec]
(b) Relaxation delay: 0.35s (d1=0.3s)
1
2
3
4
5
6
7
8
20
40
60
80
ω1 (13Cα; 13Cαβ) [ppm]
L-optimized
Not L-optimized
L-optimized
Not L-optimized

….GFT NMR for the aromatic rings …

L-optimization of aromatic protons

(nearly) complete resonance assignment of aromatic protons is required for:

-> high-quality structure determination

-> using aromatic rings to probe protein dynamics

L-GFT-TROSY (4,3)D HCCH

Longitudinal (L-) Relaxation Optimization
for Aromatic Protons:
Water and aliphatic ^{1}H magnetization along +z
at the start of signal detection

Evaluation in 2D NMR

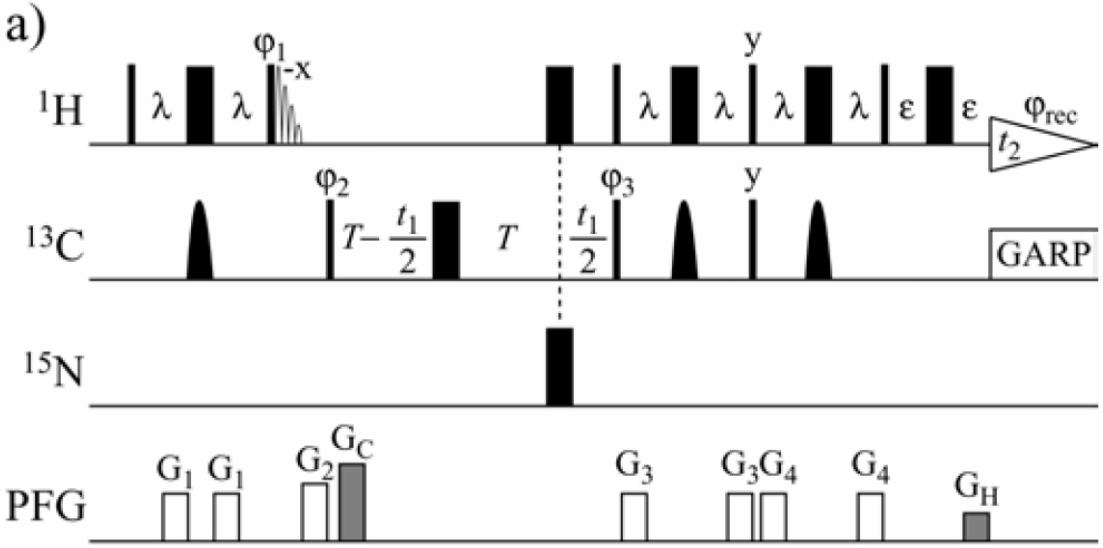

HSQC

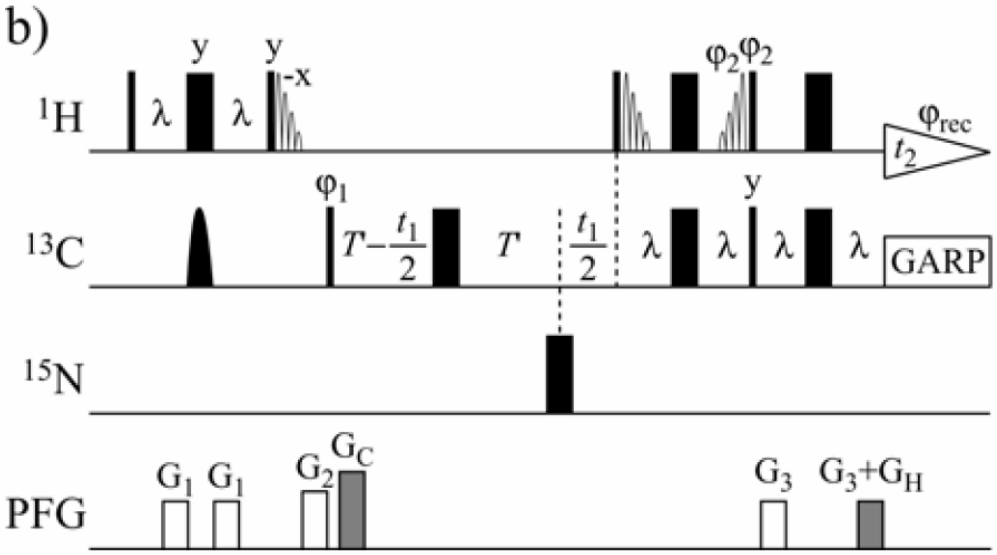

TROSY

L-optimization for ^{13}C-$^{1}H^{aromatic}$

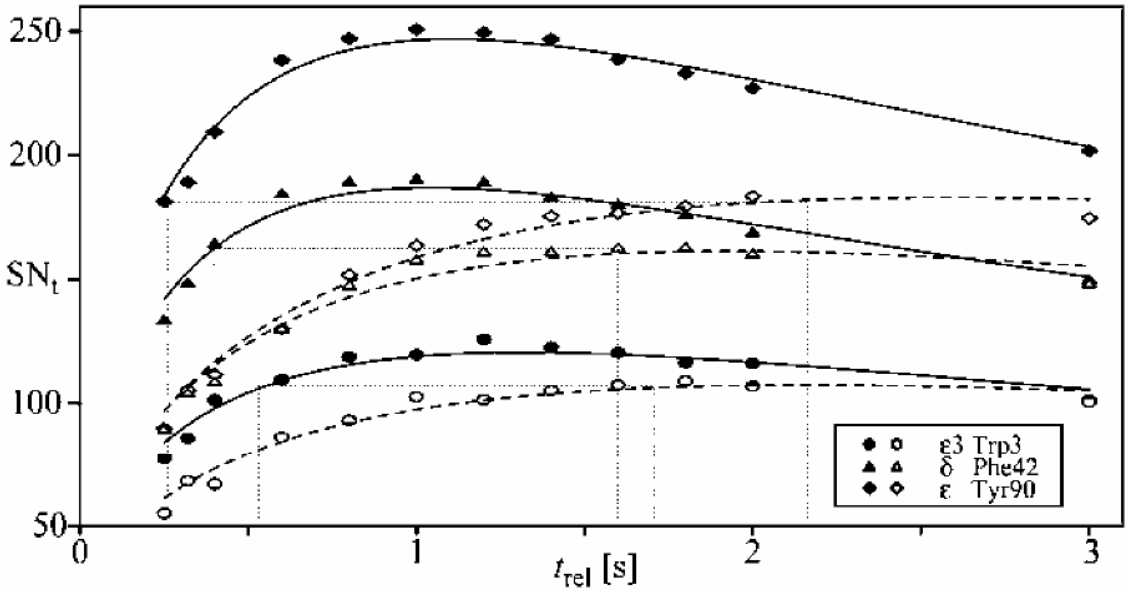

Figure 1. SN_t in *ct* 2D [^{13}C,^{1}H]-HSQC versus t_{rel} for three peaks of protein PfR13 (20 °C; 750 MHz). Filled (open) symbols and solid (dashed) lines correspond to spectra acquired *with* (*without*) L-optimization. Vertical lines at ~1.6−2.2 s indicate t_{rel}^{opt} *without* L-optimization, and those at ~0.2−0.5 s indicate t_{rel}^{match} (Table S1) where L-optimized congeners reach the same intrinsic sensitivity.

$$SN_t = A\frac{1-\exp(-R_1(t_{rel}+t_{acq}))}{\sqrt{t_{rel}+t_{acq}+t_{seq}}}$$

L-GFT-TROSY (4,3)D HCCH

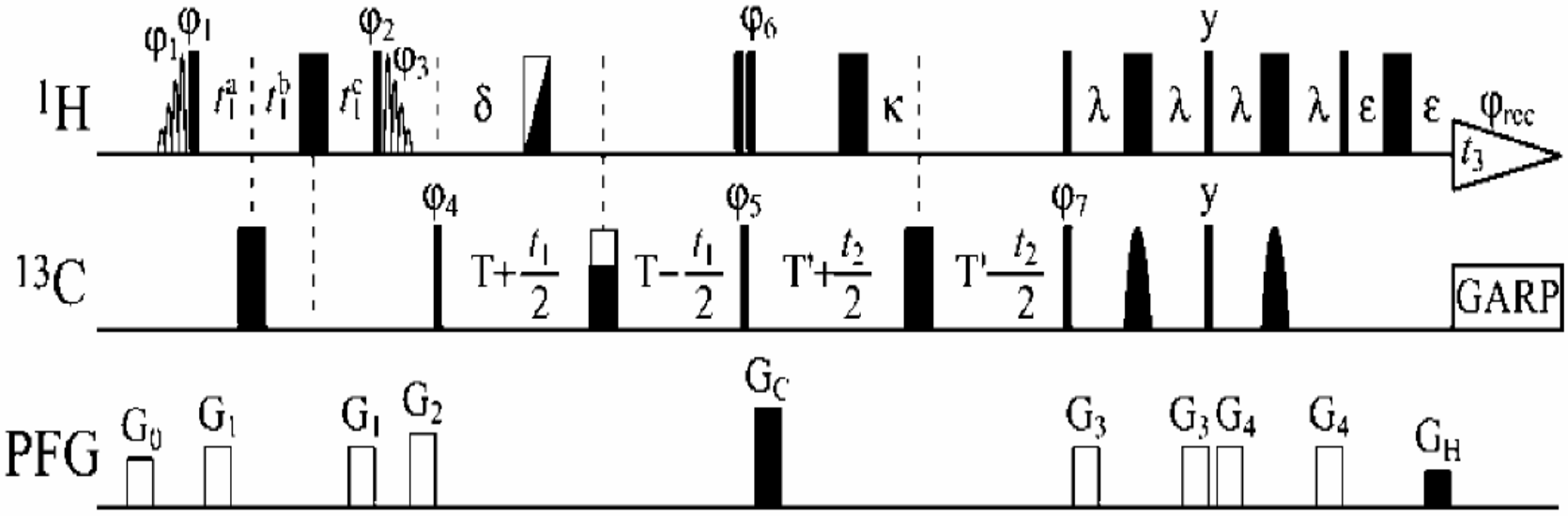

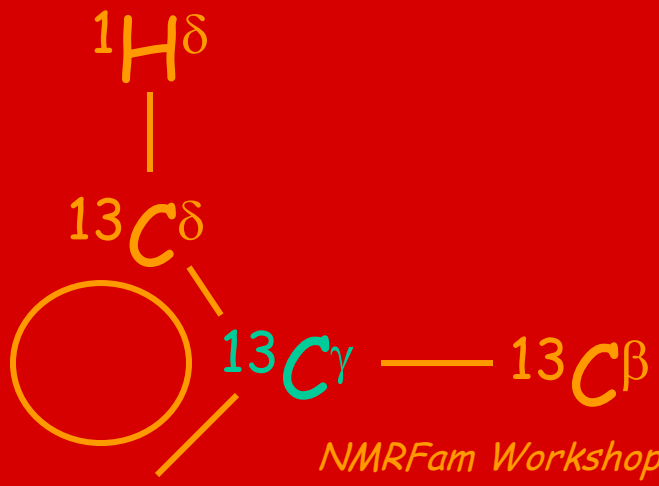

L-GFT-TROSY (4,3)D HCCH to avoid sampling limited data acquisition: 4D HCCH-information in 25 minutes

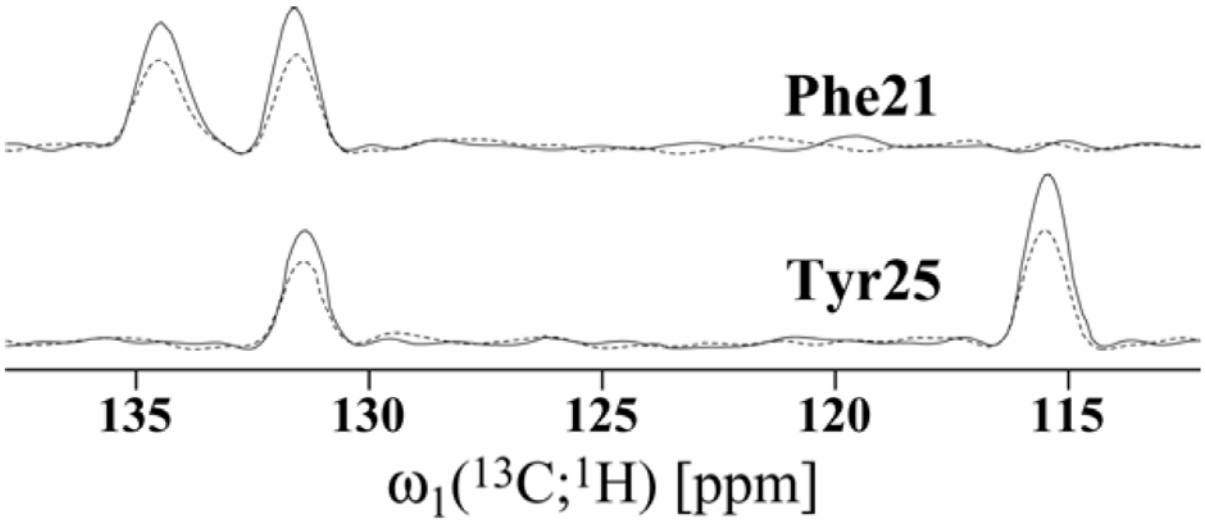

Figure S6. Cross sections taken along the GFT dimension from L-GFT (4,3)D HCCH (solid traces) and GFT (4,3)D HCCH (dotted traces) acquired for 11 kDa protein MaR11 in 25 min each.

L-GFT-TROSY (4,3)D HCCH for 21 kDa HR41

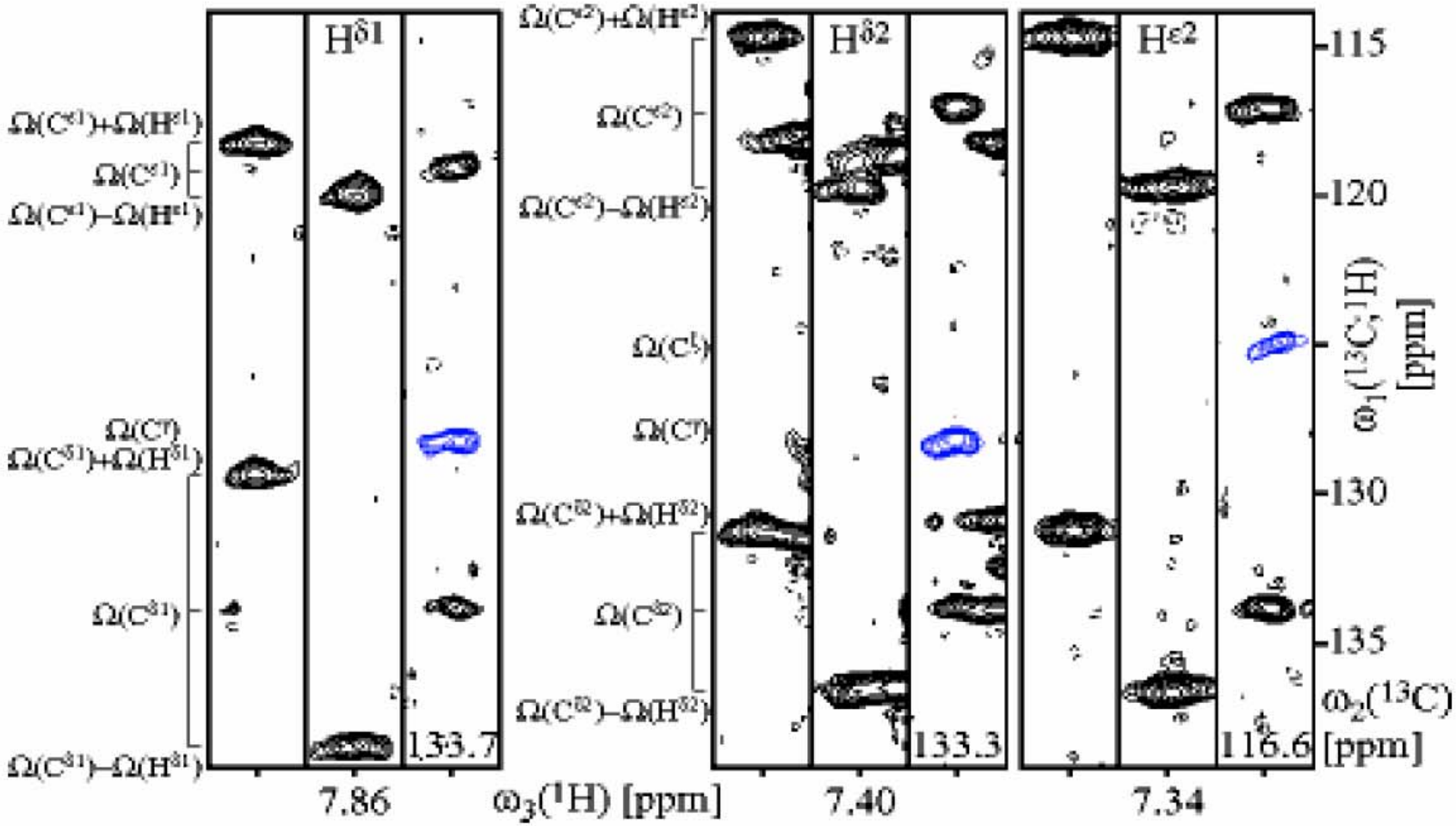

Figure 3. $[\omega_1(^{13}C^{(1)};^{1}H^{(1)}),\omega_3(^{1}H^{(2)})]$-strips taken along the GFT dimension of L-GFT-TROSY (4,3)D HCCH recorded at 750 MHz for 21 kDa HR41 with $t_{rel} = 1$ s. Peaks belong to the slowly flipping ring of Tyr 90. Central peaks arising from $^{13}C^{\gamma/\zeta}$ polarization are depicted in blue.

Aromatic ^{1}H linewidths in HR41

Table S6: $^{1}H^{aromatic}$ line-widths of HR41 at 25 °C from 2D [^{13}C,^{1}H] TROSY and (4,3)D HCCH

Res. No.	Res.	Atom Type	^{1}H linewidth [Hz] 2D [^{13}C,^{1}H] TROSY	L-GFT (4,3)D HCCH	Average
28	Trp	$H^{\delta 1}$	32	-	32
28	Trp	$H^{\varepsilon 3}$	42	40	41
28	Trp	$H^{\eta 2}$	40	41	41
28	Trp	$H^{\zeta 2}$	38	-	38
28	Trp	$H^{\zeta 3}$	-	42	42
36	Tyr	H^{δ}	-	21	21
36	Tyr	H^{ε}	-	21	21
42	Tyr	H^{δ}	-	35	35
42	Tyr	H^{ε}	-	32	32
53	Trp	$H^{\delta 1}$	35	-	35
53	Trp	$H^{\eta 2}$	43	41	42
53	Trp	$H^{\zeta 2}$	-	35	35
53	Trp	$H^{\zeta 3}$	-	39	39
54	Phe	H^{ε}	52	-	52
54	Phe	H^{ζ}	44	-	44
65	Trp	$H^{\delta 1}$	-	<37[a]	<37[a]
65	Trp	$H^{\eta 2}$	-	39	39
65	Trp	$H^{\zeta 2}$	38	34	36
66	Phe	H^{δ}	-	25	25
66	Phe	H^{ε}	27	24	25
66	Phe	H^{ζ}	25	26	26
70	Trp	$H^{\delta 1}$	33	39	36
70	Trp	$H^{\varepsilon 3}$	-	34	34
70	Trp	$H^{\eta 2}$	-	42	42
70	Trp	$H^{\zeta 2}$	-	33	33
70	Trp	$H^{\zeta 3}$	-	<36[a]	<36[a]
71	Tyr	H^{δ}	-	<29[a]	<29[a]
71	Tyr	H^{ε}	-	<33[a]	<33[a]
78	Tyr	H^{ε}	-	<35[a]	<35[a]
80	Phe	H^{δ}	-	32	32
80	Phe	H^{ε}	41	41	41
80	Phe	H^{ζ}	40	-	40
84	Phe	H^{δ}	39	35	37
84	Phe	H^{ε}	44	42	43
84	Phe	H^{ζ}	44	45	45
90	Tyr	$H^{\delta 1}$	45	34	39
90	Tyr	$H^{\delta 2}$	-	36	36
90	Tyr	$H^{\varepsilon 1}$	-	32	32
90	Tyr	$H^{\varepsilon 2}$	40	38	39
110	Tyr	H^{δ}	31	27	29
110	Tyr	H^{ε}	-	27	27
121	Phe	H^{δ}	-	<42[a]	<42[a]
121	Phe	H^{ε}	-	<42[a]	<42[a]
121	Phe	H^{ζ}	39	-	39
125	Trp	$H^{\delta 1}$	34	35	35
125	Trp	$H^{\eta 2}$	-	<41[a]	<41[a]
125	Trp	$H^{\zeta 2}$	-	<39[a]	<39[a]
132	Phe	H^{δ}	36	35	35
132	Phe	H^{ε}	37	38	38
132	Phe	H^{ζ}	39	-	39
145	Trp	$H^{\delta 1}$	37	36	37
145	Trp	$H^{\varepsilon 3}$	51	-	51
145	Trp	$H^{\eta 3}$	-	<36[a]	<36[a]
145	Trp	$H^{\zeta 2}$	43	44	43
145	Trp	$H^{\zeta 3}$	-	<48[a]	<48[a]
Completeness			**42%**	**71%**	**85%**

[a] Upper limit only due to spectral overlap.

Ring flipping and functional dynamics in the 21 kDa protein HR41

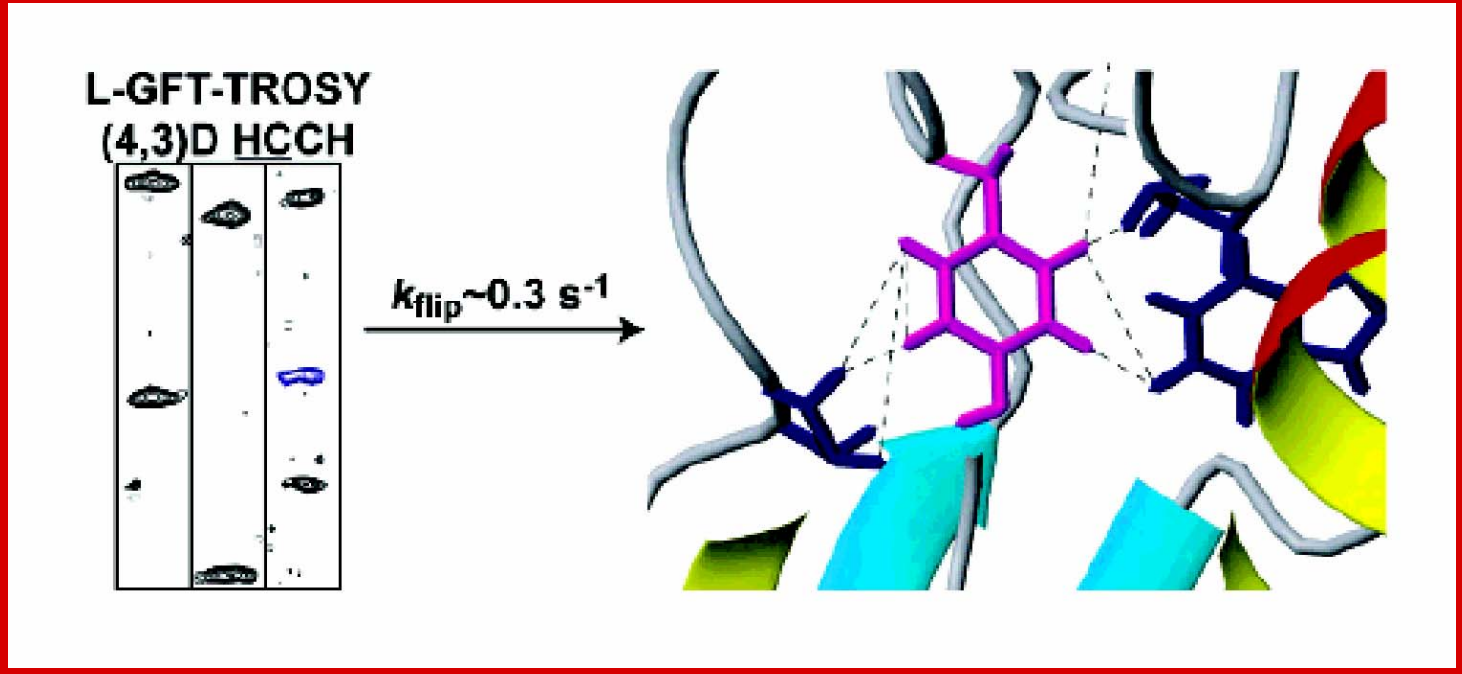

L-GFT-TROSY (4,3)D HCCH for larger proteins

- L-optimization and PFG-PEP increase intrinsic sensitivity ~2-fold
- L-optimization enables ~3-fold faster data sampling
- TROSY allows use of $^{13}C^{aro}$ polarization for central peak detection
- Nearly complete resonance assignments of aromatic resonances based on 4D spectral information enable
  - high-quality structure determination
  - use aromatic rings to explore larger amplitude motional modes

GFT NMR for high-throughput protein structure determination

Approaches for rapid NMR data collection

Approach	Acceleration	Data Processing
Basic		
Reduction of t_{max}	<~1.5 for each dimension	FT
Reduction of t_{rel}	<~2	FT
Aliasing	<~3	FT
Advanced		
Sparse sampling	<~2-3	MER or TWD/FT
L-optimization: Reduction of t_{rel}:	~2-3	FT
Simultaneous acquisition	<~2	FT
Hadamard spectroscopy	<~2	HT
Single scan ND NMR	~10-50 (each dimension)	FT
RD NMR spectroscopy	~10	FT
GFT NMR spectroscopy	~10^K for (*N*, *N*-*K*)D	G-matrix FT

From: H. Atreya & T . Szyperski. Methods Enzymol. **2005**, *394*, 78–108.

GFT projection NMR based structure determination protocol

sequence specific ^{15}N, ^{1}H, $^{13}C\alpha$ and $^{13}C\beta$ assignment

$^{1}H\alpha$ / $^{1}H\beta$ assignment

side-chain assignment (aliphatic and aromatic) → NO C-C TOCSY

structure calculation and refinement

(4,3)D HNN$C^{\alpha\beta}C^{\alpha}$ and (4,3)D $C^{\alpha\beta}C^{\alpha}$(CO)NHN

(5,2)D HACACONHN ($^{1}H\alpha$) OR (4,3)D $H^{\alpha\beta}C^{\alpha\beta}$(CO)NHN ($^{1}H\alpha$/$^{1}H\beta$)

(4,3)D HCCH

3D ^{15}N/$^{13}C^{aliph}$/$^{13}C^{arom}$ - resolved [^{1}H,^{1}H]-NOESY

CYANA/AUTOSTRUCTURE

1~2d

1~3d

5~10d

Pilot study (3.2004): structure of 14 kDa YqfB

16.9 hrs GFT spectra for
resonance assignment and
9.1 hrs for simultaneous 3D NOESY
(1 mmol solution at 25 °C
and 600 MHz w/cryogenic probe)

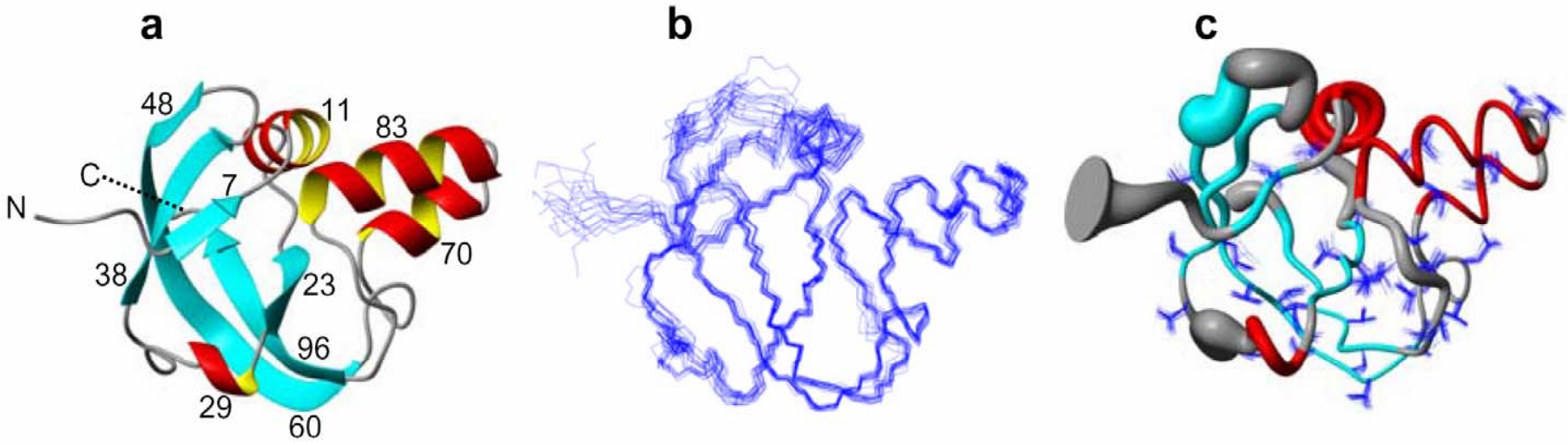

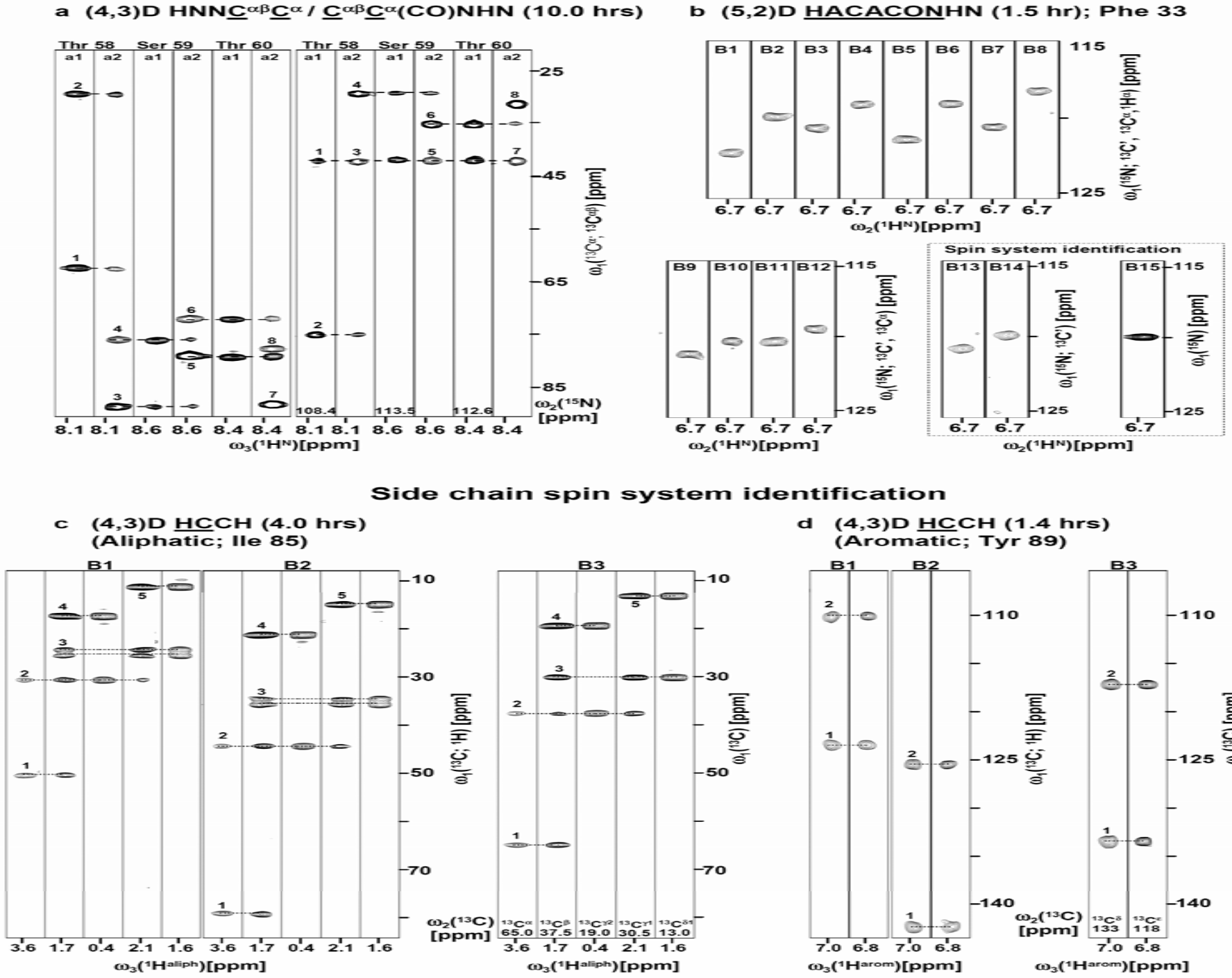
a (4,3)D HNNCαβCα / CαβCα(CO)NHN (10.0 hrs)
Thr 58
Ser 59
Thr 60
a1
a2
108.4
113.5
112.6
ω1(13Cα; 13Cαβ) [ppm]
ω2(15N) [ppm]
ω3(1HN)[ppm]
b (5,2)D HACACONHN (1.5 hr); Phe 33
B1
B2
B3
B4
B5
B6
B7
B8
B9
B10
B11
B12
B13
B14
B15
ω1(15N; 13C', 13Cα,1Hα) [ppm]
ω1(15N; 13C', 13Cα) [ppm]
ω1(15N; 13C') [ppm]
ω1(15N) [ppm]
ω2(1HN)[ppm]
Spin system identification
Side chain spin system identification
c (4,3)D HCCH (4.0 hrs)
(Aliphatic; Ile 85)
ω1(13C; 1H) [ppm]
ω2(13C) [ppm]
13Cα 65.0
13Cβ 37.5
13Cγ2 19.0
13Cγ1 30.5
13Cδ1 13.0
ω3(1Haliph)[ppm]
d (4,3)D HCCH (1.4 hrs)
(Aromatic; Tyr 89)
13Cδ 133
13Cε 118
ω3(1Harom)[ppm]

3D [H]-NOESY-[NH/$^{13}C^{ali}H$/$^{13}C^{aro}H$]

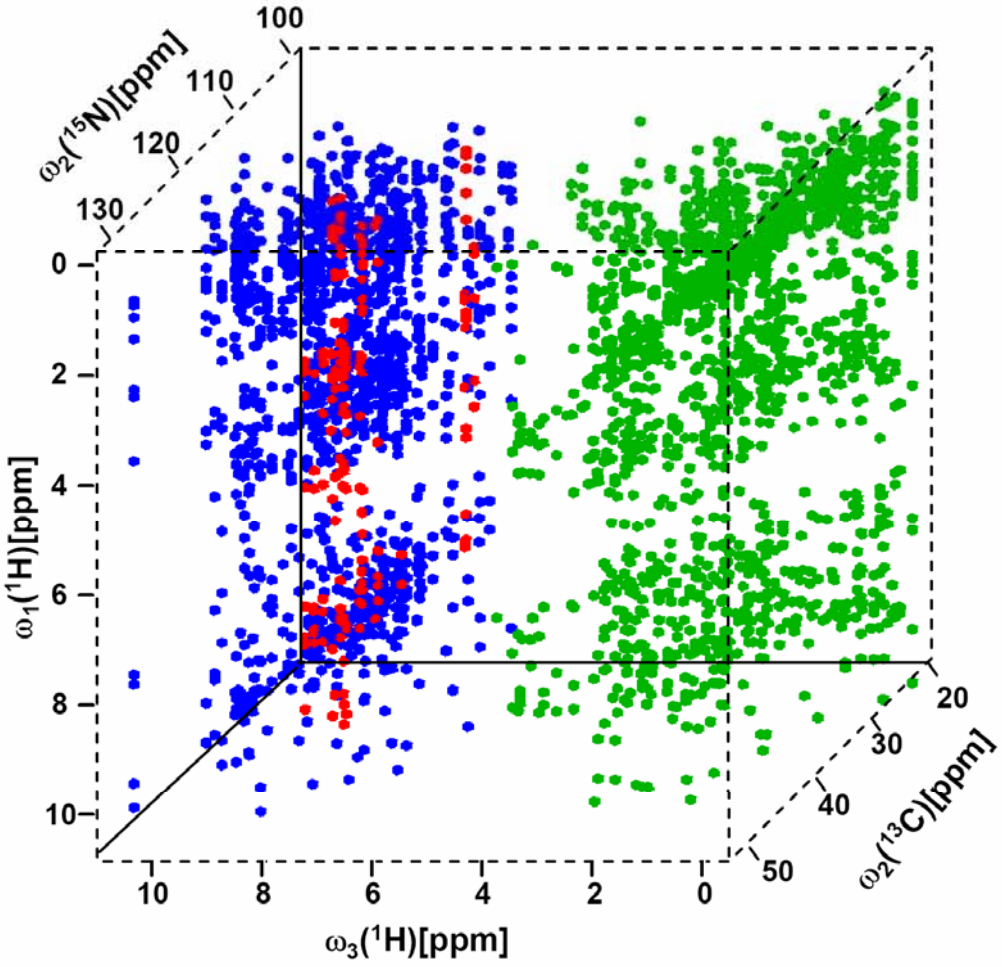

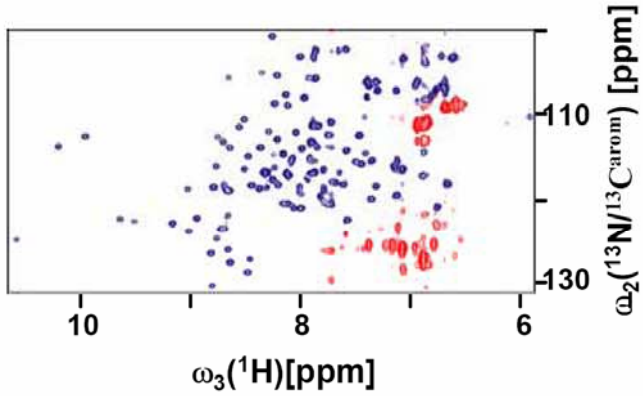

C

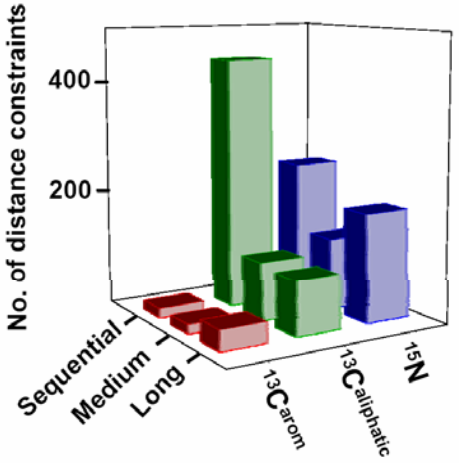

L-(4,3)D HNN(CO)$\underline{C}^{\alpha\beta}\underline{C}^{\alpha}$

Flip-back of water and aliphatic proton polarization

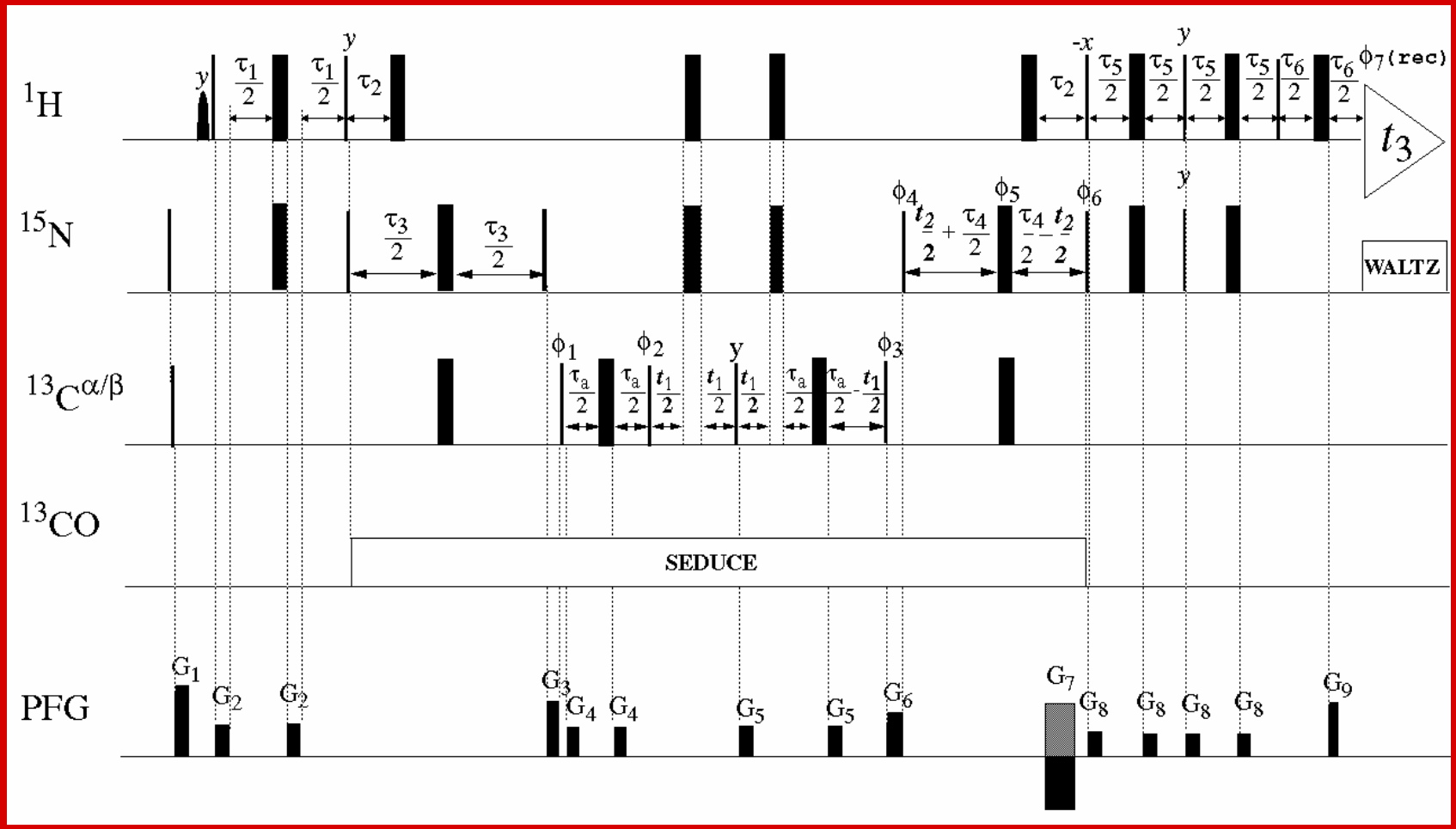

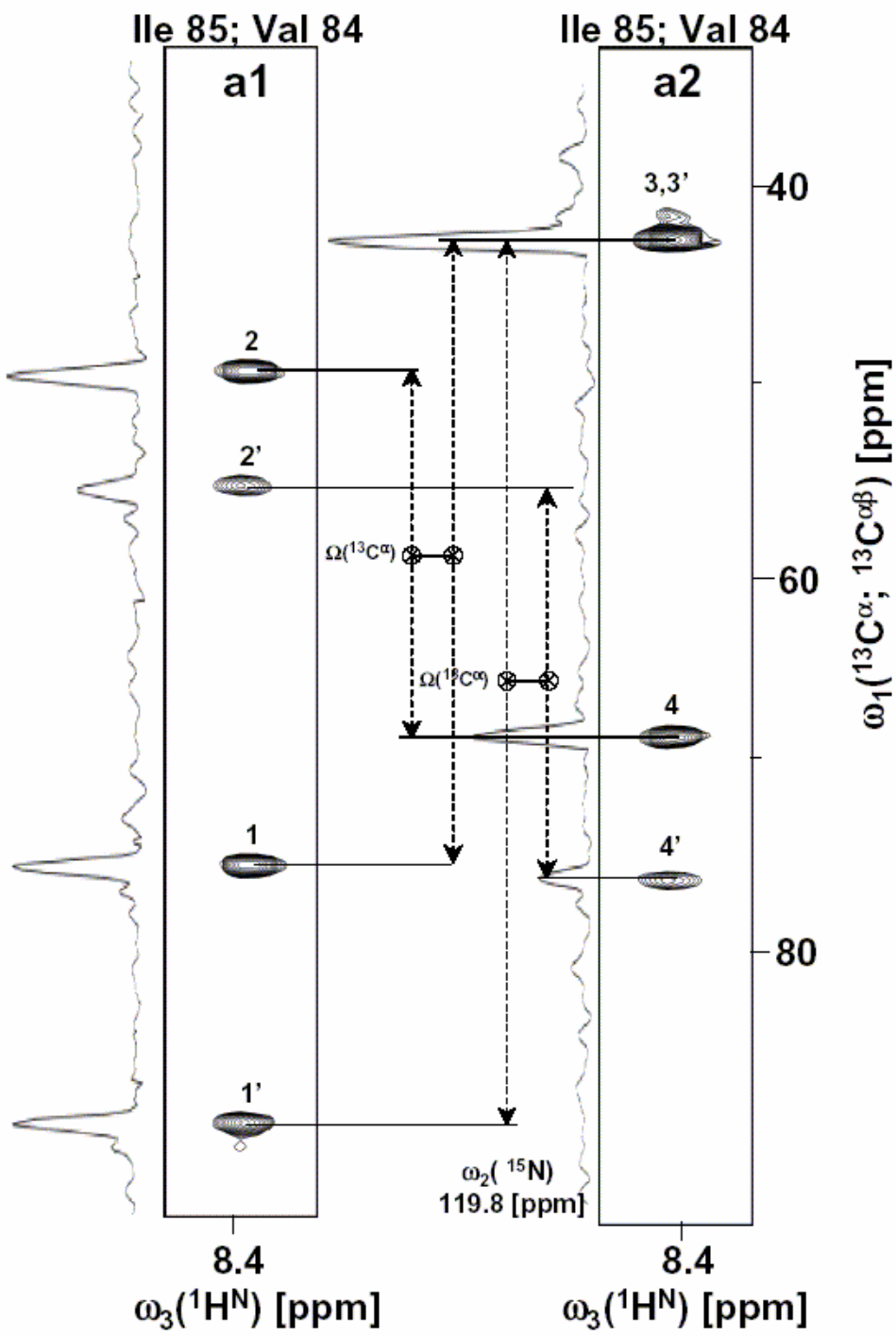

4D CACB(CO)NHN

information in

(4,3)D $\underline{C}^{\alpha\beta}\underline{C}^{\alpha}$(CO)NHN

(4,3)D HNN$C^{\alpha\beta}C^{\alpha}$/ $C^{\alpha\beta}C^{\alpha}$(CO)NHN 'sequential walk'

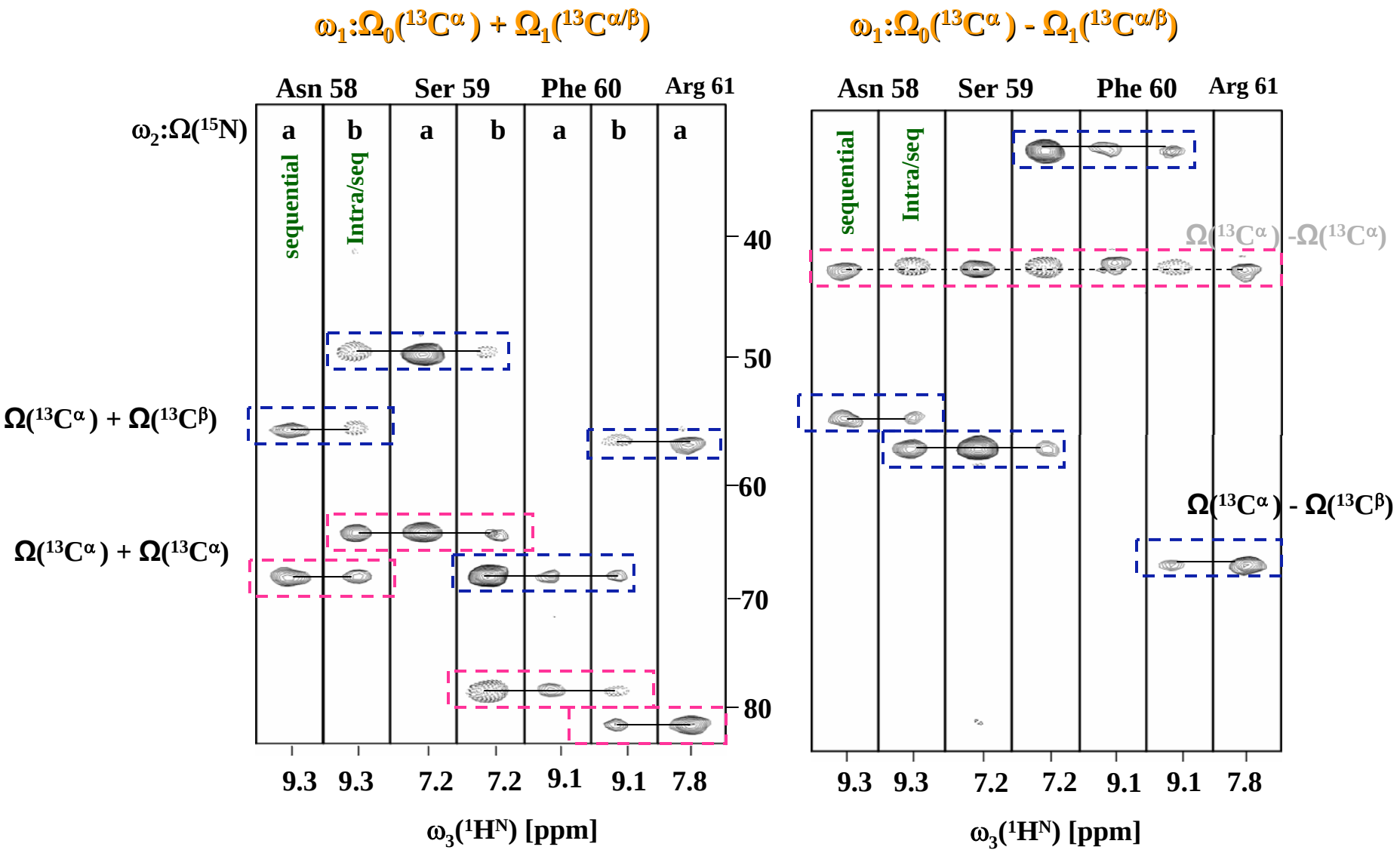

Better signal *dispersion*

(4,3)D HNN$C^{\alpha\beta}C^{\alpha}$ (B)

when compared with

3D HNNCACB (A)

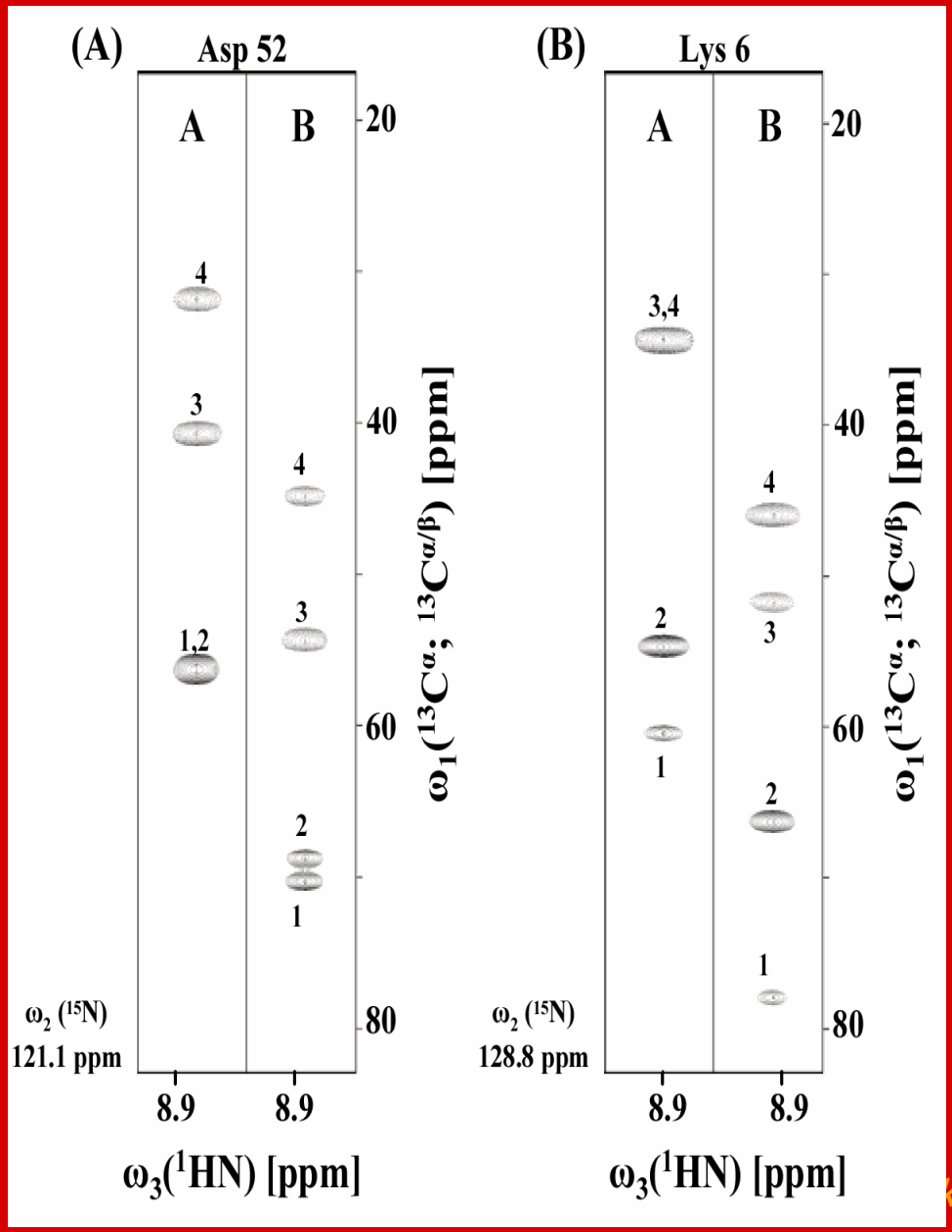

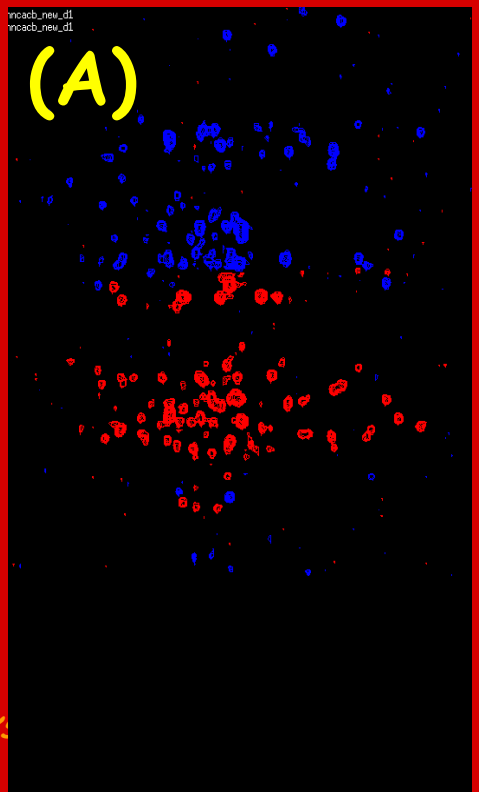

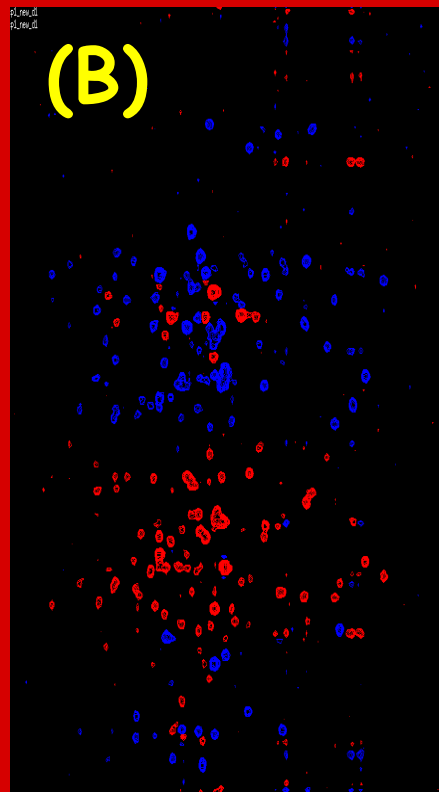

JACS
ARTICLES
Published on Web 06/07/2005

G-Matrix Fourier Transform NOESY-Based Protocol for High-Quality Protein Structure Determination

Yang Shen, Hanudatta S. Atreya, Gaohua Liu, and Thomas Szyperski*

Contribution from the Departments of Chemistry and Structural Biology, The State University of New York at Buffalo, Buffalo, New York 14260

Received January 11, 2005; E-mail: szypersk@chem.buffalo.edu

(4,3)D [HN/H^{13}C^{ali}]-NOESY-[NH/^{13}C^{ali}H]:

Rapid acquisition of highly resolved 4D NOESY information

NMRFam Workshop 06/06/06

(a) (4,3)D [HN/$^{13}C^{ali}$H]-NOESY-[NH/$^{13}C^{ali}$H] with central peak detection in (b) 3D [H]-NOESY-[NH/$^{13}C^{ali}$H/$^{13}C^{aro}$H]

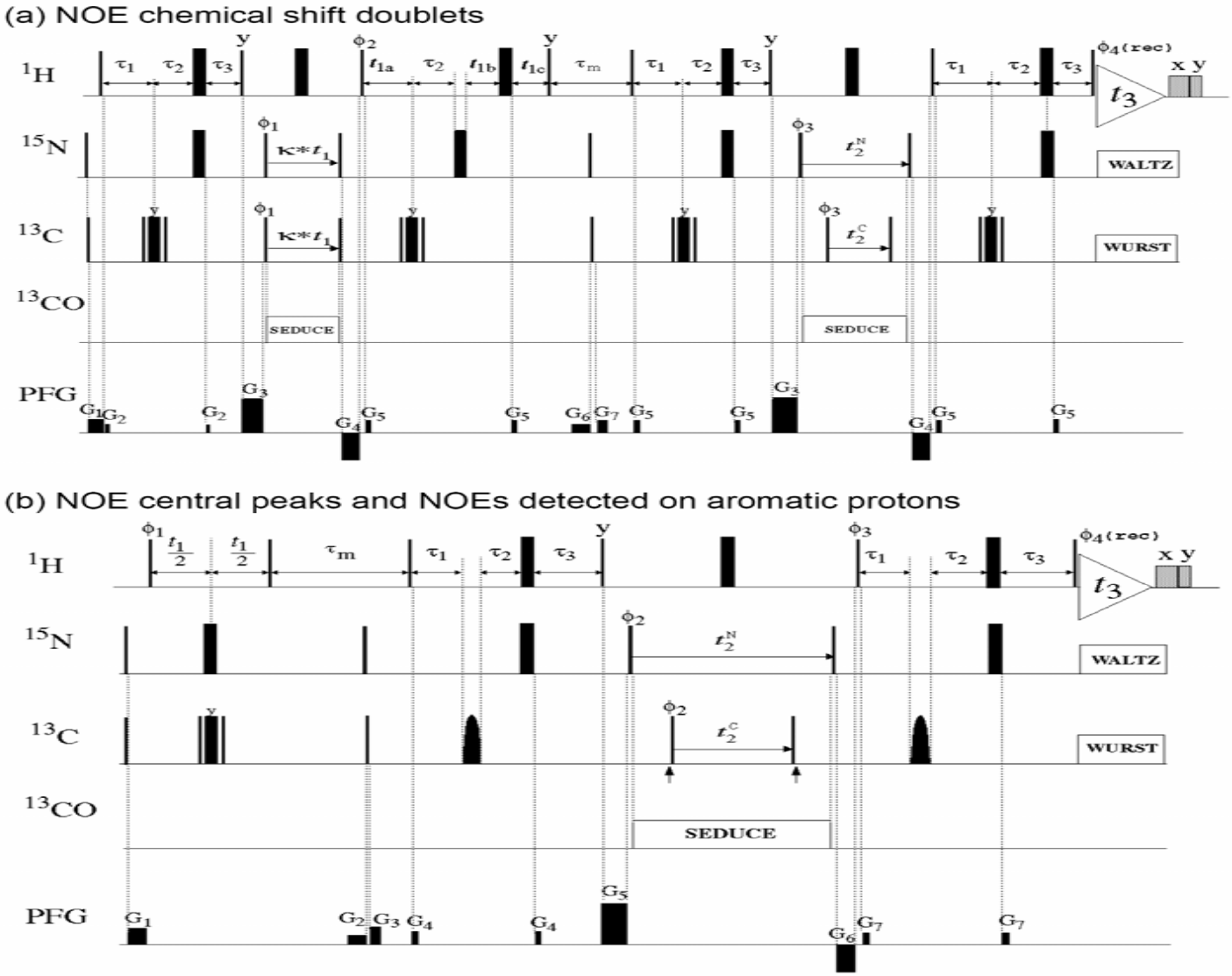

(4,3)D [HN/H$^{13}C^{ali}$]-NOESY-[NH/$^{13}C^{ali}$H] with central peak detection in 3D [H]-NOESY-[NH/$^{13}C^{ali}$H/$^{13}C^{aro}$H]

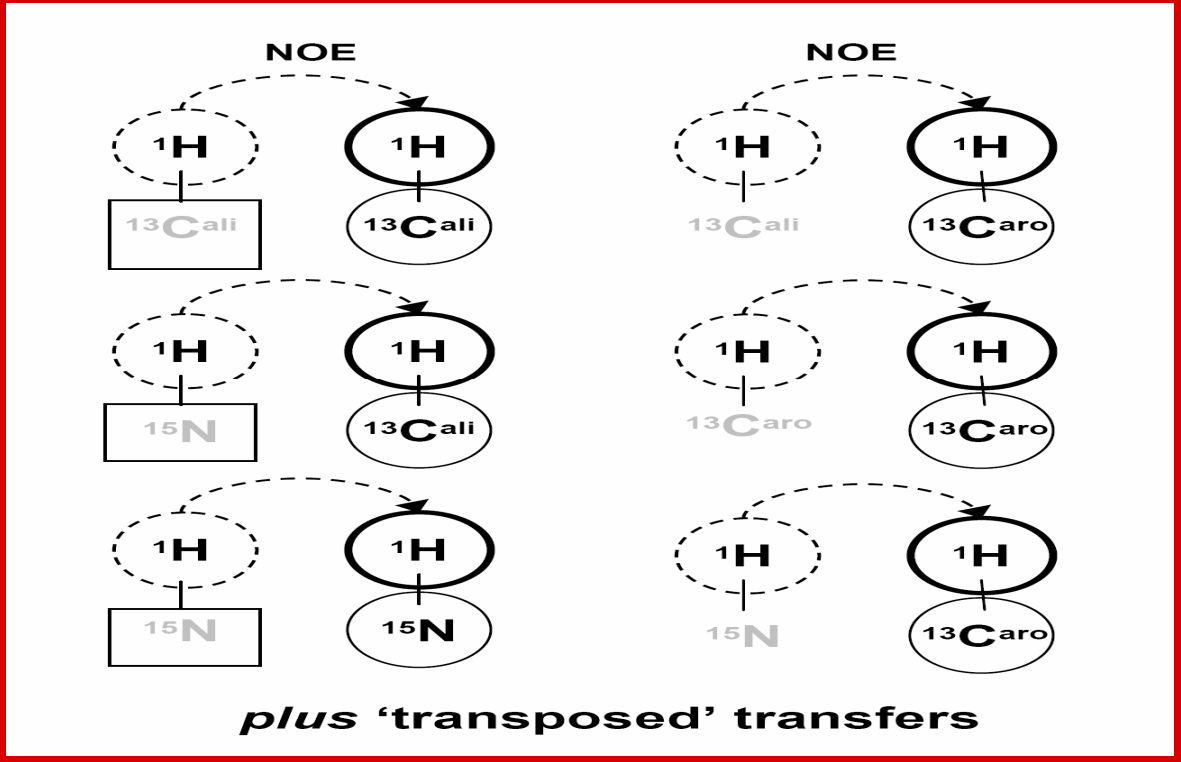

Information of three 4D and three 3D NOESY spectra

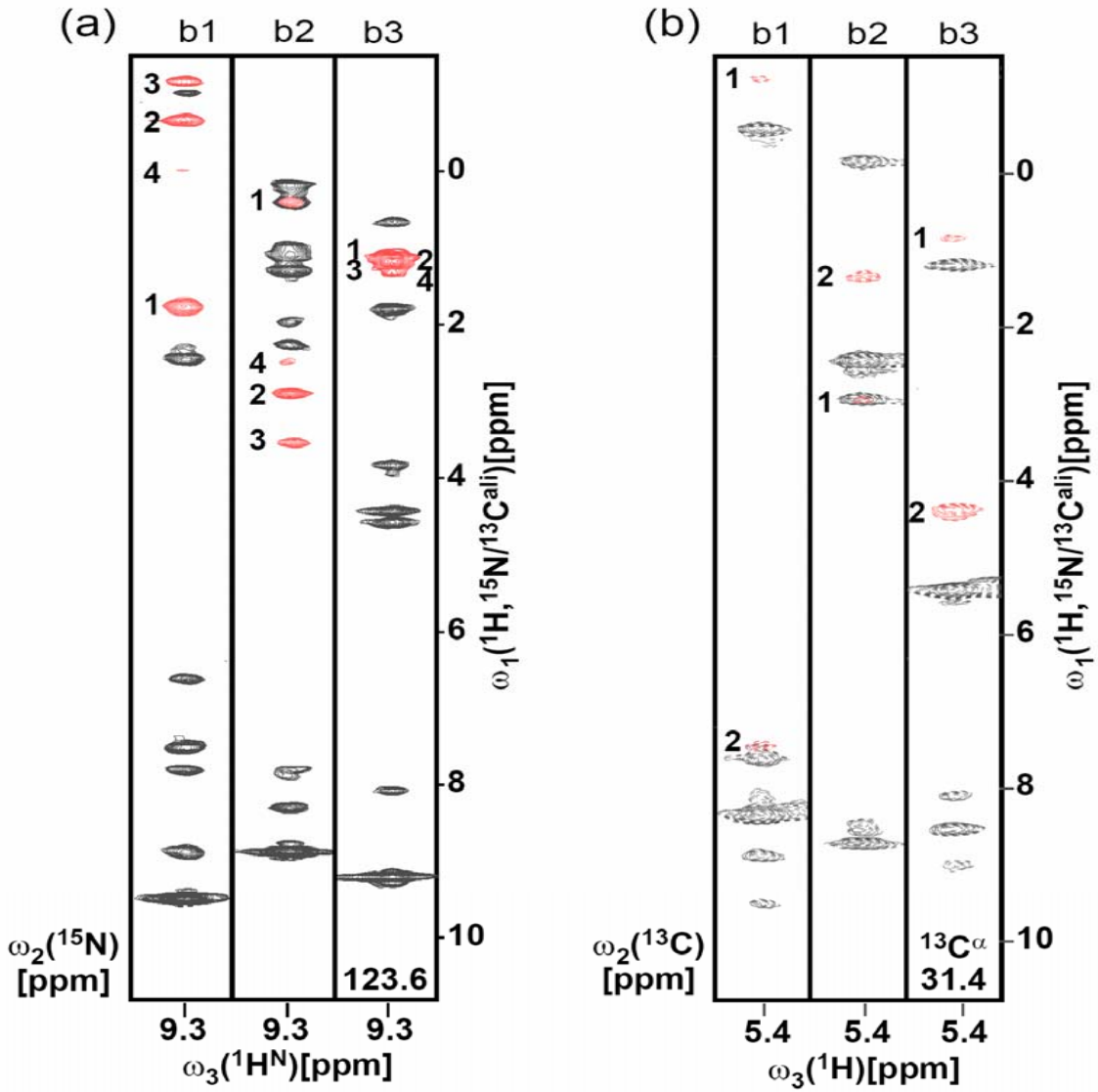

b1: $\Omega(^1H)+0.5\ \Omega(^{13}C)$

b2: $\Omega(^1H)-0.5\ \Omega(^{13}C)$

b3 : $\Omega(^1H)$

Role of (4,3)D GFT NOESY

- For medium sized proteins (τ_r~8-12 ns), sensitivity of shift doublet detection is ~3 times lower than for central peak detection
- For YqfB, 30 hours measurement time resulted in ~70% detection yield for doublets -> direct assignment of ~70% of *long-range* NOEs

=> (4,3)D GFT NOESY is primarily tool for assigning NOEs in 3D NOESY

Northeast Structural Genomics Consortium: A SG Research Network

Bioinformatics / Data Management

Barry Honig, Columbia University
Mark Gerstein, Yale University
Igor Jurisica, Ontario Cancer Inst.
Andrew Laine, Columbia University
Diana Murray, Cornell Medical
Burkhard Rost, Columbia University

X-ray Crystallography

Wayne Hendrickson, Columbia U
Peter Allen, Columbia University
George DeTitta, Hauptman-Woodward
John Hunt, Columbia University
Liang Tong, Columbia University

Protein Production / Biophysics

Gaetano Montelione, Rutgers University
Stephen Anderson, Rutgers University
Masayori Inouye, RWJMS - UMDNJ
Cheryl Arrowsmith, Ontario Cancer I.

Protein NMR

Thomas Szyperski, State U of New York
Cheryl Arrowsmith, Ontario Cancer Inst.
Michael Kennedy, Pacific Northwest Natl Labs
Ron Levy, Rutgers University
Jim Prestegard, University of Georgia
Gaetano Montelione, Rutgers University

Semi-empiric solution of 'protein folding problem'

36 RD/GFT NMR-based Structures: Molecular weight distribution

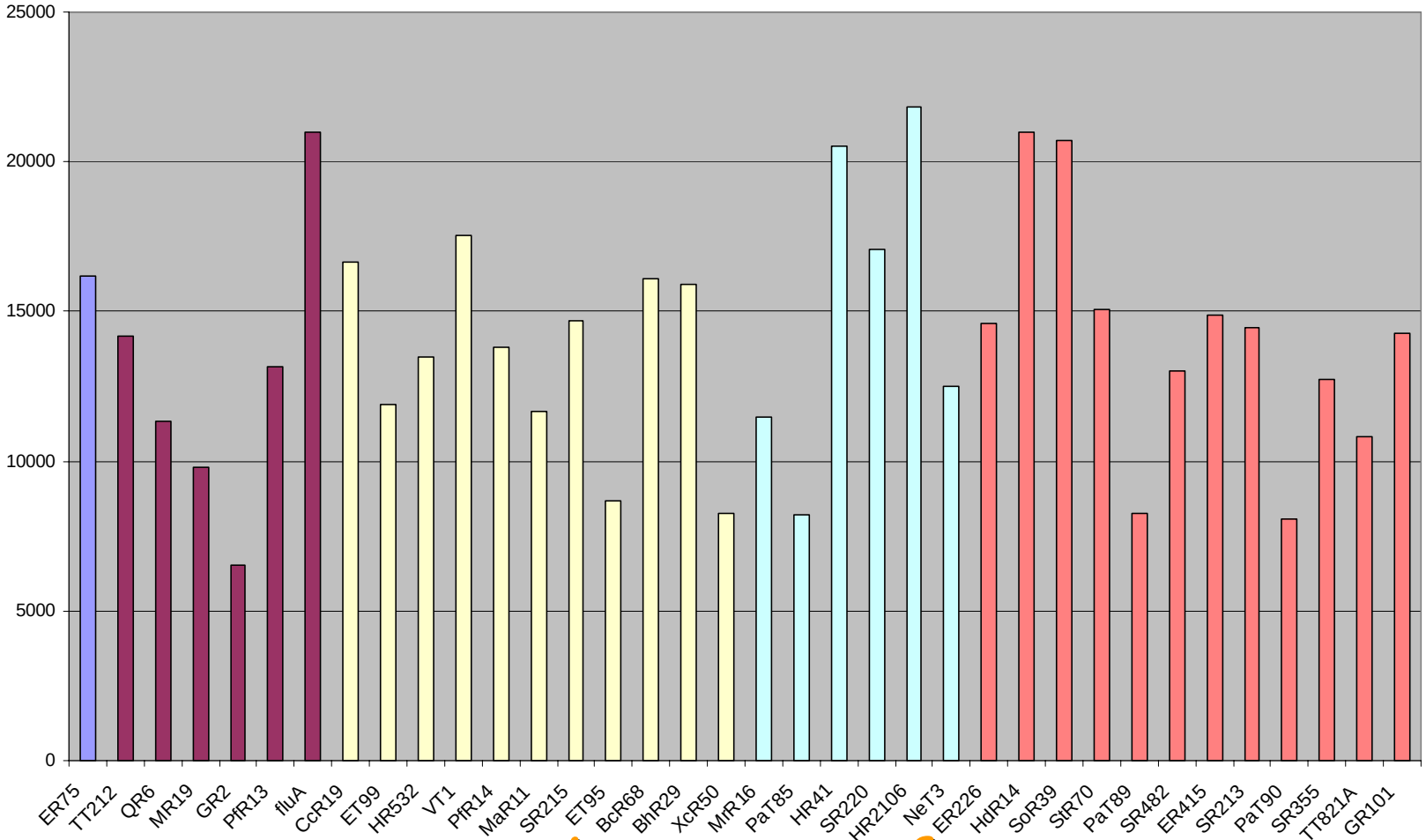

…..robustness of semi-automated GFT NMR data analysis

Wealth of structural-biological insight….

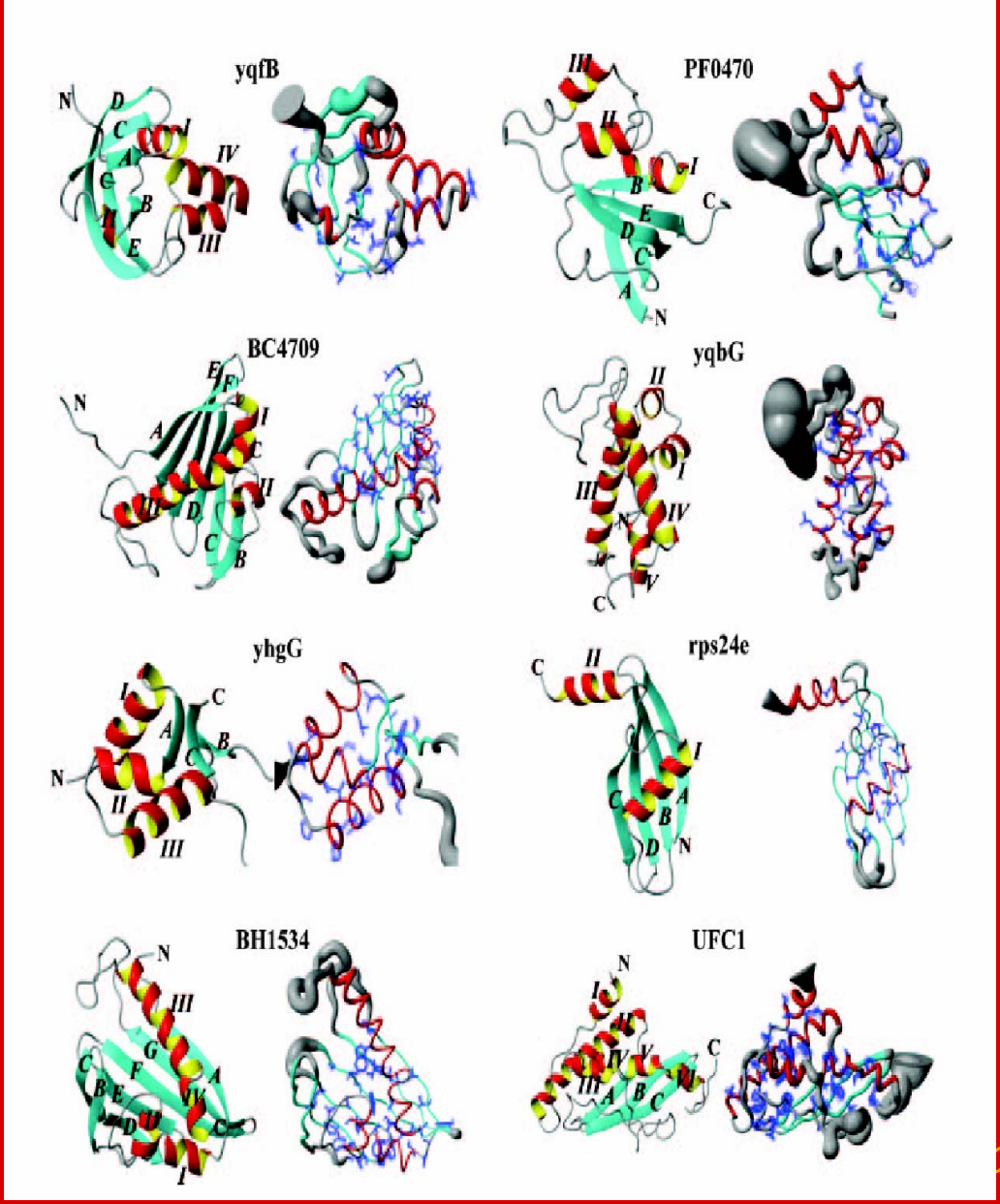

SCOP classification

yqfB and PF0470:
'PUA domain'

UFC1:
'Ubiquitin-conjugating enzyme'

BC4709 and BH1534:
'START domain'

yhgG
'winged-helix DNA-Binding domain'

rps24e:
'Yggu-like'

yqbG:
no structural homologue found

http://www.nsm.buffalo.edu/Research/GFT

G-matrix Fourier Transform (GFT) Projection NMR Spectroscopy

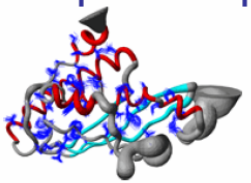

Prof. Thomas Szyperski

State University of New York at Buffalo

On GFT Projection NMR Spectroscopy

Defining features of G-matrix Fourier Transform (GFT) projection NMR spectroscopy (Kim and Szyperski, 2003):

(i) joint sampling of K+1 chemical shifts $\Omega_0, \Omega_1, \ldots, \Omega_K$ encoded in K+1 indirect evolution periods of an ND FT NMR experiment,

(ii) phase-sensitive detection of 2^K linear combinations of chemical shifts $\Omega_0 \pm \Omega_1 \pm \ldots \pm \Omega_K$,

(iii) editing of the 2^K linear combinations of shifts into 2^K (N-K)D 'basic' projected sub-spectra, so that each contains one of the linear combinations.

more...

Download RD/GFT NMR Package

References

Talks on GFT NMR

GFT NMR in the Media

By registering to the UB GFT NMR web site, you will soon receive by email additional parameter sets and pulse programs which have been recently published by Atreya et al. (J. Am. Chem. Soc. 127, 4554 - 4555), Shen et al. (J. Am. Chem. Soc. 127, 9085 - 9099) and Eletsky et al. (J. Am. Chem. Soc. 127, 14578-14579) [more...]

Support of the National Science Foundation and the National Institutes of Health is acknowledged

G-matrix Fourier Transform (GFT) Projection NMR Spectroscopy

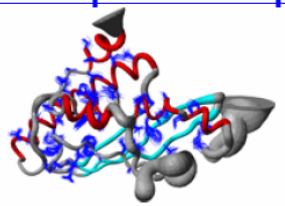

Download GFT/RD NMR Package

Contents of GFT/RD NMR packages

Please register first - *free* for academic users

Registered Users click here to download GFT NMR package

Registered Users click here to download RD NMR package

Please cite "Kim, S. and Szyperski, T. (2003) GFT NMR, a New Approach to Rapidly Obtain Precise High Dimensional NMR Spectral Information. *J. Am. Chem. Soc.* **125**, 1385-1393" and potentially additional publications describing the specific experiments (see 'References') when publishing research resulting from the use of the GFT NMR package

Please cite "Szyperski, T., Yeh, D. C., Sukumaran, D. K., Moseley, H. N. B. and Montelione, G. T. (2002) Reduced-dimensionality NMR spectroscopy for High-Throughput Resonance Assignment. *Proc. Natl. Acad. Sci. USA* **99**, 8009-8014" when publishing research resulting from the use of the RD NMR package

Support of the National Science Foundation and the National Institutes of Health is acknowledged

Relation of GFT NMR Spectroscopy and

'Projection Reconstruction' (PR) NMR

(Kupce & Freeman, JACS 2004, *126*, 6429)

NMRFam Workshop 06/06/06

MAGNETIC RESONANCE IN CHEMISTRY
Magn. Reson. Chem. 2006; **44**: 000–000
Published online in Wiley InterScience (www.interscience.wiley.com). DOI: 10.1002/mrc.1817

MRC

Principles and applications of GFT projection NMR spectroscopy†

Thomas Szyperski* and Hanudatta S. Atreya

Departments of Chemistry and Structural Biology, The State University of New York at Buffalo, The Northeast Structural Genomics Consortium, Buffalo, NY 14260, USA

Received 2 December 2005; Revised 20 January 2006; Accepted 28 February 2006

'Projection' component in 'Projection-reconstruction (PR) NMR' is equivalent to GFT projection NMR

NMRFam Workshop 06/06/06

(4,2)D GFT NMR

$S_{1r} \propto \cos(\kappa_0 \Omega_0 t)*\cos(\kappa_1 \Omega_1 t)*\cos(\kappa_2 \Omega_2 t)$

$S_{1i} \propto \sin(\kappa_0 \Omega_0 t)*\cos(\kappa_1 \Omega_1 t)*\cos(\kappa_2 \Omega_2 t)$

$S_{2r} \propto \cos(\kappa_0 \Omega_0 t)*\sin(\kappa_1 \Omega_1 t)*\cos(\kappa_2 \Omega_2 t)$

$S_{2i} \propto \sin(\kappa_0 \Omega_0 t)*\sin(\kappa_1 \Omega_1 t)*\cos(\kappa_2 \Omega_2 t)$

$S_{3r} \propto \cos(\kappa_0 \Omega_0 t)*\cos(\kappa_1 \Omega_1 t)*\sin(\kappa_2 \Omega_2 t)$

$S_{3i} \propto \sin(\kappa_0 \Omega_0 t)*\cos(\kappa_1 \Omega_1 t)*\sin(\kappa_2 \Omega_2 t)$

$S_{4r} \propto \cos(\kappa_0 \Omega_0 t)*\sin(\kappa_1 \Omega_1 t)*\sin(\kappa_2 \Omega_2 t)$

$S_{4i} \propto \sin(\kappa_0 \Omega_0 t)*\sin(\kappa_1 \Omega_1 t)*\sin(\kappa_2 \Omega_2 t)$,

so that the vector $\mathbf{T}(2)=\mathbf{G}(2)\bullet\mathbf{S}(2)$ is given in complex notation by:

$$\mathbf{T}(2) = \begin{bmatrix} e^{i(\kappa_0*\Omega_0+\kappa_1*\Omega_1+\kappa_2*\Omega_2)t} \\ e^{i(\kappa_0*\Omega_0-\kappa_1*\Omega_1+\kappa_2*\Omega_2)t} \\ e^{i(\kappa_0*\Omega_0+\kappa_1*\Omega_1-\kappa_2*\Omega_2)t} \\ e^{i(\kappa_0*\Omega_0-\kappa_1*\Omega_1-\kappa_2*\Omega_2)t} \end{bmatrix} = \begin{bmatrix} 1 & i & i & -1 & i & -1 & -1 & -i \\ 1 & i & -i & 1 & i & -1 & 1 & i \\ 1 & i & i & -1 & -i & 1 & 1 & i \\ 1 & i & -i & 1 & -i & 1 & -1 & -i \end{bmatrix} \bullet \begin{bmatrix} s_{1r} \\ s_{1i} \\ s_{2r} \\ s_{2i} \\ s_{3r} \\ s_{3i} \\ s_{4r} \\ s_{4i} \end{bmatrix} \qquad (4).$$

Hence, the four linear combinations of chemical shifts, $\kappa_0*\Omega_0\pm\kappa_1*\Omega_1\pm\kappa_2*\Omega_2$, are measured in one of the four sub-spectra each.

G-matrix transformation ⇔ 'generalized hyper-complex FT'

$$S_{+\alpha,+\beta} = 0.25[(S_{rrr} - S_{rjk} - S_{ijr} - S_{irk}) + i(S_{irr} - S_{ijk} + S_{rjr} + S_{rrk})]$$
$$S_{+\alpha,-\beta} = 0.25[(S_{rrr} + S_{rjk} - S_{ijr} + S_{irk}) + i(S_{irr} + S_{ijk} + S_{rjr} - S_{rrk})]$$
$$S_{-\alpha,+\beta} = 0.25[(S_{rrr} + S_{rjk} + S_{ijr} - S_{irk}) + i(S_{irr} + S_{ijk} - S_{rjr} + S_{rrk})]$$
$$S_{-\alpha,-\beta} = 0.25[(S_{rrr} - S_{rjk} + S_{ijr} + S_{irk}) + i(S_{irr} - S_{ijk} - S_{rjr} - S_{rrk})]$$

Kupce E, Freeman R. *J. Am. Chem. Soc.* 2004; **126**: 6429-6440.

The equivalence of G-matrix Eq. (4) with this system of equations becomes readily apparent when considering the correspondence of the following parameters and expressions:

$S_{+\alpha,+\beta} \leftrightarrow e^{i(\kappa_0 * \Omega_0 + \kappa_1 * \Omega_1 + \kappa_2 * \Omega_2)t}$, $S_{+\alpha,-\beta} \leftrightarrow e^{i(\kappa_0 * \Omega_0 - \kappa_1 * \Omega_1 + \kappa_2 * \Omega_2)t}$, $S_{-\alpha,+\beta} \leftrightarrow e^{i(\kappa_0 * \Omega_0 + \kappa_1 * \Omega_1 - \kappa_2 * \Omega_2)t}$,

$S_{+\alpha,+\beta} \leftrightarrow e^{i(\kappa_0 * \Omega_0 - \kappa_1 * \Omega_1 - \kappa_2 * \Omega_2)t}$, and

$S_{rrr} \leftrightarrow S_{1r}$, $S_{rjk} \leftrightarrow S_{4r}$, $S_{ijr} \leftrightarrow S_{3i}$, $S_{irk} \leftrightarrow S_{2i}$, $S_{irr} \leftrightarrow S_{1i}$, $S_{ijk} \leftrightarrow S_{4i}$, $S_{rjr} \leftrightarrow S_{3r}$, $S_{rrk} \leftrightarrow S_{2r}$.

Moreover, the scaling factors κ_j in Eq (4) are adapted to the use of projection angles α and β (Fig. 1) by setting $\kappa_0 = \cos\alpha \cos\beta$, $\kappa_1 = \sin\alpha \cos\beta$ and $\kappa_2 = \sin\beta$.[30]

Hence, the projection formalism of PR NMR is equivalent to the GFT NMR formalism.

Scaling of shift evolution periods ⇔ 'tilt angles of plane projection'

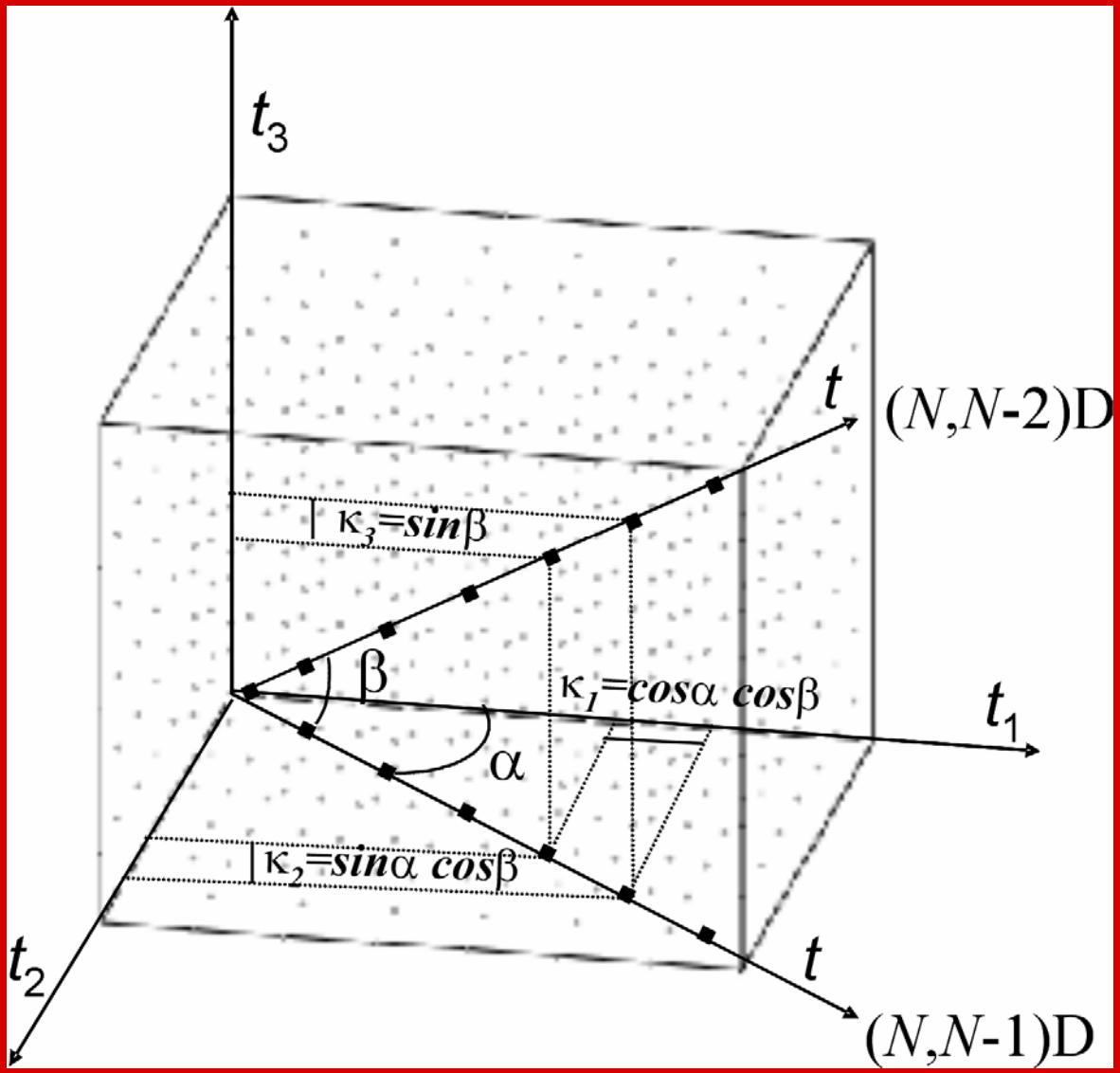

Generalized Reconstruction of *n*-D NMR Spectra from Multiple Projections: Application to the 5-D HACACONH Spectrum of Protein G B1 Domain

Brian E. Coggins,† Ronald A. Venters,‡ and Pei Zhou*,†

Department of Biochemistry and Duke University NMR Center, Duke University Medical Center, Durham, North Carolina 27710

Received November 5, 2003; E-mail: peizhou@biochem.duke.edu

Simultaneously incrementing the evolution parameters has been employed by several groups to speed up multidimensional experiments.[1,5−8] The resulting intermodulation of chemical shifts can be disentangled, for example, by the G-matrix methodology to produce a set of "base spectra".[8] These base spectra, in fact, represent tilted projections at fixed angles. Taking the GFT 5-D HACACONH experiment, for example, base spectra 1−8 are projections at angles (60°/120°, 60°/120°, 60°/120°, 60°) relative to the orthogonal C^{α}, H^{α}, C′, and N axes, respectively. Depending

… an urgent demand for a **unified nomenclature** to name projected NMR experiments arises…

Table 1. GFT/G²FT NMR experiments

Research group; Experiment name	Magnetization transfer pathway[a]	Linear combination of chemical shifts observed in the GFT dimension(s) (ω_1/ω_2)
Szyperski and co-workers		
1. Backbone and $^1H^\beta/^{13}C^\beta$ resonance assignments		
(5,2)D HACACONHN[3]	$^1H^\alpha_{i-1}$ (t_1) → $^{13}C^\alpha_{i-1}$ (t_1) → $^{13}C'_{i-1}$ (t_1) → $^{15}N_i$ (t_2) → ^1HN_i (t_2)	$\Omega(^{15}N_i) \pm \Omega(^{13}C'_{i-1}) \pm \Omega(^{13}C^\alpha_{i-1}) \pm \Omega(^1H^\alpha_{i-1})$
(5,3)D HACACONHN[12]	(t_1) (t_1) (t_1) (t_2) (t_3)	$\Omega(^{13}C'_{i-1}) \pm \Omega(^{13}C^\alpha_{i-1}) \pm \Omega(^1H^\alpha_{i-1})$
(5,2)D HACA, CONHN[12]	$^1H^\alpha_i$ (t_1) → $^{13}C^\alpha_i$ (t_1) → $^{13}C'_i$ (t_1) → $^{13}C^\alpha_i$ → $^{15}N_i$ (t_1) → ^1HN_i (t_2)	$\Omega(^{15}N_i) \pm \Omega(^{13}C'_i) \pm \Omega(^{13}C^\alpha_i) \pm \Omega(^1H^\alpha_i)$
(5,3)D HACA, CONHN[12]	(t_1) (t_1) (t_1) (t_2) (t_3)	$\Omega(^{13}C'_{i-1}) \pm \Omega(^{13}C^\alpha_{i-1}) \pm \Omega(^1H^\alpha_{i-1})$
(4,3)D CBCACONHN[12]	$^1H^{\alpha\beta}_{i-1}$ → $^{13}C^{\alpha\beta}_{i-1}$ (t_1) → $^{13}C^\alpha_{i-1}$ → $^{13}C'_{i-1}$ (t_1) → $^{15}N_i$ (t_2) → ^1HN_i (t_3)	$\Omega(^{13}C'_{i-1}) \pm \Omega(^{13}C^\alpha_{i-1})$; $\Omega(^{13}C'_{i-1}) \pm \Omega(^{13}C^\beta_{i-1})$
(4,3)D CBCA, CONHN[12]	$^1H^{\alpha\beta}_i$ → $^{13}C^{\alpha\beta}_i$ (t_1) → $^{13}C^\alpha_i$ → $^{13}C'_i$ (t_1) → $^{15}N_i$ (t_2) → ^1HN_i (t_3)	$\Omega(^{13}C'_i) \pm \Omega(^{13}C^\alpha_i)$; $\Omega(^{13}C'_i) \pm \Omega(^{13}C^\beta_i)$
(4,3)D HNNC$^{\alpha\beta}$ ulnC$^\alpha$[13]	^1HN_i → $^{15}N_i$ → $^{13}C^\alpha_{i/i-1}$ → $^{13}C^{\alpha\beta}_{i/i-1}$ (t_1) → $^{13}C^\alpha_{i/i-1}$ (t_1) → $^{15}N_i$ (t_2) → ^1HN_i (t_3)	$\Omega(^{13}C^\alpha_{i/i-1}) \pm \Omega(^{13}C^\alpha_{i/i-1})$; $\Omega(^{13}C^\alpha_{i/i-1}) \pm \Omega(^{13}C^\beta_{i/i-1})$
(4,3)D HNN(CO)C$^{\alpha\beta}$C$^\alpha$[13]	^1HN_i → $^{15}N_i$ → $^{13}C'_{i-1}$ → $^{13}C^\alpha_{i-1}$ (t_1) → $^{13}C^{\alpha\beta}_{i-1}$ → $^{13}C^\alpha_{i-1}$ (t_1) → $^{13}C'_{i-1}$ (t_1) → $^{15}N_i$ (t_2) → ^1HN_i (t_2)	$\Omega(^{13}C^\alpha_{i-1}) \pm \Omega(^{13}C^\alpha_{i-1})$; $\Omega(^{13}C^\alpha_{i-1}) \pm \Omega(^{13}C^\beta_{i-1})$
(4,3)D C$^{\alpha\beta}$C$^\alpha$ (CO)NHN[13]	$^1H^{\alpha\beta}_{i-1}$ → $^{13}C^{\alpha\beta}_{i-1}$ (t_1) → $^{13}C^\alpha_{i-1}$ (t_1) → $^{13}C'_{i-1}$ → $^{15}N_i$ (t_2) → ^1HN_i (t_3)	$\Omega(^{13}C^\alpha_{i-1}) \pm \Omega(^{13}C^\alpha_{i-1})$;
(5,3)D H$^{\alpha\beta}$C$^{\alpha\beta}$C$^\alpha$ (CO)NHN[13]	(t_1) (t_1) (t_2) (t_3)	$\Omega(^{13}C^\alpha_{i-1}) \pm \Omega(^{13}C^{\alpha/\beta}_{i-1})$;
(6,3)D H$^{\alpha\beta}$C$^{\alpha\beta}$C$^\alpha$ (CO)NHN[13]	(t_1) (t_1) (t_1) (t_2) (t_3)	$\Omega(^{13}C^{\alpha/\beta}_{i-1}) \pm \Omega(^{13}C^{\alpha/\beta}_{i-1}) \pm \Omega(^1H^{\alpha/\beta}_{i-1})$;
2. Side-chain resonance assignments		
(5,3)D HCC-CH[13]	$^1H^{(1)}$ (t_1) → $^{13}C^{(1)}$ (t_1) → $^{13}C^{(2)}$ (t_1) → $^{13}C^{(2)}$ (t_2) → $^1H^{(2)}$ (t_3)	$\Omega(^{13}C^{(2)}) \pm \Omega(^{13}C^{(1)}) \pm \Omega(^1H^{(1)})$ 'cross peak'; $\Omega(^{13}C^{(2)}) \pm \Omega(^{13}C^{(2)}) \pm \Omega(^1H^{(2)})$ 'diagonal peak'
(4,2)D HCCH[13] (aliphatic/aromatic)	$^1H^{(1)}$ (t_1) → $^{13}C^{(1)}$ (t_1) → $^{13}C^{(2)}$ (t_1) → $^1H^{(2)}$ (t_2)	$\Omega(^{13}C^{(2)}) \pm \Omega(^{13}C^{(1)}) \pm \Omega(^1H^{(1)})$ 'cross peak'; $\Omega(^{13}C^{(2)}) \pm \Omega(^{13}C^{(2)}) \pm \Omega(^1H^{(2)})$ 'diagonal peak'
(4,3)D HCCH[40] (aliphatic/aromatic)	(t_1) (t_1) (t_2) (t_3)	$\Omega(^{13}C^{(1)}) \pm \Omega(^1H^{(1)})$ 'cross peak'; $\Omega(^{13}C^{(2)}) \pm \Omega(^1H^{(2)})$ 'diagonal peak'
ι-TROSY-(4,3)D HCCH[41] (aromatic)	$^1H^{(1)}$ (t_1) → $^{13}C^{(1)}$ (t_1) → $^{13}C^{(2)}$ (t_2) → $^1H^{(2)}$ (t_3)	$\Omega(^{13}C^{(1)}) \pm \Omega(^1H^{(1)})$ 'cross peak'; $\Omega(^{13}C^{(2)}) \pm \Omega(^1H^{(2)})$ 'diagonal peak'
3. GFT NOESY		
(4,3)D [HC^{ali}/HN]–NOESY–CH^{ali}/NH][42]	$^1H^{ali(1)}$ (t_1) → $^{13}C^{(1)}$ (t_1); $^1H^{N(1)}$ (t_1) → $^{15}N^{(1)}$ (t_1); NOE: $^1H^{ali(1)}/^1H^{N(1)}$ → $^1H^{ali}/^1H^{N(2)}$; $^{13}C^{(2)}$ (t_2) → $^1H^{ali(2)}$ (t_3); $^{15}N^{(2)}$ (t_2) → $^1H^{N(2)}$ (t_3)	$\Omega(^1H^{ali(1)}) \pm \Omega(^{13}C^{ali(1)}) \Omega(^1H^{N(1)}) \pm \Omega(^{15}N^{(1)})$ 'cross peak'; $\Omega(^1H^{ali(2)}) \pm \Omega(^{13}C^{ali(2)}) \Omega(^1H^{N(2)}) \pm \Omega(^{15}N^{(2)})$ 'cross peak';

(continued overleaf)

Table 1. *(Continued)*

Research group; experiment name	Magnetization transfer pathway[a]	Linear combination of chemical shifts observed in the GFT dimension(s)(ω_1/ω_2)
4. G²FT NMR experiments[38]		
ι-(5,3)D HN{N, CO}{C$^{\alpha\beta}$C$^\alpha$}	^1HN_i → $^{15}N_i$ → $^{13}C^\alpha_{i/i-1}$ → $^{13}C^{\alpha\beta}_{i/i-1}$ (t_1) → $^{13}C^\alpha_{i/i-1}$ (t_1) → $^{15}N_i$ (t_2) → ^1HN_i (t_3); $^{13}C'_{i-1}$ (t_2)	ω_1: $\Omega(^{13}C^\alpha_{i/i-1}) \pm \Omega(^{13}C^\alpha_{i/i-1})$; $\Omega(^{13}C^\alpha_{i/i-1}) \pm \Omega(^{13}C^\beta_{i/i-1})$ ω_2 : $\Omega(^{15}N_i) \pm \Omega(^{13}C'_{i-1})$
ι-(5,3)D HN{NCO}{C$^{\alpha\beta}$C$^\alpha$}	^1HN_i → ^{15}Ni → $^{13}C'_{i-1}$ → $^{13}C^\alpha_{i-1}$ → $^{13}C^{\alpha\beta}_{i-1}$ (t_1) → $^{13}C^\alpha_{i-1}$ (t_1) → $^{13}C'_{i-1}$ (t_2) → $^{15}N_i$ (t_2) → ^1HN_i (t_3)	ω_1 : $\Omega(^{13}C^\alpha_{i-1}) \pm \Omega(^{13}C^\alpha_{i-1})$; $\Omega(^{13}C^\alpha_{i-1}) \pm \Omega(^{13}C^\beta_{i-1})$ ω_2 : $\Omega(^{15}N_i) \pm \Omega(^{13}C'_{i-1})$
(5,3)D {C$^{\alpha\beta}$C$^\alpha$}{CON}HN	$^1H^{\alpha\beta}_{i-1}$ → $^{13}C^{\alpha\beta}_{i-1}$ (t_1) → $^{13}C^\alpha_{i-1}$ (t_1) → $^{13}C'_{i-1}$ (t_2) → $^{15}N_i$ (t_2) → ^1HN_i (t_3)	ω_1 : $\Omega(^{13}C^\alpha_{i-1}) \pm \Omega(^{13}C^\alpha_{i-1})$; ω_2 : $\Omega(^{15}N_i) \pm \Omega(^{13}C'_{i-1})$
(6,3)D {H$^{\alpha\beta}$C$^{\alpha\beta}$C$^\alpha$}{CON}HN	(t_1) (t_1) (t_1) (t_2) (t_2) (t_3)	ω_1 : $\Omega(^{13}C^\alpha_{i-1}) \pm \Omega(^{13}C^{\alpha/\beta}_{i-1}) \pm \Omega(^1H^{\alpha/\beta}_{i-1})$; ω_2 : $\Omega(^{15}N_i) \pm \Omega(^{13}C'_{i-1})$
(5,3)D HN{N, CO}{C$^\alpha$H$^\alpha$}	^1HN_i → $^{15}N_i$ → $^{13}C^\alpha_{i/i-1}$ → $^1H^\alpha_{i/i-1}$ (t_1) → $^{13}C^\alpha_{i/i-1}$ (t_1) → $^{15}N_i$ (t_2) → ^1HN_i (t_3); $^{13}C'_{i-1}$ (t_2)	ω_1 : $\Omega(^{13}C^\alpha_{i/i-1}) \pm \Omega(^1H^\alpha_{i/i-1})$; ω_2 : $\Omega(^{15}N_i) \pm \Omega(^{13}C'_{i-1})$
(5,3)D {H$^\alpha$C$^\alpha$}{CON}HN	$^1H^\alpha_{i-1}$ (t_1) → $^{13}C^\alpha_{i-1}$ (t_1) → $^{13}C'_{i-1}$ (t_2) → $^{15}N_i$ (t_2) → ^1HN_i (t_3)	ω_1 : $\Omega(^{13}C^\alpha_{i-1}) \pm \Omega(^{13}H^\alpha_{i-1})$; ω_2 : $\Omega(^{15}N_i) \pm \Omega(^{13}C'_{i-1})$
ι-(5,3)D HN{N, C$^\alpha$}{C$^{\alpha\beta}$C$^\alpha$}	^1HN_i → $^{15}N_i$ → $^{13}C^\alpha_{i/i-1}$ (t_2) → $^{13}C^{\alpha\beta}_{i/i-1}$ (t_1) → $^{13}C^\alpha_{i/i-1}$ (t_1) → $^{15}N_i$ (t_2) → ^1HN_i (t_3)	ω_1 : $\Omega(^{13}C^\alpha_{i/i-1}) \pm \Omega(^{13}C^\alpha_{i/i-1})$; $\Omega(^{13}C^\alpha_{i/i-1}) \pm \Omega(^{13}C^\beta_{i/i-1})$ ω_2 : $\Omega(^{15}N_i) \pm \Omega(^{13}C^\alpha_i)$
ι-(5,3)D HN{N(CO)C$^\alpha$}{C$^{\alpha\beta}$C$^\alpha$}	^1HN_i → $^{15}N_i$ → $^{13}C'_{i-1}$ → $^{13}C^\alpha_{i-1}$ (t_2) → $^{13}C^{\alpha\beta}_{i-1}$ (t_1) → $^{13}C^\alpha_{i-1}$ (t_1) → $^{13}C'_{i-1}$ → $^{15}N_i$ (t_2) → ^1HN_i (t_3)	ω_1 : $\Omega(^{13}C^\alpha_{i-1}) \pm \Omega(^{13}C^\alpha_{i-1})$; $\Omega(^{13}C^\alpha_{i-1}) \pm \Omega(^{13}C^\beta_{i-1})$ ω_2 : $\Omega(^{15}N_i) \pm \Omega(^{13}C'_{i-1})$
Gao and co-workers[43]		
1. Backbone and $^{13}C^\beta$ resonance assignments		
(3,2)D HNNCO[22]	^1HN_i → $^{15}N_i$ → $^{13}C'_{i-1}$ (t_1) → $^{15}N_i$ (t_1) → ^1HN_i (t_2)	$\Omega(^{15}N_i) \pm \Omega(^{13}C'_{i-1})$
(3,2)D HNNCA	^1HN_i → $^{15}N_i$ → $^{13}C^\alpha_{i/i-1}$ (t_1) → $^{15}N_i$ (t_1) → ^1HN_i (t_2)	$\Omega(^{15}N_i) \pm \Omega(^{13}C^\alpha_{i/i-1})$
(3,2)D HNNCACB	^1HN_i → $^{15}N_i$ → $^{13}C^\alpha_{i/i-1}$ → $^{13}C^{\alpha\beta}_{i/i-1}$ (t_1) → $^{13}C^\alpha_{i/i-1}$ → $^{15}N_i$ (t_1) → ^1HN_i (t_2)	$\Omega(^{15}N_i) \pm \Omega(^{13}C^\alpha_{i/i-1})/\Omega(^{13}C^\beta_{i/i-1})$
(3,2)D HNN(CO)CA	^1HN_i → $^{15}N_i$ → $^{13}C'_{i-1}$ → $^{13}C^\alpha_{i-1}$ (t_1) → $^{13}C'_{i-1}$ → $^{15}N_i$ (t_1) → ^1HN_i (t_2)	$\Omega(^{15}N_i) \pm \Omega(^{13}C^\alpha_{i-1})$
(3,2)D HNN(CA)CO	^1HN_i → $^{15}N_i$ → $^{13}C^\alpha_i$ → $^{13}C'_i$ (t_1) → $^{13}C^\alpha_i$ → $^{15}N_i$ (t_1) → ^1HN_i (t_2)	$\Omega(^{15}N_i) \pm \Omega(^{13}C'i)$
(3,2)D HNN(CO)CACB	^1HN_i → $^{15}N_i$ → $^{13}C'_{i-1}$ → $^{13}C^\alpha_{i-1}$ → $^{13}C^{\alpha\beta}_{i-1}$ (t_1) → $^{13}C^\alpha_{i-1}$ → $^{13}C'_{i-1}$ → $^{15}N_i$ (t_1) → ^1HN_i (t_2)	$\Omega(^{15}N_i) \pm \Omega(^{13}C^\alpha_{i-1})/\Omega(^{13}C^\beta_{i-1})$
(3,2)D CBCANHN	$^1H^{\alpha\beta}_{i/i-1}$ → $^{13}C^{\alpha\beta}_{i/i-1}$ (t_1) → $^{13}C^\alpha_{i/i-1}$ → $^{15}N_i$ (t_2) → ^1HN_i (t_1)	$\Omega(^{15}N_i) \pm \Omega(^{13}C^\alpha_{i/i-1})/\Omega(^{13}C^\beta_{i/i-1})$

Table 2: Translation of Projection (Reconstruction) NMR experiments to GFT-NMR nomenclature

Research Group; Projection NMR experiments (with Tilt angles)	Equivalent GFT NMR experiment(s)[a] (with corresponding scaling factors)
Marion and co-workers	
1. 3D $^{13}C/^{15}N$ filtered NOESY[15]	(4,3)D [HC^{ali}]-NOESY-[NH]
Kozminski and co-workers	
1. 2D RD-HNCA[41]	(3,2)D HNNCA
2. 2D RD-HN(CO)CA[41]	(3,2)D HNN(CO)CA
3. 2D RD-HACANH[41]	(4,2)D HACANH
4. 2D DQ-HN{CACB}[42]	(4,2)D HNN$C^{\alpha\beta}C^{\alpha}$
5. 2D DQ-HN(CO){CACB}[42]	(4,2)D HNN(CO)$C^{\alpha\beta}C^{\alpha}$
6. 2D HNCO[43]	(3,2)D HNNCO
7. 2D HNCA[43]	(3,2)D HNNCA
8. 2D HN(CO)CA[43]	(3,2)D HNN(CO)CA
9. 2D H(N)COCA[43]	(3,2)D HN(N)COCA
Brutscher and co-workers	
1. 2D DQ/ZQ HNCA[44]	(3,2)D HNNCA
2. 2D DQ/ZQ HN(CO)CA[44]	(3,2)D HNN(CO)CA
3. 2D DQ/ZQ HNCACB[44]	(3,2)D HNN$C^{\alpha\beta}C^{\alpha}$
4. 2D DQ/ZQ HN(COCA)CB[44]	(3,2)D HNN(COCA)CB
5. 2D DQ/ZQ HN(CA)HA[44]	(3,2)D HNN(CA)HA
6. 2D DQ/ZQ HN(COCA)HA[44]	(3,2)D HNN(COCA)HA
Kupce and Freeman	
1. 3D HNCO[27]	**1. (3,2)D HNNCO**
Tilt angles: $\alpha=30^0$	Scaling factors (κ): N=0.5; CO=0.87
Tilt angles: $\alpha=0^0, 90^0$	2D [$^{13}C'$, ^1H] Projection of 3D HNNCO, 2D [^{15}N, ^1H] HSQC
2. 3D HNCA[28]	**2. (3,2)D HNNCA**
Tilt angles: $\alpha=\pm30^0$	Scaling factors (κ): N=0.5; CA=0.87
Tilt angles: $\alpha=0^0, 90^0$	2D [$^{13}C'$, ^1H] Projection of 3D HNNCA, 2D [^{15}N, ^1H] HSQC
3. 3D HN(CO)CA[28]	**3. (3,2)D HNN(CO)CA**
Tilt angles: $\alpha=\pm60^0$	Scaling factors (κ): N=0.87; CA=0.5
Tilt angles: $\alpha=0^0, 90^0$	2D [$^{13}C'$, ^1H] Projection of 3D HNN(CO)CA, 2D [^{15}N, ^1H] HSQC
4. 4D HNCOCA[30]	**4. (4,2)D HNNCOCA**
Tilt angles: $\alpha=\pm45^0$; $\beta=\pm45^0$	Scaling factors(κ): N=0.71; CO=0.5; CA=0.5
Tilt angles: $\alpha=0^0$; $\beta=0^0$ $\alpha=90^0$; $\beta=0^0$ $\alpha=0^0$; $\beta=90^0$	2D [$^{13}C'$, ^1H] Projection of 4D HNNCOCA 2D [$^{13}C^{\alpha}$, ^1H] Projection of 4D HNNCOCA 2D [^{15}N, ^1H] HSQC
5. The 'TILT' experiment: 3D ^{15}N-NOESY-HSQC and ^{15}N-TOCSY-HSQC[45]	**5. (3,2)D [H]-NOESY-[NH] /(3,2)D [H]-TOCSY-[NH]**
Tilt angle: $\alpha=0^0$, $\alpha=\pm30^0$	Scaling factors(κ): H=1.0, N=0.0 H=0.87, N=0.5

Zhou and co-workers	
1. 5-D HACACONH[33]	**1. (5,2)D HACACONHN**
Tilt angles: N=±60, CO=±60, CA=±60, HA=±60	Scaling factor (κ): N=0.5, CO=0.5, CA=0.5, HA=0.5
Tilt angles: $N=0^0$, $CO=90^0$, $CA=90^0$, $HA=90^0$ $N=90^0$, $CO=0^0$, $CA=90^0$, $HA=90^0$ $N=90^0$, $CO=90^0$, $CA=0^0$, $HA=90^0$ $N=90^0$, $CO=90^0$, $CA=90^0$, $HA=0^0$	2D [^{15}N, ^1H] HSQC 2D [$^{13}C'$, ^1H] Projection of 4D/5D HACACONHN 2D [$^{13}C^{\alpha}$, ^1H] Projection of 4D/5D HACACONHN 2D [$^1H^{\alpha}$, ^1H] Projection of 4D/5D HACACONHN
2. (4,2)D PR-HNCACB[34]	**2. (4,2)D HNN$C^{\alpha\beta}C^{\alpha}$**
Tilt angles: $N=86.0^0$, $CA=15.5^0$, $CB=75.0^0$ $N=73.9^0$, $CA=33.7^0$, $CB=61.3^0$ $N=54.7^0$, $CA=54.7^0$, $CB=54.7^0$ $N=33.7^0$, $CA=73.9^0$, $CB=61.3^0$ $N=15.5^0$, $CA=86.0^0$, $CB=75.0^0$	Scaling factors(κ): $N=0.07$, $C^{\alpha}=0.96$, $C^{\beta}=0.26$ $N=0.28$, $C^{\alpha}=0.83$, $C^{\beta}=0.48$ $N=0.58$,$C^{\alpha}=0.58$, $C^{\beta}=0.58$ $N=0.83$, $C^{\alpha}=0.28$, $C^{\beta}=0.48$ $N=0.96$, $C^{\alpha}=0.07$, $C^{\beta}=0.26$
Tilt angles: $N=0^0$, $CA=90^0$, $CB=90^0$ $N=90^0$, $CA=0^0$, $CB=90^0$ $N=90^0$, $CA=90^0$, $CB=0^0$	2D [^{15}N, ^1H] HSQC 2D [$^{13}C^{\alpha}$, ^1H] Projection of 3D/4D HNNCACB 2D [$^{13}C^{\beta}$, ^1H] Projection of 4D HNNCACB
3. (4,2)D PR-HN(CO)CACB[34] Tilt angles same as in (2)	**3. (4,2)D HNN(CO)$C^{\alpha\beta}C^{\alpha}$** Scaling Factors same as in (2)
4. (4,2)D PR-Intra-HNCACB[34] Tilt angles same as in (2)	**4. (4,2)D Intra-HNN$C^{\alpha\beta}C^{\alpha}$** Scaling Factors same as in (2)
5. (4,2)D PR-HNCACO[34] Tilt angles same as in (2) with CB shift evolution replaced by CO	**5. (4,2)D Intra-HNNCACO** Scaling Factors same as in (2) with C^{β} shift evolution replaced by CO
6. (4,2)D PR-HNCOCA[34] Tilt angles same as in (2) with CA shift evolution replaced by CO and CB shift evolution replaced by CA	**6. (4,2)D HNNCOCA** Scaling Factors same as in (2) with C^{α} replaced by CO and C^{β} replaced by CA
7. (4,2)D PR-HNC$O_{i-1}CA_i$[34] Tilt angles same as in (2) with CA shift evolution replaced by CO and CB shift evolution replaced by CA	**7. (4,2)D HNN<CO,CA>** Scaling Factors same as in (2) with C^{α} shift evolution replaced by CO and C^{β} shift evolution replaced by CA
8. (4,2)D PR-HACANH[34] Tilt angles same as in (2) with CA shift evolution replaced by HA and CB shift evolution replaced by CA	**8. (4,2)D HACANHN** Scaling Factors same as in (2) with C^{α} shift evolution replaced by HA and C^{β} shift evolution replaced by CA
9. (4,2)D PR-HACA(CO)NH[34] Tilt angles same as in (2) with CA shift evolution replaced by HA and CB shift evolution replaced by CA	**9. (4,2)D HACA(CO)NH** Tilt angles same as in (2) with CA shift evolution replaced by HA and CB shift evolution replaced by CA

10. (4,2)D PR CH_3-N NOESY[46]	**10. (4,2)D [HC^{ali}]-NOESY-[NH]**
Tilt angles: 100 Projection angles distributed evenly in angle space: N=α_i; H= β_i; C=γ_i; i=1..100	Scaling factors(κ): N = cos(α_i), H = cos(β_i), C^{ali}= cos(γ_i); i=1..100
11. (4,3)D HC(CO)NH-TOCSY and (4,3)D HC(C)NH-TOCSY[47]	**11. (4,3)D HC(CO)NH-TOCSY and (4,3)D HC(C)NH-TOCSY**
Tilt angles: $\alpha=0^0$, $\pm18^0$, $\pm36^0$, $\pm54^0$, $\pm72^0$, 90^0	Scaling factors(κ): ^{1}H=1.0, 0.95, 0.81, 0.58, 0.31, 0.0 ^{13}C=0.0, 0.31, 0.58, 0.81, 0.95, 1.0
Wüthrich and co-workers[48]	
1. 4D APSY-HNCOCA	**1. Set of (3,2)D and (4,2)D GFT NMR experiments:**
Tilt angles: $\alpha=\pm30^0$; $\beta=0^0$ $\alpha=\pm60^0$; $\beta=0^0$	**(3,2)D HN(N)COCA** Scaling factors(κ): CO=0.5; CA=0.87; CO=0.87; CA=0.5
Tilt angles: $\alpha=0^0$; $\beta=\pm30^0$ $\alpha=0^0$; $\beta=\pm60^0$	**(3,2)D HNN(CO)CA** Scaling factors(κ): N=0.5; CA=0.87 N=0.87; CA=0.5
Tilt angles: $\alpha=90^0$; $\beta=\pm30^0$ $\alpha=90^0$; $\beta=\pm60^0$	**(3,2)D HNNCO** Scaling factors(κ): N=0.5; CO=0.87 N=0.87; CO=0.5
Tilt angles: $\alpha=\pm30^0$; $\beta=\pm30^0$ $\alpha=\pm60^0$; $\beta=\pm30^0$ $\alpha=\pm45^0$; $\beta=\pm60^0$	**(4,2)D HNNCOCA** Scaling factors(κ): N=0.5; CO=0.44; CA=0.75 N=0.5; CO=0.75; CA=0.44 N=0.87; CO=0.35; CA=0.35
Tilt angles: $\alpha=0^0$; $\beta=0^0$ $\alpha=90^0$; $\beta=0^0$ $\alpha=0^0$; $\beta=90^0$	2D [$^{13}C^{\alpha}$, ^{1}H] Projection of 4D HNNCOCA 2D [^{13}C', ^{1}H] Projection of 4D HNNCOCA 2D [^{15}N, ^{1}H] HSQC
2. 5D APSY-HACACONH	**2. A set of (3,2)D GFT NMR experiments**
Tilt angles: $\alpha=\pm30^0$; $\beta=0^0$; $\gamma=0^0$ $\alpha=\pm60^0$; $\beta=0^0$; $\gamma=0^0$	**(3,2)D (HACA)CONHN** Scaling factors(κ): N= 0.87; CO=0.5 Scaling factors(κ): N= 0.5; CO=0.87
Tilt angles: $\alpha=0^0$; $\beta=\pm30^0$; $\gamma=0^0$ $\alpha=0^0$; $\beta=\pm60^0$; $\gamma=0^0$	**(3,2)D (HA)CA(CO)NHN** Scaling factors(κ): N= 0.87; CA=0.5 N= 0.5; CA=0.87
Tilt angles: $\alpha=0^0$; $\beta=0^0$; $\gamma=\pm30^0$ $\alpha=0^0$; $\beta=0^0$; $\gamma=\pm60^0$	**(3,2)D HA(CACO)NHN** Scaling factors(κ): N= 0.87; HA=0.5 N= 0.5; HA=0.87
Tilt angles: $\alpha=90^0$; $\beta=\pm30^0$; $\gamma=0^0$ $\alpha=90^0$; $\beta=\pm60^0$; $\gamma=0^0$	**(3,2)D (HA)CACO(N)HN** Scaling factors(κ): CA= 0.5; CO=0.87 CA= 0.87; CO=0.5
Tilt angles: $\alpha=90^0$; $\beta=0^0$; $\gamma=\pm30^0$ $\alpha=90^0$; $\beta=0^0$; $\gamma=\pm60^0$	**(3,2)D HA(CA)CO(N)HN** Scaling factors(κ): CO= 0.87; HA=0.5 CO= 0.5; HA=0.87
Tilt angles: $\alpha=0^0$; $\beta=90^0$; $\gamma=\pm30^0$ $\alpha=0^0$; $\beta=90^0$; $\gamma=\pm60^0$	**(3,2)D HACA(CON)HN** Scaling factors(κ): CA= 0.87; HA=0.5 CA= 0.5; HA=0.87
Tilt angles: $\alpha=0^0$; $\beta=0^0$; $\gamma=0^0$ $\alpha=90^0$; $\beta=0^0$; $\gamma=0^0$ $\alpha=0^0$; $\beta=90^0$; $\gamma=0^0$ $\alpha=0^0$; $\beta=0^0$; $\gamma=90^0$	2D [^{15}N, ^{1}H] HSQC 2D [^{13}C', ^{1}H] Projection of 4D HNNCOCA 2D [$^{13}C^{\alpha}$, ^{1}H] Projection of 4D HNNCOCA 2D [$^1H^{\alpha}$, ^{1}H] Projection of 4D HNNCOCA
Wagner and co-workers[49]	
3D RD-HCcoNH-TOCSY	**(4,3)D HC(CO)NHN-TOCSY**
Markely and co-workers[37]	
1. 3D HNCO[b]	**1. (3,2)D HNNCO**
Tilt angles: $\alpha=50^0$, 35^0, 10^0, 70^0, 20^0, 25^0, 45^0	Scaling factors(κ): N=0.76, 0.57, 0.17, 0.94, 0.34, 0.42, 0.71 CO =0.64, 0.82, 0.98, 0.34, 0.94, 0.90, 0.71
2. 3D HNCACB[b]	**2. (3,2)D HNNCACB**
Tilt angles: $\alpha=20^0$, 10^0, 30^0, 40^0, 50^0, 60^0, 70^0	Scaling factors(κ):N=0.34, 0.17, 0.50, 0.64, 0.76, 0.87, 0.94 CA/CB=0.94, 0.98, 0.87, 0.76, 0.64, 0.50, 0.34
3. 3D CBCA(CO)NHN[b]	**3. (3,2)D CBCA(CO)NHN**
Tilt angles: $\alpha=50^0$, 55^0, 40^0, 70^0, 30^0, 65^0, 20^0	Scaling factors(κ):N=0.76, 0.82, 0.65, 0.94, 0.87, 0.90, 0.34 CA/CB=0.64, 0.57, 0.76, 0.34, 0.50, 0.42, 0.94

[a] Only basic spectra are considered, unless otherwise indicated.
[b] The tilt angles for mouse protein Mm202773 are considered.[37]

Classification of 'Projected NMR spectra'

- Which chemical shifts are jointly sampled?
- Which orthogonal projections are acquired?
- What is the 'dimensionality' of the spectral information?
- Are conventional ND spectra reconstructed?
- How many 'GFT dimensions'?

Seho Kim, Hanudatta Atreya, Gaohua Liu, Yang Shen,
Alexander Eletski, Jeffrey Mills, David Parish, Duanxiang Xu,
Catherine du Penhoat, Qi Zhang, Kiran Singarapu

Dinesh Sukumaran

Gaetano Montelione

Cheryl Arrowsmith

National Science Foundation (MCB)

National Institutes of Health (PSI)